1 **Hitchhiking on condensed chromatin promotes plasmid persistence in yeast without**

2 **perturbing chromosome function**

3

4 **Authors**: Hemant Kumar Prajapati[1][§], Deepanshu Kumar[2][§], Xian-Mei Yang[3], Chien-Hui Ma[3],

5 Priyanka Mittal[1], Makkuni Jayaram[3]* and Santanu K. Ghosh[2]*

6 [1] National Institute of Child Health and Human Development, National Institutes of Health,

7 Bethesda, MD, 20892.

8 [2]Department of Biosciences and Bioengineering, Indian Institute of Technology, Bombay,

9 Powai, Mumbai-400076, India.

10 [3] Section of Molecular Genetics and Microbiology, University of Texas, Austin, TX 78712, USA.

11 [§] Equal contribution

12 * Corresponding author

13
14 Email: santanughosh@iitb.ac.in, jayaram@austin.utexas.edu

15
16 Tel. (+ 91) 22 2576 7766;
17 Fax (+ 91) 222572 3480.

18

19

20 **Running head:** The association of 2 micron plasmid with chromosome

21 **Abbreviations:** *CEN*: Centromere; *TEL*: Telomere; 3-AT: 3-Amino-1,2,4-triazole

22 **Keywords:** 2-micron plasmid, extra-chromosomal element, budding yeast, centromere,

23 telomere, condensin complex, chromosome condensation.

24

25

26

27

28

Abstract

Equipartitioning by chromosome hitchhiking and copy number correction by DNA amplification are at the heart of the evolutionary success of the selfish yeast 2-micron plasmid. The present analysis reveals plasmid presence near centromeres and telomeres in mitotic cells, with a preference towards the latter. The observed correlation of plasmid missegregation with non-disjunction of rDNA and telomeres under Cdc14 inactivation, higher plasmid missegregation upon induced missegregation of chromosome XII but not chromosome III, requirement of condensin for plasmid stability and the interaction of the condensin subunit Brn1 with the plasmid partitioning system lend functional credence to condensed chromatin being favored for plasmid tethering. By homing to condensed/quiescent chromosome locales, and not over-perturbing genome homeostasis, the plasmid may minimize fitness conflicts with its host. Analogous persistence strategies may be utilized by other extrachromosomal selfish genomes, for example, episomes of mammalian viruses that also hitchhike on host chromosomes for their stable maintenance.

Introduction

Eukaryotes, in contrast to prokaryotes, rarely harbor stably propagating extra-chromosomal DNA elements in their nuclei. However, circular plasmids have been identified in the budding yeast lineage and in the slime mold *Dictyostelium* (Broach, 1982; Hughes & Welker, 1999). In addition, papilloma and gammaherpes viruses exist as episomes in infected mammalian cells during long periods of latency (Coursey & McBride, 2019; Frappier, 2004; McBride, 2008). Eukaryotic nuclei also contain extra-chromosomal circular DNA molecules, called eccDNA that are excised from chromosomes (Cohen & Segal, 2009; Møller et al., 2015; Shibata et al., 2012). Their formation, often associated with DNA replication/repair events, may be important in the evolutionary sizing and shaping of genomes. A subset of these circles has been associated with human diseases (Autiero et al., 2002; Cohen et al., 1997).

The multi-copy 2-micron plasmid of *Saccahromyces cerevisiae*, present as 40-60 molecules per haploid genome content, is the most well characterized among yeast DNA plasmids (Broach & Volkert, 1991; Liu et al., 2014; Rizvi et al., 2018; Sau et al., 2019). Current evidence suggests that plasmid molecules are organized into clusters of 3-5 foci that act as units of segregation during cell division (Ghosh et al., 2007; Liu et al., 2013; Velmurugan et al., 2000). The plasmid genome has a bi-partite functional organization, namely, a replication-partitioning module and a copy number amplification module. The host replication machinery recognizes the plasmid origin, and duplicates each plasmid molecule once during S phase (Zakian et al., 1979). The plasmid partitioning system, comprised of the plasmid coded Rep1 and Rep2 proteins and the *cis*-acting *STB* locus, segregates the replicated molecules equally, or nearly so, to daughter cells (Liu et al., 2014; Rizvi et al., 2018; Sau et al., 2019). The amplification system, constituted by the plasmid coded Flp site-specific recombinase and its target *FRT* sites arranged in head-to-head orientation within the plasmid genome, compensates for copy number reduction resulting from rare missegregation events. Iterative copying of the

79   plasmid template is triggered by a Flp-mediated recombination event coupled to bidirectional

80   plasmid replication (Futcher, 1986; Petes & Williamson, 1994; Volkert & Broach, 1986). The

81   expression of *FLP* is negatively regulated by a putative Rep1-Rep2 repressor, and positively by

82   the plasmid coded Raf1 protein—an antagonist of the repressor (A. Rizvi et al., 2017; Murray et

83   al., 1987; Reynolds et al., 1987; Som et al., 1988). The Flp protein levels and activity are

84   controlled via post-translational modification by the host sumoylation machinery, which signals

85   subsequent proteasome-mediated turnover of Flp (Chen et al., 2005; Ma et al., 2019; Xiong et

86   al., 2009). Thus, mutually reinforcing regulatory mechanisms harbored by the plasmid and

87   imposed by the host protect against any undue drop or runaway increase in plasmid population.

88   Equal segregation and copy number optimization account for the evolutionary persistence of the

89   2-micron plasmid as a selfish DNA element that neither enhances nor significantly diminishes

90   host fitness (Futcher & Cox, 1983; Mead et al., 1986).

91   The current model for 2-micron plasmid propagation, supported by several lines of

92   circumstantial evidence, posits plasmid segregation in physical association with chromosomes

93   (hitchhiking) (Liu et al., 2016; Liu et al., 2013; Mehta et al., 2002). Furthermore, plasmid sisters

94   formed by replication of a single copy *STB*-reporter hitchhike on sister chromatids in a one-to-

95   one fashion (Ghosh et al., 2007). This chromosome-like segregation is not only dependent on

96   the Rep-*STB* system but also on plasmid replication. Apparently, the Rep-*STB* system, in

97   conjunction with replication, directs the symmetric tethering of plasmid sisters to sister

98   chromatids (Liu et al., 2016). In the absence of replication, the Rep-*STB*-assisted plasmid-

99   chromosome tethering becomes random, and plasmid segregation follows the random

100   assortment of chromosomes. Extrapolation of the single-copy plasmid behavior to the native

101   multi-copy plasmid foci suggests a high-order organization within each focus for coordinating

102   the replication of plasmid molecules and the symmetric attachment of the replicated copies to

103   sister chromatids.

104   The orchestration of plasmid segregation by Rep1-Rep2-*STB* is mediated with the

105 assistance of several host factors that interact with the partitioning system in a cell cycle

106 dependent fashion (Cui et al., 2009; Ghosh et al., 2007; Ghosh et al., 2010; Hajra et al., 2006;

107 Huang et al., 2011; Ma et al., 2012; Mehta et al., 2002; Mehta et al., 2005; Prajapati et al., 2017;

108 Wong et al., 2002). Nearly all of these factors play a role in centromere (*CEN*)-mediated

109 chromosome segregation as well. It has been speculated that the unusually short, and

110 genetically defined, point-*CEN* of budding yeast chromosomes and the plasmid-*STB* have

111 diverged from a common ancestor that once directed the segregation of both plasmids and

112 chromosomes (Huang et al., 2011; Malik & Henikoff, 2009). Fluorescence tagged *STB*-reporter

113 plasmids have suggested their tendency to be localized near centromeres and spindle pole

114 bodies in mitotic cells (Velmurugan et al., 2000) whereas, in meiotic cells, their preferred

115 localization is at or near telomeres (*TEL*s) (Sau et al., 2014). Plasmid-telomere association is

116 dependent on the bouquet proteins Ndj1 and Csm1, which are meiosis-specific (Chu, 1998;

117 Chua & Roeder, 1997; Conrad et al., 1997; Primig et al., 2000; Rabitsch et al., 2001). Subtle

118 variations in the mode of plasmid-chromosome association and in the host factors responsible

119 for this process may be necessitated by the two distinct cell cycle programs, even though the

120 common hitchhiking theme is conserved in both cases. The role of the mitotic spindle, the

121 spindle associated motor Kip1 and the microtubule plus end binding proteins, Bik1 and Bim1 in

122 2-micron plasmid segregation during mitosis (Cui et al., 2009; Mehta et al., 2005; Prajapati et

123 al., 2017) suggests spindle-mediated recruitment of the 2-micron plasmid to chromosome sites

124 in the vicinity of centromeres. The association of the *CEN*-specific histone H3 variant Cse4 with

125 *STB* (Hajra et al., 2006), which has been additionally detected at centromere-like regions

126 (CLRs) present near *CEN*s (Lefrancois et al., 2013), would also be consistent with the proximity

127 between plasmid and *CEN*s.

128   The apparent differential plasmid localization on chromosomes in mitotic versus meiotic

129   cells may, in principle, be reconciled by structural or organizational features common to

130   centromeres and telomeres, and perhaps shared by other plasmid tethering sites on

131   chromosomes. To address more definitively the still unresolved questions regarding

132   chromosome locations utilized by the 2-micron plasmid for hitchhiking, we have now mapped

133   the positions of a single-copy *STB*-reporter plasmid with respect to *CEN V* and *TEL V* (also *TEL*

134   *V* and *TEL VII*) simultaneously. We find that the plasmid is located near *CEN* or *TEL* in ≥ 65% of

135   the mitotic cells (≤ 0.5 μm), with a clear *TEL* preference over *CEN*. Interestingly, we observed

136   that 2-micron plasmid segregation is impaired when the disjunction of strongly condensed loci

137   such as telomeres or rDNA is blocked by Cdc14 inactivation. Consistent with this observation,

138   induced missegregation of a highly condensin-dependent chromosome (Chr XII) has a stronger

139   negative effect on equal plasmid segregation than the missegregation of a chromosome that is

140   less dependent on condensin (Chr III). Genetic assays and chromatin immunoprecipitation

141   (ChIP) analyses reveal the interaction of the condensin subunit Brn1 with the Rep-*STB* system,

142   suggesting that condensin is an authentic plasmid partitioning factor appropriated from the host.

143   Condensin requirement for plasmid segregation may be mandated by the need for multiple

144   plasmid molecules within a focus to be condensed in order for them to co-segregate with a

145   chromosome as one physical entity. Preferential localization at chromosome loci where

146   condensin is enriched may reflect a plasmid strategy to satisfy this requirement. Alternatively,

147   condensin acquisition by the clustered plasmid molecules, and presumably their condensation,

148   may facilitate the tethering of plasmid foci to condensed chromosome locales. By hitchhiking on

149   condensed, quiescent chromatin such as telomeres, the plasmid may minimize potential

150   deleterious effects on chromosome function and on the host's fitness.

151

152

153 **Results**

154 **Strategy for mapping plasmid positions with respect to centromeres, telomeres and the**

155 **spindle pole body at different stages of mitosis**

156 Current evidence suggests that the 2-micron plasmid tends to localize preferentially near the

157 centromere cluster and the spindle pole body in mitotic cells (Mehta et al., 2005), but migrates

158 towards the nuclear periphery as diploid cells enter the meiotic program (Sau et al., 2014; Sau

159 et al., 2015). These localizations were carried out primarily using fluorescence-tagged multi-

160 copy *STB*-reporter plasmids (Mehta et al., 2005; Sau et al., 2014), and a nearly single-copy

161 reporter plasmid in one instance (Cui et al., 2009). Visualization of the native 2-micron plasmid

162 in mitotic cells using FISH also reveals a significantly higher number of plasmid foci

163 unassociated with the nuclear membrane than those localizing with it (Heun et al., 2001a).

164 Meiotic plasmid localization at the nuclear periphery increases from early meiosis to the

165 pachytene stage, and requires the bouquet proteins Ndj1 and Csm4 (Sau et al., 2014). In

166 pachytene chromosome spreads, over half the plasmid foci are situated on chromosomes,

167 predominantly at or near telomeres (Sau et al., 2014). The sum of the available data, viewed in

168 light of a shared chromosome-hitchhiking mechanism for plasmid segregation during mitosis as

169 well as meiosis, is consistent with the following interpretation. The 2-micron plasmid exploits

170 certain chromatin features characteristic of centromeres or telomeres, or regions proximal to

171 them, for its chromosome localization. Plasmid presence distal to these loci may be accounted

172 for by similar chromatin features present at a subset of other chromosome regions as well.

173 Differential plasmid localization with respect to the nuclear periphery during mitosis and meiosis

174 may reflect changes in chromatin organization, and/or altered spatial arrangements, of

175 chromosome locales between mitotic and meiotic cells.

176 In order to gain further insights into the chromosome-associated segregation of the 2-

177 micron plasmid, we sought to map plasmid positions in mitotic cells at higher resolution by

7

178   simultaneously fluorescence-tagging chromosome V (Chr V) at the centromere and the

179   telomere on the right arm. Furthermore, in order to avoid any imprecision posed by multiple

180   plasmid foci, we employed a previously described *STB*-reporter plasmid (pSG1) present at one

181   copy (and as a single focus) in ≥ 80% of the cells (Ghosh et al., 2007). The segregation

182   behavior of this plasmid is quite similar to that of an *STB*-reporter plasmid excised from a

183   chromosome by site-specific recombination at G1, and therefore has a copy number of exactly

184   one prior to DNA replication (Liu et al., 2013). A unique advantage of pSG1, which also contains

185   a *GAL* promoter-regulated centromere (*CEN*), is that it can be induced to behave as a *CEN*-

186   plasmid, *STB*-plasmid or an *ARS*-plasmid (lacking partitioning activity) under appropriate

187   experimental conditions (Figure 1- figure supplement 1). When cells harboring pSG1 are grown

188   in medium with glucose as the carbon source (to repress the *GAL* promoter), it is referred to as

189   pSG1-*CEN* to indicate an active centromere. The *CEN*-mediated partitioning function of pSG1-

190   *CEN* is not affected by the presence or absence of the native 2-micron plasmid in the host cells

191   ([Cir$^+$] or [Cir^0], respectively). When present in [Cir$^+$] cells, and the carbon source is galactose,

192   *CEN* is inactivated (by high level transcription from the *GAL* promoter), and the plasmid is

193   referred to as pSG1-*STB* to denote its segregation by a functional Rep-*STB* partitioning system.

194   When placed in [Cir^0] cells, with galactose as the carbon source, the absence of the Rep

195   proteins makes the plasmid behave as pSG1-*ARS* in segregation (Figure 1- figure supplement

196   1).

197   We distinguished *CEN V* and *TEL V* in cells expressing TetR-GFP by their distinct

198   fluorescence intensities conferred by [TetO]$_{224}$ and [TetO]$_{448}$ arrays inserted at *CEN V* and *TEL*

199   *V* loci, respectively (Alexandru et al., 2001; Michaelis et al., 1997) (Figure 1- figure supplement

200   2). We verified that the two loci could be identified unambiguously at various stages of mitosis

201   by marking their positions relative to the spindle pole body (SPB) tagged with Spc42-mCherry

202   (Figure 1- figure supplement 2). In *S. cerevisiae*, centromeres remain congressed as a single

203   cluster in close proximity to SPB during interphase as well as mitosis, while the rosette of three

204   to six telomere clusters is positioned at the nuclear periphery distal to SPB in a Rabl-like pattern

205   (Gotta et al., 1996; Guacci et al., 1997; Heun et al., 2001b; Jin et al., 2000; Jin et al., 1998;

206   Kupiec, 2014; Taddei & Gasser, 2012). Consistent with this spatial organization, we observed

207   partial overlap or close proximity of SPB to the fainter of the two GFP foci (*CEN V*), with the

208   brighter GFP focus *(TEL V)* located away from it (Figure 1- figure supplement 2). These three

209   nuclear landmarks provided a frame of reference for mapping the spatial positions of reporter

210   plasmids.

211

212   **Mitotic localization of pSG1-*CEN* and pSG1-*STB* with respect to *CEN V* and *TEL V***

213   In order to follow plasmid localization in the nucleus, we introduced pSG1 into isogeneic [Cir$^+$]

214   and [Cir^0] strains containing the marked *CEN V*, *TEL V* and SPB, and expressing cyan-LacI.

215   Plasmid foci were visualized by repressor interaction with the plasmid-borne [LacO]$_{256}$ array

216   (Straight et al., 1996). As already noted, by using [Cir$^+$] and [Cir^0] backgrounds and manipulating

217   the carbon source, we could induce pSG1 to behave as pSG1-*CEN*, pSG1-*STB* or pSG1-*ARS*

218   (Figure 1- figure supplement 1, Ghosh et al., 2007).

219   The localization of pSG1-*CEN* ([Cir$^+$]; glucose) at different stages of the mitotic cell cycle

220   (Figure 1A, B) at or close to SPB (≤ 0.5 μm) was akin to that of chromosome centromeres

221   (Figure 1- figure supplement 2), as expected. The spatial distribution of pSG1-*STB* ([Cir$^+$];

222   galactose), however, was different (Figure 2 and 3). In G1/S (Figure 2A, B) and in metaphase

223   (Figure 2C, D) cells, 40-45% of the cyan foci were proximal to the *TEL V* (≤ 0.5 μm), 20-25%

224   were close to *CEN V* (≤ 0.5 μm) and the rest showed no spatial linkage to either *CEN V* or *TEL*

225   *V* (> 0.5 μm) (Figure 2A-D).The pSG1-*STB* sisters were seen in metaphase cells as a single

226   coalesced focus in the majority of cases (60-65%), as would be consistent with the bridging of

227   plasmid sisters by the cohesin complex (Ghosh et al., 2010; Liu et al., 2013; Mehta et al., 2002)

228 and/or their symmetric attachment to sister chromatids (Liu et al., 2016), which are also paired

229 by cohesin. For the purpose of precise positioning, the cells (35-40%) showing plasmids with

230 more than a single focus were excluded from the distance analysis. As the average copy

231 number of pSG1 was only approximately one (Ghosh et al., 2007), not every cell in the

232 population contained a single plasmid molecule prior to replication. At least a subset of the

233 metaphase cells with two separated plasmid foci might indicate copy number deviation from

234 unity, rather than a lack of pairing between plasmid sisters. Higher foci number seen in a very

235 small fraction of cells could only be due to the presence of more than one plasmid per nucleus.

236 As a more stringent test of the apparent tendency of pSG1-*STB* to remain telomere-

237 proximal, we observed its localization in a selected subset of anaphase cells in which the *CEN*

238 *V*s were well separated from each other, and from the unsegregated *TEL V*s that remained at

239 the spindle mid-zone (Figure 3A). In this population, the fraction of cells showing pSG1-*STB*

240 proximity to *TEL V* was ~45%; *CEN V* proximity was seen in ~15% (Figure 3B). For the pSG1-

241 *ARS* plasmid, the proximal (≤ 0.5 μm from *CEN V* or *TEL V*) and distal (> 0.5 μm from *CEN V*

242 and *TEL V*) locations of foci were roughly evenly divided among G1/S cells (Figure 2- figure

243 supplement 1). As an *ARS*-plasmid does not physically associate with chromosomes, as

244 revealed by chromosome spread assays (Liu et al., 2014; Mehta et al., 2002), the data in Figure

245 2- figure supplement 1 refer to the overall nuclear distribution of the plasmid and not its location

246 on chromosomes.

247 Finally, we verified the mapping of plasmid positions by determining the three-

248 dimensional disposition of pSG1 with respect to *CEN V* and *TEL V* in live cells. The dot plots of

249 distances in 'Figure 2- figure supplement 2' were derived by defining the centroids of the

250 plasmid and chromosome fluorescent foci from imaging a series of nuclear stacks (Figure 2-

251 figure supplement 2A). The distribution of pSG1-*STB* showed a discernible bias towards

252 telomere proximity (Figure 2- figure supplement 2B), while that of pSG1-*ARS* ([Cir^0]; galactose)

253   was essentially random (Figure 2- figure supplement 1 and 2C). The expected centromere-

254   proximal localization of pSG1-*CEN* was also evident (Figure 1, Figure 2- figure supplement 2D).

255   The combined results from Figure 2 and Figure 3 suggest that telomeres and their

256   proximal loci are more frequently habited by the 2-micron plasmid than centromeres and nearby

257   regions. At all the stages of the cell cycle, a third population of cells showed no association of

258   pSG1-*STB* with *CEN V* or *TEL V* locus (> 0.5 μm in Figure 2 and 3). It is likely that the 2-micron

259   plasmid associates with other tethering sites distributed along chromosome arms, albeit at a

260   lower frequency.

261

262   **Association of the 2-micron plasmid with *TEL VII***

263   Unlike centromeres, which are congressed into one tightly knit cluster in mitotic cells, telomeres

264   form a rosette of 3-6 clusters (Kupiec, 2014; Taddei & Gasser, 2012). The premise of our

265   assays (Figure 2 and Figure 3) is that *TEL V* is equally likely to associate with any of these

266   clusters. In order to probe potential variations among telomeres in plasmid association, we

267   assayed plasmid localization with respect to two telomeres, *TEL V* and *TEL VII* (on the right arm

268   of Chr VII), differentially tagged by [TetO]$_{448}$-[TetR-GFP] and [TetO]$_{\sim50}$-[TetR-GFP] fluorescence,

269   respectively.

270   In the experimental strain *TEL V* was distinguished from *TEL VII* by the difference in

271   their fluorescence intensities. The observed pSG1 association with *TEL V* was ~48% and that

272   with *TEL VII* was 24% (Figure 2- figure supplement 3). These results, while upholding the

273   telomere preference of the 2-micron plasmid, suggest that all telomeres may not be equal in

274   plasmid occupancy. Such differences might arise from differences in high-order chromatin

275   organization and/or epigenetic features at or near individual telomeres. Some variability might

276   also result if individual telomeres are not entirely bias-free in their associations during cluster

277　formation. Furthermore, 'proximity' is somewhat broadly defined in our assays because of the

278　resolution limits of fluorescence microscopy and the cut-off distance of 0.5 μm employed.

279　　　From the perspective of the hitchhiking model for segregation, the combined results from

280　Figure 2 and Figure 3 suggest that telomere- and centromere-association together constitutes a

281　major segregation route for the 2-micron plasmid. Furthermore, telomeres are better preferred

282　as hitchhiking sites by the plasmid than centromeres. Thus, preferential plasmid segregation as

283　a telomere appendage observed during meiosis (Sau et al., 2014) appears to hold for mitosis as

284　well, a fact that was not appreciated from prior published results. While Rep1 and Rep2 proteins

285　are essential for mediating plasmid-chromosome association in both mitosis and meiosis, the

286　host proteins involved in plasmid linkage to telomeres are likely different between the two cell

287　cycle programs (Sau et al., 2014).

288

289　**Blocking segregation of condensed chromosome loci causes *STB*-plasmid non-**

290　**disjunction**

291　Chromosome sites preferentially occupied by the condensin complex in budding yeast include

292　telomere-proximal regions, which are organized as condensed, transcriptionally quiescent

293　heterochromatin (Wang et al., 2005). Chromosome condensation is influenced by centromeres

294　in their role as *cis*-acting mediators. They promote recruitment of condensin, cohesin and

295　associated signaling molecules to pericentric regions, which have characteristic chromatin

296　composition and organization (Biggins, 2013; Kruitwagen et al., 2018; Stephens et al., 2011;

297　Yong-Gonzalez et al., 2007). Genome-wide mapping studies reveal quantitative differences in

298　condensin occupancy along chromosome arms, as well as cell cycle dependent modulations in

299　occupancy at individual loci (Wang et al., 2005). In mitotic yeast cells, in addition to sub-

300　telomeric and pericentric regions, the rDNA gene cluster is also prominent in condensin

301　enrichment. The non-random localization of an *STB*-plasmid in the nucleus, favoring the vicinity

302   of telomeres and centromeres (Figure 2 and 3; Figure 2- figure supplement 2, Figure 2- figure

303   supplement 3), prompted us to examine a potential role for condensin in 2-micron plasmid

304   segregation, and to address the possible coupling between condensed chromosome loci and

305   the plasmid in segregation.

306   Telomeres and rDNA differ subtly from chromosomes as a whole in their segregation

307   mechanism. In addition to early anaphase cleavage of cohesin that holds together sister

308   chromatids in pairs, these loci require a second 'late' condensin-dependent step to complete

309   unlinking and segregation (Machin et al., 2016). The extra condensin recruitment is mediated by

310   Cdc14 phosphatase, which is released from its sequestered state at the onset of anaphase by

311   the FEAR (Fourteen Early Anaphase Release) network (Stegmeier & Amon, 2004; Sullivan et

312   al., 2004). Upon inactivation of Cdc14, rDNA and telomeres are delayed in disjunction relative to

313   the rest of the chromosomes (Clemente-Blanco et al., 2011). If the 2-micron plasmid

314   preferentially utilizes condensed chromatin for its hitchhiking mode of segregation, lack of

315   Cdc14 function is expected to increase the frequency of plasmid missegregation. We tested this

316   prediction using a multi-copy *STB*-reporter plasmid pSV5-*STB* (Figure 4) that we had utilized in

317   prior plasmid segregation assays (Mehta et al., 2002). The control reporter plasmids for this

318   analysis were derivatives of pSV5 in which *STB* was either deleted (pSV6-*ARS*) or replaced by

319   *CEN* (pSV7-*CEN*) (Figure 4- figure supplement 1 and 2).

320   The pSV5 plasmid, fluorescence tagged by [LacO]-[CFP-LacI] interaction, is organized

321   into 2-5 foci per nucleus. Prior experiments suggest that each plasmid focus is an independent

322   unit in segregation (Velmurugan et al., 2000). As the number of plasmid molecules in individual

323   foci is unknown, and occasionally foci tend to overlap, segregation estimates from counting foci

324   numbers in mother and daughter nuclei are only semi-quantitative. Nevertheless, there is good

325   agreement between data obtained from multi-copy and single-copy plasmid reporters in

326   segregation assays (Ghosh et al., 2007; Liu et al., 2013; Velmurugan et al., 2000)

327   In the *cdc14-3* (Ts) strain at 33ºC (non-permissive), a significant fraction of the cells

328   showed non-disjunction of telomeres marked by [*TEL V*-LacO]-[GFP-LacI] (~35%; Type III plus

329   Type IV, Figure 4A) or the r-DNA locus marked by [rDNA–LacO]-[GFP-LacI] (~40%; Type III

330   plus Type IV, Figure 4B), as expected from prior studies (D'Amours et al., 2004). In the wild type

331   strain, these loci segregated normally in ≥ 90% of the cells (Type I plus Type II, Figure 4A, B).

332   The corresponding equal segregation of ~70% for pSV5-*STB* (Type I plus Type III, Figure 4A,

333   B;), which is consistent with prior results for multi-copy and single-copy reporter plasmids

334   (Ghosh et al., 2007; Velmurugan et al., 2000), dropped to ~40-50% in the *cdc14* mutant (Type I

335   plus Type III, Figure 4A, B). Significantly, pSV5-*STB* and *TEL V* or rDNA were well correlated in

336   their segregation, equal as well as unequal, in the wild type and mutant strains (Type I + Type

337   IV >> Type II + Type III Figure 4A, B). In the majority of cells in which plasmid missegregation

338   was coupled to the block in *TEL V* or rDNA segregation (Type IV, Figure 4A, B), the entire

339   cluster of pSV5-*STB* foci, or a majority of the foci, was trapped in the mother or at the bud neck.

340   In contrast to pSV5-*STB*, pSV6-*ARS* (Mehta et al., 2002), lacking *STB*, showed high

341   missegregation in the wild type and mutant strains (Type II plus Type IV, Figure 4- figure

342   supplement 1 A, B). On the other hand, pSV7-*CEN* segregated equally in most of the cells

343   irrespective of the strain background (Type I and Type III, Figure 4- figure supplement 2 A, B).

344   To further verify the apparent distinction between an *STB*-plasmid and an *ARS*- or a *CEN*-

345   plasmid in segregation under Cdc14 inactivation, we followed the single copy reporter plasmids

346   (pSG1-*STB*, pSG1-*CEN* and pSG1-*ARS*) with respect to Nop1 in the *cdc14* mutant strain

347   (Figure 4- figure supplement 3). Consistent with the results from Figure 4, Figure 4- figure

348   supplement 1 and Figure 4- figure supplement 2, pSG1-*STB* alone showed the correlation with

349   Nop1 in segregation (Figure 4- figure supplement 3).

350   Thus, Cdc14 assisted segregation of *TEL V* or rDNA also impacts plasmid segregation

351   directed by the Rep1-Rep2-*STB* system, but has no effect on *CEN* mediated segregation or

352 segregation in the absence of a partitioning system. The correlation between *STB*-plasmid

353 missegregation and the block in *TEL V* or rDNA segregation is consistent with condensed

354 chromosome loci being preferred sites for hitchhiking by the 2-micron plasmid.

355

356 **Missegregation of chromosome XII causes missegregation of the 2-micron plasmid**

357 Faithful chromosome segregation in yeast, as in all eukaryotes, requires chromosome

358 condensation, which facilitates compaction of chromosome arms, unlinking of catenated sister

359 chromatids, and their organization into functional segregation units (Hayes & Barilla., 2006).

360 While condensation is easily visualized in the large chromosomes of plants and metazoans,

361 more sensitive tools utilizing FRET or fluorescence quenching are needed to monitor

362 condensation of the relatively short yeast chromosomes (Kruitwagen et al., 2018). However,

363 condensation of the rDNA locus on chromosome XII (comprised of ~150 copies of a 9.1 kbp

364 repeat unit or 1.5 Mbp DNA) has been revealed by standard microscopy in conjunction with

365 FISH (fluorescence in situ hybridization) (Lavoie et al., 2004). As already pointed out,

366 segregation of the rDNA and telomere loci requires a Cdc14-dependent extra step of condensin

367 recruitment and action. Interruption of this step perturbs the segregation of these loci and of the

368 2-micron plasmid, while chromosome segregation overall proceeds normally.

369 When gross missegregation of yeast chromosomes is induced by a conditional mutation,

370 the majority of foci formed by a fluorescence-tagged multi-copy *STB*-plasmid segregates to the

371 nuclear compartment containing the bulk of the chromosome mass (Mehta et al., 2002;

372 Velmurugan et al., 2000). When the entire set of replicated sister chromatids is forced into either

373 the mother or the daughter nucleus, a single-copy *STB*-plasmid is almost always localized in the

374 chromosome-containing nucleus (Liu et al., 2016). These observations are consistent with

375 plasmid hitchhiking sites being distributed on more than one (or perhaps all) chromosomes.

376 However, the correlation between plasmid and Nop1 (rDNA) during segregation under Cdc14

377   inactivation suggests that missegregation of chromosome XII, housing the rDNA array and

378   critically dependent on condensin for segregation, is likely to affect 2-micron plasmid

379   segregation more severely than missegregation of a smaller chromosome with less stringent

380   dependence on condensin. We tested this hypothesis by following plasmid behavior in cells

381   missegregating either chromosome XII (the longest yeast chromosome) or chromosome III,

382   which is roughly one-third as long.

383   The pSV5-*STB* plasmid was introduced into isogenic strains in which either *CEN III* or

384   *CEN XII* could be inactivated conditionally by *GAL* promoter driven transcription through them

385   (Reid et al., 2008). The expression of GFP-LacI and Nop1-RFP in these strains permitted

386   plasmid segregation and chromosome XII segregation (by Nop1 as proxy) to be monitored

387   simultaneously against chromosome segregation as a whole visualized by DAPI staining.

388   Missegregation of chromosome XII, but not of chromosome III, resulted in a significant increase

389   in plasmid missegregation (Figure 5A-C). Furthermore, in cells showing missegregation of both

390   pSV5-*STB* and Nop1 (Type III; Figure 5A;), the majority of plasmid foci was present in the

391   nucleus containing Nop1.

392   The above results suggest that chromosome XII is a more preferred target for 2-micron

393   plasmid association than chromosome III (and likely the other individual chromosomes). The

394   size advantage of chromosome XII over chromosome III should have only minimal effect on

395   plasmid association/segregation, as it would be more than offset by the fifteen normally

396   segregating chromosomes in each of the assays.

397

398   **Absence of condensin function disrupts faithful *STB*-plasmid segregation**

399   The bias towards condensed chromatin in the chromosome-association of the 2-micron plasmid

400   suggests two possible roles, which need not be mutually exclusive, for the condensin complex

401   in plasmid physiology. The multiple plasmid copies present within a chromosome associated

402   plasmid focus, which appears to be the unit in segregation (Sau et al., 2019; Velmurugan et al.,

403   2000), may need to be condensed as a prerequisite for segregation by hitchhiking. Or

404   condensin may facilitate preferential plasmid association, and segregation in concert, with

405   condensed chromosome loci. In support of the latter role, condensin is known to bridge DNA

406   loci that are distal to each other on the genome. For example, it binds to tRNA genes dispersed

407   throughout the chromosomes, and promotes their congregation into a cluster at the nucleolus

408   (Haeusler et al., 2008). In order to probe potential condensin requirement for 2-micron plasmid

409   segregation, we compared the rates of missegregation of *STB*-plasmids with those of *CEN*- or

410   *ARS*-plasmids following inactivation of the condensin component Brn1.

411   At 36°C, the instability of the *STB*-plasmid (pRS422; *ADE2*) (Brachmann et al., 1998)

412   was elevated ~4-fold in the temperature sensitive *brn1-60* mutant (Ouspenski et al., 2000) over

413   the wild type (Figure 6A). We also noted a comparable increase in the loss rate of the control

414   *CEN*-plasmid (pRS412; *ADE2*) (Brachmann et al., 1998), but not an *ARS*-plasmid (YRp17,

415   *TRP1*) (Botstein and Davis 1981) in the mutant background (Figure 6A). The *CEN*-plasmid

416   instability is consistent with the previously demonstrated role of condensin in centromere

417   function (Yong-Gonzalez et al., 2007). These stability results were further verified by assaying

418   the segregation of fluorescence-tagged *STB*-reporter and *CEN*-reporter plasmids (pSV5-*STB*

419   and pSV7-*CEN*, respectively) in the wild type and mutant strains (Figure 6B). A fluorescence-

420   tagged *ARS*-plasmid (pSV6-*ARS*), by contrast, was not altered in its segregation by the loss of

421   condensin function (Figure 6B).

422   The difference in the responses of *ARS*- versus *STB*- and *CEN*-plasmids to condensin

423   inactivation suggests that the observed segregation results are unlikely to have resulted from

424   the pleiotropic effects of condensin on chromatin organization and function. However, they do

425   not address whether condensin plays similar or distinct roles in its contribution towards the

426   segregation functions of *STB* and *CEN*.

427

Brn1 interacts with the 2-micron plasmid partitioning system

429   Since condensin is required for chromosome segregation, and the 2-micron plasmid is

430   dependent on chromosomes for its own segregation, it is difficult to decipher whether

431   condensin's effect on the plasmid is direct or indirect. Proximity of the plasmid to condensed

432   chromosome loci may lead to incidental plasmid-condensin association, and likely plasmid

433   condensation as a result. Alternatively, condensin acquisition by the plasmid (and perhaps

434   condensation) may be functionally related to the localization of a plasmid focus at condensed

435   chromatin and its chromosome associated segregation. One reasonable criterion for the direct

436   involvement of condensin in 2-micron plasmid segregation would be its interaction with the Rep-

437   *STB* system. Such interactions by host factors that assist plasmid partitioning have been

438   demonstrated in previous studies through genetic interaction, chromatin immunoprecipitation

439   (ChIP), and affinity enrichment-mass spectrometry assays (Cui et al., 2009; Hajra et al., 2006;

440   Ma et al., 2013; Mehta et al., 2002; Prajapati et al., 2017). We have now subjected condensin to

441   similar tests using the Brn1 subunit of the complex as its representative.

442   Interaction between *STB* and Brn1 was detected in a monohybrid assay, in which Brn1

443   fused to Gal4 transcriptional activation domain (Brn1-AD) increased the transcription of a *HIS3*

444   reporter gene harboring *STB* as an upstream activator sequence (UAS) (Figure 7- figure

445   supplement 1). This transcriptional activation was abolished in the absence of Rep1 and Rep2

446   ([Cir^o] host) (Figure 7- figure supplement 1), suggesting that Brn1-*STB* interaction is mediated

447   by Rep1 or Rep2, or by both. Consistent with Rep protein mediated condensin recruitment at

448   *STB*, yeast dihybrid assays revealed the interaction of Brn1 with Rep1 and Rep2 (Figure 7-

449   figure supplement 2).

450   The results from the genetic assays were confirmed by the enrichment of *STB* DNA

451   during chromatin immunoprecipitation (ChIP) in a [Cir$^+$] strain using anti-HA antibodies directed

452   to Brn1-6HA (Figure 7A). The authenticity of Brn1-*STB* association was verified by centromere

453   (*CEN III*) enrichment, but not the tubulin locus *TUB2*, in the immunoprecipitate. *TUB2* has been

454   designated as weak or negative in condensin localization (Wang et al., 2005). Furthermore,

455   ChIP in a [Cir^0] strain (lacking Rep1 and Rep2) failed to bring down *STB*, with little or no effect

456   on *CEN III* (Figure 7B). Finally, consistent with the higher missegregation of *STB-* plasmids

457   under Cdc14 inactivation (Figure 4, Figure 4- figure supplement 3), ChIP in the *cdc14-3* mutant

458   revealed a nearly complete absence of condensin at *STB* (Figure 7A, B).

459   The Rep-protein-dependent association of condensin with *STB*, the loss of this

460   association upon Cdc14 inactivation, and the rise in *STB*-plasmid instability upon Brn1 or Cdc14

461   inactivation argue for condensin being an authentic host coded 2-micron plasmid partitioning

462   factor. The appropriation of the host's DNA compaction and/or high-order DNA organization

463   factors (condensin and cohesin, for example) by the 2-micron plasmid would be consistent with

464   the evolutionary attunement of plasmid segregation to chromosome segregation.

465

466   **Discussion**

467   We have characterized chromatin attributes exploited by the 2-micron plasmid for its hitchhiking

468   mode of segregation during mitosis. Our findings suggest that condensed or condensin enriched

469   chromatin and/or silent heterochromatin-like regions of chromosomes are preferred targets for

470   plasmid-chromosome association. Furthermore, the condensin complex interacts with the

471   plasmid partitioning system, and facilitates equal plasmid segregation.

472

473   **2-micron plasmid localization on yeast chromosomes**

474   The chromosome-hitchhiking model for 2-micron plasmid segregation (Liu et al., 2016; Liu et al.,

475   2013; Rizvi et al., 2018; Sau et al., 2014) is based on a confluence of circumstantial, albeit

476   persuasive, evidence. Strictly, plasmid association with a nuclear entity that segregates with the

477   same characteristics as chromosomes cannot be ruled out. Direct demonstration of plasmid-

478   chromosome association is impeded by the inability to resolve individual mitotic yeast

479   chromosomes. Nevertheless, multi-copy and single-copy *STB*-reporter plasmids localize to

480   yeast mitotic chromosome spreads in a Rep1-Rep2 dependent fashion, and colocalize with

481   these proteins (Ghosh et al., 2006; Mehta et al., 2002). In mammalian cells, co-expressed Rep1

482   and Rep2 form merged foci on mitotic chromosomes collectively, and along the arms of

483   individual chromosomes in metaphase spreads (Liu et al., 2016). Based on Rep1-Rep2

484   association with *STB* (Mehta et al., 2002; Scott-Drew & Murray, 1998; Velmurugan et al., 2000),

485   and assuming the mammalian system to recapitulate the native yeast system, it follows that the

486   2-micron plasmid is tethered to yeast chromosomes with assistance from the Rep proteins.

487   Meiotic yeast chromosome spreads, with considerably higher resolution than mitotic spreads,

488   reveal *STB*-plasmid foci to be coalesced with a subset of Rep foci localized on chromosomes

489   (Sau et al., 2014). The preferential plasmid localization at telomeres or subtelomeric regions in

490   these spreads differs from the reported centromere proximity of plasmid in mitotic cells (Mehta

491   et al., 2002). Higher accuracy mapping has now localized the 2-micron plasmid near *CEN* and

492   *TEL* in a majority of the cell population, with a clear bias towards *TEL* (Figure 2 and Figure 3). In

493   over a third of the population, the plasmid location is distal to *CEN* or *TEL*. It is possible that

494   these 'other' chromosome sites that the plasmid tethers to share organizational features with

495   *CEN* and *TEL*, for example, chromatin architecture and/or transcriptional quiescence.

496

A role for chromatin organization in the selection of plasmid tethering sites?

498   *S. cerevisiae* lacks the canonical eukaryotic machinery for silenced heterochromatin assembly

499   (Briggs et al., 2001; Grunstein & Gasser, 2013), but is still capable of transcriptional repression

500   through specialized chromatin architecture. Silencing at telomeres, rDNA and the *HML*/*HMR* loci

501   requires one or more components of the Sir protein complex (Sir1-4) along with other

502 companion proteins that are shared among, or unique to, individual loci (Huang et al., 2002;

503 Kueng et al., 2013). The atypical, genetically defined point centromeres of *S. cerevisiae*

504 chromosomes do not conform to the classical definition of heterochromatin observed at

505 epigenetically determined regional centromeres. Nevertheless, Sir1 is associated with *CEN*, and

506 contributes to mitotic chromosome stability (Sharp et al., 2003), which can be modulated by

507 driving transcription through *CEN* (Hill & Bloom, 1989; Ohkuni & Kitagawa, 2012). By a more

508 inclusive definition, 'heterochromatin' of *S. cerevisiae* encompasses not only transcriptionally

509 inactive chromatin but also functional *CEN* chromatin. The plasmid partitioning system may

510 recognize tethering sites, including the preferred *TEL* and *CEN*, by a chromatin signature

511 shared within this broad class of chromosome regions.

512 The *S. cerevisiae* point centromere, despite being genetically specified, manifests a

513 certain degree of epigenetic character. Established *CEN*s are functionally propagated through

514 many generations in strains carrying kinetochore mutations that block *de novo CEN*

515 establishment (Mythreye & Bloom, 2003). By one postulate, centromeres originated from

516 telomeres in parallel with the microtubule based cytoskeletal segregation machinery in response

517 to the formation of multiple linear chromosomes from an ancestral single circular genophore

518 (Villasante et al., 2007). *CEN* and *TEL* do share organizational or functional features in a limited

519 set of biological contexts. In the fission yeast, centromere-centrosome contact can replace

520 telomere-centrosome contact to support spindle formation and successful meiosis (Fennell et

521 al., 2015). In fruit fly oocytes, the clustering of centromeres resembles bouquet formation by

522 telomeres, which is emblematic of eukaryotic meiosis in general (Takeo et al., 2011). Both *TEL*s

523 and *CEN*s being tethering sites for the native yeast plasmid would be consistent with some

524 epigenetic mark that was conserved during their separate evolutionary trajectories, which might

525 also be retained within *CEN*-adjacent centromere like regions (*CLR*s) (Lefrancois et al., 2013).

526

2-micron plasmid missegregation upon Cdc14 inactivation

The functional relevance of telomere proximity of the 2-micron plasmid on chromosomes is upheld by the increase in plasmid missegregation when telomere (and rDNA) disjunction is impeded by inactivating Cdc14. However, total missegregation of all plasmid foci in tandem with *TEL* or rDNA (represented by Nop1) is rarely seen (Figure 4). This is the expected outcome if plasmid tethering sites were present at chromosome locales other than *TEL*s, including *CEN*-proximal regions as revealed in the localization assays. According to a prior study, when the entire set of chromosomes is confined to either the mother or daughter nucleus, there is near perfect correlation between an *STB*-plasmid and chromosomes in their localization (Liu et al., 2016). Taken together, these results support a non-random distribution of plasmid tethering sites on chromosomes, *TEL*s or nearby loci being high density or high affinity sites. Cdc14 inactivation has pleiotropic consequences, one of which is compromised spindle integrity (Khmelinskii & Schiebel, 2008; Marston et al., 2003). The mitotic spindle and spindle associated proteins play a role, even if indirect, in 2-micron plasmid segregation (Mehta et al., 2002; Mehta et al., 2005; Prajapati et al., 2017). Hence, potential contribution of spindle defect to plasmid missegregation under loss of Cdc14 function cannot be ruled out. However, such an effect is likely modest, as overall chromosome segregation (revealed by DAPI staining) appears to be normal in our assays. Furthermore, *STB* plasmid missegregation can also be induced by inactivating the condensin component Brn1, which is not known to be involved in spindle function.

A role for the condensin complex in 2-micron plasmid segregation

As noted, Cdc14-promoted condensin recruitment late in the cell cycle at rDNA and *TEL*s is a pre-requisite for their proper segregation (D'Amours et al., 2004; Sullivan et al., 2004). The possibility that this instalment of condensin resolves rDNA sisters independent of chromosome

552 condensation and Topo II activity has been raised (D'Amours et al., 2004). However, full

553 condensation of rDNA, approximately equal to that of condensed euchromatin, is completed

554 only in anaphase (Sullivan et al., 2004). Resolution of the interlinks between rDNA sisters by

555 recruitment of Topo II in a condensin dependent step, or remodeling of the interlinks by

556 condensin to a configuration favored by Topo II, has not been ruled out (Charbin et al., 2014;

557 Sullivan et al., 2004). The increased missegregation of the 2-micron plasmid in a condensin

558 mutant (Figure 6) may result from a direct effect of condensin on the plasmid itself, or an indirect

559 effect manifested through chromosomes on which it hitches a ride.

560   By being a chromosome appendage, the plasmid becomes subjected to the same

561 physical and conformational constraints that a chromosome experiences during segregation.

562 Chromosome condensation and plasmid condensation may thus be coincidental events.

563 However, the interaction of Brn1 with the Rep proteins and its localization at *STB* with Rep

564 protein assistance (Figure 7, Figure 7- figure supplement 1 and 2) would be consistent with a

565 more direct role for condensin in plasmid segregation. Interestingly, Brn1 association with *STB*

566 is reduced by Cdc14 inactivation (Figure 7). Perhaps Cdc14 dependent condensin assembly is

567 shared by repeated loci that include rDNA and telomeres on chromosomes and the extra-

568 chromosomal (but chromosome associated) 2-micron plasmid. Cohesin-mediated pairing of

569 plasmid sisters (Ghosh et al., 2010; Mehta et al., 2002), in conjunction with possible condensin-

570 assisted DNA compaction, may promote the organization of replicated plasmid molecules into

571 two equally populated sister clusters that tether symmetrically to sister chromatids. Such a

572 mechanism is consistent with the segregation pattern observed for single-copy *STB* plasmids

573 whose sister copies segregate one-to-one in most cells (Ghosh et al., 2007; Liu et al., 2016; Liu

574 et al., 2014). Condensin associated with *STB* may also serve to recruit Topo II to the plasmid

575 and/or assist decatenation of plasmid sisters. Topo II inactivation causes an accumulation of

576 replicated 2-micron plasmids as catenanes (DiNardo et al., 1984).

577

578 **Hitchhiking on host chromosomes by selfish DNA elements: choice of tethering sites**

579 The 2-micron plasmid resembles viral episomes in infected mammalian cells in hitchhiking on

580 chromosomes (Kanda et al., 2007; Nanbo et al., 2007; Coursey & McBride, 2019; Sau et al.,

581 2019) even though their respective hosts are separated in evolution by ~1.5 billion years. Given

582 the high fidelity of chromosome dissemination to daughter cells, it is not surprising that the yeast

583 plasmid and mammalian viruses have converged on the common strategy of exploiting the

584 host's chromosome segregation machinery for self-preservation. The telomere- and

585 centromere-proximal localization of the 2-micron plasmid in mitotic cells suggest a propensity for

586 plasmid tethering sites to be embedded in chromosome regions sparsely populated by genes or

587 those organized into silent chromatin. Such localization would not only minimize fitness costs to

588 the host but would also be advantageous to the plasmid. On the one hand, the host would be

589 largely protected against perturbations to gene functions; on the other, the probability of plasmid

590 dislodgement from the chromosome due to gene activity would be small.

591 Strikingly, the tethering sites on mammalian chromosomes for viral episomes also

592 appear to be enriched for condensed chromatin (Aydin & Schelhaas, 2016). The

593 heterochromatin regions that the episomes localize to include pericentromeric, peritelomeric and

594 rDNA loci (Griffiths & Whitehouse, 2007; Kelley-Clarke et al., 2007; Krithivas et al., 2002;

595 Oliveira et al., 2006; Poddar et al., 2009; Sekhar et al., 2010). A recent genome-wide Hi-C

596 analysis has identified repressive chromatin as preferred tethering sites for Epstein-Barr virus

597 (Moquin et al., 2017). Thus, the logic of associating with chromosomes for long-term

598 persistence with as little disturbance to host genome structure and homeostasis as possible

599 appears to be preserved among highly diverse eukaryotic selfish DNA elements.

600

601

602   **Materials and methods**

603

604   **Yeast strains and plasmids**

605   The yeast strains used in this study (W303 background) and their relevant genotypes are listed

606   in Table S1. Strains containing or lacking the native 2-micron plasmid are referred to as [Cir$^+$] or

607   [Cir^0], respectively. The [Cir$^+$] designation does not include [Cir^0] strains transformed with 2-

608   micron derived or other artificial plasmid constructs. In the strains for chromatin

609   immunoprecipitation (ChIP) assays, the *BRN1* locus on chromosome II was tagged with 6-HA

610   by inserting a PCR amplified DNA fragment containing the epitope tag via homologous

611   recombination (Janke et al., 2004). Gene fusion and expression of the tagged proteins were

612   verified by PCR using total extracted DNA as template, and by immunostaining chromatin

613   spreads with HA-antibody, respectively

614   The plasmid constructs employed in this work and their salient features are summarized

615   in Table S1. The plasmid pRS402CFP-LacI (*ADE2*) was obtained by replacing the coding region

616   for GFP in pRS402GFP-LacI (Velmurugan et al., 2000) with that of CFP.

617

618   **Tagging *TEL VII* with TetO**

619   CRISPR (Cas9-sgRNA) technology was used to tag *TEL VII* with a [TetO]$_n$ array in a strain

620   expressing [TetR-GFP] and containing [TetO]$_{448}$ inserted at *TEL V* (Ma et al., 2019). The PCR

621   amplified DNA containing [TetO]$_n$ (obtained from pRS306-[TetO]$_{224}$ as template) flanked by

622   chromosome homology at either end was inserted between *IMA1* and *MAL13* genes on the right

623   arm of Chr VII (~22 kbp from the end). Viable colonies obtained following transformation were

624   screened by fluorescence microscopy to identify successful integrants. Based on the sizes of

625   PCR products amplified using isolated total DNA, the number of [TetO] copies was < 50, and

25

626 varied in individual transformants. One transformant showing two green fluorescent foci

627 (bright *TEL V* and faint *TEL VII*) in most individual cells was saved for further analysis.

628

629 **Cell cycle synchronization**

630 Cells were arrested in G1/S with α-factor, and released into the cell cycle by washing off the

631 pheromone. Reporter plasmids were localized in the arrested cells and following their release.

632 Cells harvested at intervals during cell cycle progression were examined by microscopy.

633 Metaphase and anaphase cells were identified by their characteristic morphological features, as

634 described previously (Cui et al., 2009; Ghosh et al., 2007).

635

636 **Plasmid stability assays**

637 Cultures of transformant colonies containing a reporter plasmid were grown overnight in

638 selective liquid medium, and were diluted into YPDA medium (non-selective). The inocula were

639 grown for 'n' generations in non-selective media (n varied from 5 to 10, depending on the

640 experiment). The fractions of plasmid containing cells in the population at the start (f_0) and at the

641 end (f_n) of growth in the non-selective media were estimated by plating equal aliquots of the

642 cultures on selective and non-selective plates. The plasmid loss rate per generation (%) was

643 estimated as 'i' = $(1/n) \times \ln(f_0/f_n)$ (Murray & Cesareni, 1986). The average values were plotted in

644 a graph where error bars represented the standard deviation from the mean values acquired

645 from three independent experiments. p-values were calculated using *t*-test (assuming unequal

646 variances) after comparing the values from WT and *cdc14-3*.

647

648 **Plasmid segregation under induced missegregation of chromosomes**

649 For inducing chromosome III or XII to missegregate in galactose medium, the *GAL1* promoter

650 was inserted immediately upstream of *CEN III* or *CEN XII* as described previously (Reid et al.,

651   2008). Cells harboring the *GAL-CEN* cassette were grown till mid-log phase in SC (-Leu, -Trp,

652   raffinose) medium at 30°C before being transferred to SC (-Leu,-Trp) medium supplemented

653   with either 2% galactose or 2% glucose for 5 hr at 30°C. Cells were harvested, stained with

654   DAPI, and reporter plasmids ([LacO]-[GFP-LacI]) and rDNA (DsRed-Nop1) were observed by

655   fluorescence microscopy to follow the segregation pattern of plasmid with respect to rDNA. The

656   average values were plotted in a graph where error bars represented the standard deviation

657   from the mean values acquired from three independent experiments.

658

659   **Monohybrid and di-hybrid assays**

660   The monohybrid assay was performed as described earlier (Prajapati et al., 2017) to detect the

661   interaction between *STB* locus and Brn1. The experimental strain was engineered to express

662   *BRN1*-AD (AD = *GAL4* activation domain), and harbored *STB* placed upstream of the *HIS3*

663   reporter locus as its UAS. Enhanced *HIS3* transcription as a result of Brn1-*STB* interaction

664   (revealed by growth on medium lacking histidine) was assayed by inhibiting the His3 activity

665   resulting from basal expression with 40 mM 3-AT (3-amino-1,2,4-triazole).

666   In the strain for di-hybrid assays (Finley et al., 1996), the bait protein was expressed as

667   a fusion to LexA DNA binding domain, and LexO was integrated upstream of the *LEU2* reporter

668   gene. A prey protein to be tested was fused to the B42 transcription activation domain, and was

669   expressed by galactose induction from the *GAL1* promoter. The interaction between the bait

670   and its putative prey was certified by colony growth in the absence of leucine. A positive

671   response was verified by reciprocally swapping the bait and prey in the fusion proteins.

672   Expression of the activation domain alone (without fusion to the bait) provided the negative

673   control. Physical interaction between Rep1 and Rep2 was used as positive control for the

674   assay.

675

27

676 **Chromatin immunoprecipitation assays**

677 Chromatin immunoprecipitation (ChIP) assays were performed as described previously

678 (Prajapati et al., 2018; Verzijlbergen et al., 2014). Brn1 fused to 6XHA at the carboxyl-terminus

679 was immunoprecipitated using a polyclonal antibody to HA (Rabbit polyclonal HA11, Abcam,

680 UK). The specificity of the association was verified using a chromosomal locus '*TUB2*'

681 designated to be weak or negative in condensin association (Wang et al., 2005). The relative

682 amounts of immunoprecipitated DNA were quantitated using qPCR (Prajapati et al., 2018).

683 Corrections were applied to account for primer efficiencies below 100% (amplification factors <

684 2.0) using standardization graphs of CT values against dilutions of the input DNA. The

685 amplification factor ε was estimated as $10^{(-1/slope)}$ of the regression line, and the primer

686 efficiency E (%) as $\{[10^{(-1/slope)}] - 1\} \times 100$. The fraction of immunoprecipitated DNA in a

687 ChIP sample relative to the input DNA was calculated as $\varepsilon^{(-\Delta CT)}$, $\Delta CT = CT (ChIP) - [CT$

688 $(Input) - \log_{\varepsilon}(Input\ dilution\ factor)]$. The average values were plotted in a graph where error bars

689 represented the standard deviation from the mean values acquired from three independent

690 experiments. p-values were calculated using *t*-test (assuming unequal variances) after

691 comparing the values from WT and *cdc14-3*.

692

693 **Fluorescence microscopy and distance measurement**

694 Fluorescence microscopy was performed in live or mildly fixed cells. Fixing was performed in *p*-

695 formaldehyde (4% v/v) by incubating on ice for 5-10 min. After two washes with 0.1 M

696 phosphate buffer (pH 7.4), cells were imaged using a Zeiss Axio Observer Z1 fluorescence

697 microscope and the Axiovision software. Images were acquired using the z-stack mode, with a

698 0.20 μm interval between two successive planes (Bystricky et al., 2005). They were opened in

699 Imaris software (Bitplane, Imaris 8.0.2), and 'slice tool' was utilized to measure the spacing

700 between the centroids of two fluorescent foci (Mittal et al., 2020). The distances were grouped

701 into two types, ≤ 0.5 μm and > 0.5 μm. The average values were plotted in a graph where error

702 bars represented the standard deviation from the mean values acquired from three independent

703 experiments.

704

Acknowledgements

712

713 **Conflict of Interest:** The authors declare that they have no conflict of interest.

714

References

716 A. Rizvi, S. M., Prajapati, H. K., Nag, P., & Ghosh, S. K. (2017). The 2-μm plasmid encoded
717   protein Raf1 regulates both stability and copy number of the plasmid by blocking the
718   formation of the Rep1–Rep2 repressor complex. *Nucleic Acids Res, 45*(12), 7167-7179.
719   https://doi.org/10.1093/nar/gkx316
720 Alexandru, G., Uhlmann, F., Mechtler, K., Poupart, M.-A., & Nasmyth, K. (2001).
721   Phosphorylation of the Cohesin Subunit Scc1 by Polo/Cdc5 Kinase Regulates Sister
722   Chromatid Separation in Yeast. *Cell, 105*(4), 459-472.
723   https://doi.org/10.1016/S0092-8674(01)00362-2
724 Autiero, M., Camarca, A., Ciullo, M., Debily, M. A., El Marhomy, S., Pasquinelli, R., Capasso, I.,
725   D'Aiuto, G., Anzisi, A. M., & Piatier-Tonneau, D. (2002). Intragenic amplification and
726   formation of extrachromosomal small circular DNA molecules from the PIP gene on
727   chromosome 7 in primary breast carcinomas. *Int J Cancer, 99*(3), 370-377.
728 Aydin, I., & Schelhaas, M. (2016). Viral Genome Tethering to Host Cell Chromatin: Cause and
729   Consequences. *Traffic, 17*(4), 327-340.
730   https://doi.org/10.1111/tra.12378
731 Biggins, S. (2013). The Composition, Functions, and Regulation of the Budding Yeast
732   Kinetochore. *Genetics, 194*(4), 817.
733   https://doi.org/10.1534/genetics.112.145276

734   Brachmann, C. B., Davies, A., Cost, G. J., Caputo, E., Li, J., Hieter, P., & Boeke, J. D. (1998).
735   Designer deletion strains derived from Saccharomyces cerevisiae S288C: a useful set of
736   strains and plasmids for PCR-mediated gene disruption and other applications. *Yeast,*
737   *14*(2), 115-132.
738   https://doi.org/10.1002/(SICI)1097-0061(19980130)14:2<115::AID-YEA204>3.0.CO;2-2
739   Briggs, S. D., Bryk, M., Strahl, B. D., Cheung, W. L., Davie, J. K., Dent, S. Y., Winston, F., &
740   Allis, C. D. (2001). Histone H3 lysine 4 methylation is mediated by Set1 and required for
741   cell growth and rDNA silencing in Saccharomyces cerevisiae. *Genes Dev, 15*(24), 3286-
742   3295.
743   https://doi.org/10.1101/gad.940201
744   Broach, J. R. (1982). The yeast plasmid 2 mu circle. *Cell, 28*(2), 203-204.
745   https://doi.org/10.1016/0092-8674(82)90337-3
746   Broach, J. R., & Volkert, F. C. (1991). 6 Circular DNA Plasmids of Yeasts. *Cold Spring Harbor*
747   *Monograph Archive, 21*, 297-331.
748   http://dx.doi.org/10.1101/0.297-331
749   Bystricky, K., Laroche, T., van Houwe, G., Blaszczyk, M., & Gasser, S. M. (2005). Chromosome
750   looping in yeast: telomere pairing and coordinated movement reflect anchoring efficiency
751   and territorial organization. *J Cell Biol, 168*(3), 375-387.
752   https://doi.org/10.1083/jcb.200409091
753   Charbin, A., Bouchoux, C., & Uhlmann, F. (2014). Condensin aids sister chromatid decatenation
754   by topoisomerase II. *Nucleic Acids Res, 42*(1), 340-348.
755   https://doi.org/10.1093/nar/gkt882
756   Chen, X. L., Reindle, A., & Johnson, E. S. (2005). Misregulation of 2μm circle copy number in a
757   SUMO pathway mutant. *Mol Cell Biol, 25*(10), 4311-4320.
758   https://dx.doi.org/10.1128/2FMCB.25.10.4311-4320.2005
759   Chu, S. (1998). The transcriptional program of sporulation in budding yeast (vol 282, pg 699,
760   1998). *Science, 282*(5393), 1421-1421.
761   https://doi.org/10.1126/science.282.5389.699
762   Chua, P. R., & Roeder, G. S. (1997). Tam1, a telomere-associated meiotic protein, functions in
763   chromosome synapsis and crossover interference. *Genes Dev, 11*(14), 1786-1800.
764   https://doi.org/10.1101/gad.11.14.1786
765   Clemente-Blanco, A., Sen, N., Mayan-Santos, M., Sacristan, M. P., Graham, B., Jarmuz, A.,
766   Giess, A., Webb, E., Game, L., Eick, D., Bueno, A., Merkenschlager, M., & Aragon, L.
767   (2011). Cdc14 phosphatase promotes segregation of telomeres through repression of
768   RNA polymerase II transcription. *Nat Cell Biol, 13*(12), 1450-1456.
769   https://doi.org/10.1038/ncb2365
770   Cohen, S., Regev, A., & Lavi, S. (1997). Small polydispersed circular DNA (spcDNA) in human
771   cells: association with genomic instability. *Oncogene, 14*(8), 977-985.
772   https://doi.org/10.1038/sj.onc.1200917
773   Cohen, S., & Segal, D. (2009). Extrachromosomal circular DNA in eukaryotes: possible
774   involvement in the plasticity of tandem repeats. *Cytogenet Genome Res, 124*(3-4), 327-
775   338.
776   https://doi.org/10.1159/000218136
777   Conrad, M. N., Dominguez, A. M., & Dresser, M. E. (1997). Ndj1p, a meiotic telomere protein
778   required for normal chromosome synapsis and segregation in yeast. *Science,*
779   *276*(5316), 1252-1255.
780   https://doi.org/10.1126/science.276.5316.1252
781   Coursey, T. L., & McBride, A. A. (2019). Hitchhiking of Viral Genomes on Cellular
782   Chromosomes. *Annu Rev Virol, 6*(1), 275-296.
783   https://doi.org/10.1146/annurev-virology-092818-015716

784   Cui, H., Ghosh, S. K., & Jayaram, M. (2009). The selfish yeast plasmid uses the nuclear motor
785   Kip1p but not Cin8p for its localization and equal segregation. *J Cell Biol, 185*(2), 251-
786   264.
787   https://doi.org/10.1083/jcb.200810130
788   D'Amours, D., Stegmeier, F., & Amon, A. (2004). Cdc14 and condensin control the dissolution of
789   cohesin-independent chromosome linkages at repeated DNA. *Cell, 117*(4), 455-469.
790   https://doi.org/10.1016/s0092-8674(04)00413-1
791   DiNardo, S., Voelkel, K., & Sternglanz, R. (1984). DNA topoisomerase II mutant of
792   Saccharomyces cerevisiae: topoisomerase II is required for segregation of daughter
793   molecules at the termination of DNA replication.*PNAS, 81*(9), 2616-2620.
794   https://dx.doi.org/10.1073/pnas.81.9.2616
795   Fennell, A., Fernández-Álvarez, A., Tomita, K., & Cooper, J. P. (2015). Telomeres and
796   centromeres have interchangeable roles in promoting meiotic spindle formation. *J Cell
797   Biol , 208*(4), 415-428.
798   https://dx.doi.org/10.1083/jcb.201409058
799   Finley, R. L., Thomas, B. J., Zipursky, S. L., & Brent, R. (1996). Isolation of Drosophila cyclin D,
800   a protein expressed in the morphogenetic furrow before entry into S phase.*PNAS, 93*(7),
801   3011-3015.
802   https://dx.doi.org/10.1073/2Fpnas.93.7.3011
803   Frappier, L. (2004). Viral plasmids in mammalian cells. In *Plasmid Biology* (pp. 325-340).
804   American Society of Microbiology.
805   Chapter DOI: 10.1128/9781555817732.ch15
806   Futcher, A. B. (1986). Copy number amplification of the 2 micron circle plasmid of
807   Saccharomyces cerevisiae. *J Theor Biol, 119*(2), 197-204.
808   https://doi.org/10.1016/s0022-5193(86)80074-1
809   Futcher, A. B., & Cox, B. S. (1983). Maintenance of the 2 microns circle plasmid in populations
810   of Saccharomyces cerevisiae. *J Bacteriol, 154*(2), 612-622.
811   http://www.ncbi.nlm.nih.gov/pubmed/6341357
812   Ghosh, S. K., Hajra, S., & Jayaram, M. (2007). Faithful segregation of the multicopy yeast
813   plasmid through cohesin-mediated recognition of sisters.*PNAS, 104*(32), 13034-13039.
814   https://doi.org/10.1073/pnas.0702996104
815   Ghosh, S. K., Hajra, S., Paek, A., & Jayaram, M. (2006). Mechanisms for chromosome and
816   plasmid segregation. *Annu Rev Biochem, 75*, 211-241.
817   https://doi.org/10.1146/annurev.biochem.75.101304.124037
818   Ghosh, S. K., Huang, C. C., Hajra, S., & Jayaram, M. (2010). Yeast cohesin complex embraces
819   2 micron plasmid sisters in a tri-linked catenane complex. *Nucleic Acids Res, 38*(2), 570-
820   584.
821   https://doi.org/10.1093/nar/gkp993
822   Gotta, M., Laroche, T., Formenton, A., Maillet, L., Scherthan, H., & Gasser, S. M. (1996). The
823   clustering of telomeres and colocalization with Rap1, Sir3, and Sir4 proteins in wild-type
824   Saccharomyces cerevisiae. *J Cell Biol, 134*(6), 1349-1363.
825   https://doi.org/10.1083/jcb.134.6.1349
826   Griffiths, R., & Whitehouse, A. (2007). Herpesvirus saimiri episomal persistence is maintained
827   via interaction between open reading frame 73 and the cellular chromosome-associated
828   protein MeCP2. *J Virol, 81*(8), 4021-4032.
829   https://doi.org/10.1128/jvi.02171-06
830   Grunstein, M., & Gasser, S. M. (2013). Epigenetics in Saccharomyces cerevisiae. *Cold Spring
831   Harb Perspect Biol, 5*(7), a017491.
832   https://doi.org/10.1101/cshperspect.a017491

833 Guacci, V., Hogan, E., & Koshland, D. (1997). Centromere position in budding yeast: evidence
834   for anaphase A. *Mol Biol Cell, 8*(6), 957-972.
835   https://doi.org/10.1091/mbc.8.6.957
836 Haeusler, R. A., Pratt-Hyatt, M., Good, P. D., Gipson, T. A., & Engelke, D. R. (2008). Clustering
837   of yeast tRNA genes is mediated by specific association of condensin with tRNA gene
838   transcription complexes. *Genes Dev, 22*(16), 2204-2214.
839   https://doi.org/10.1101/gad.1675908
840 Hajra, S., Ghosh, S. K., & Jayaram, M. (2006). The centromere-specific histone variant Cse4p
841   (CENP-A) is essential for functional chromatin architecture at the yeast 2-microm circle
842   partitioning locus and promotes equal plasmid segregation. *J Cell Biol, 174*(6), 779-790.
843   https://doi.org/10.1083/jcb.200603042
844 Hayes, F., & Barilla, D. (2006). The bacterial segrosome: a dynamic nucleoprotein machine for
845   DNA trafficking and segregation [Review Article]. *Nat Rev Microbiol, 4*(2), 133-143.
846   https://doi.org/10.1038/nrmicro1342
847 Heun, P., Laroche, T., Raghuraman, M. K., & Gasser, S. M. (2001a). The positioning and
848   dynamics of origins of replication in the budding yeast nucleus. *J Cell Biol, 152*(2), 385-
849   400.
850   http://www.ncbi.nlm.nih.gov/pubmed/11266454
851 Heun, P., Laroche, T., Shimada, K., Furrer, P., & Gasser, S. M. (2001b). Chromosome
852   dynamics in the yeast interphase nucleus. *Science, 294*(5549), 2181-2186.
853   https://doi.org/10.1126/science.1065366
854 Hill, A., & Bloom, K. (1989). Acquisition and processing of a conditional dicentric chromosome in
855   Saccharomyces cerevisiae. *Mol Cell Biol, 9*(3), 1368-1370.
856   https://doi.org/10.1128/mcb.9.3.1368
857 Huang, C. C., Chang, K. M., Cui, H., & Jayaram, M. (2011). Histone H3-variant Cse4-induced
858   positive DNA supercoiling in the yeast plasmid has implications for a plasmid origin of a
859   chromosome centromere.*PNAS, 108*(33), 13671-13676.
860   https://doi.org/10.1073/pnas.1101944108
861 Huang, Y., Xu, L., Sun, Y., & Nabel, G. J. (2002). The assembly of Ebola virus nucleocapsid
862   requires virion-associated proteins 35 and 24 and posttranslational modification of
863   nucleoprotein. *Mol Cell, 10*(2), 307-316.
864   https://doi.org/10.1016/s1097-2765(02)00588-9
865 Hughes, J. E., & Welker, D. L. (1999). Nuclear plasmids of Dictyostelium. *Genet Eng (N Y), 21*,
866   1-14.
867   https://doi.org/10.1007/978-1-4615-4707-5_1
868 Janke, C., Magiera, M. M., Rathfelder, N., Taxis, C., Reber, S., Maekawa, H., Moreno-Borchart,
869   A., Doenges, G., Schwob, E., & Schiebel, E. (2004). A versatile toolbox for PCR-based
870   tagging of yeast genes: new fluorescent proteins, more markers and promoter
871   substitution cassettes. *Yeast, 21*(11), 947-962.
872   https://doi.org/10.1002/yea.1142
873 Jin, Q.-W., Fuchs, J., & Loidl, J. (2000). Centromere clustering is a major determinant of yeast
874   interphase nuclear organization. *J Cell Sci, 113*(11), 1903-1912.
875   http://www.ncbi.nlm.nih.gov/pubmed/10806101
876 Jin, Q.-w., Trelles-Sticken, E., Scherthan, H., & Loidl, J. (1998). Yeast nuclei display prominent
877   centromere clustering that is reduced in nondividing cells and in meiotic prophase. *J Cell
878   Biol, 141*(1), 21-29.
879   https://doi.org/10.1083/jcb.141.1.21
880 Kanda, T., Kamiya, M., Maruo, S., Iwakiri, D., & Takada, K. (2007). Symmetrical localization of
881   extrachromosomally replicating viral genomes on sister chromatids. *J Cell Sci, 120*(Pt 9),

882   1529-1539.
883   https://doi.org/10.1242/jcs.03434
884 Kelley-Clarke, B., Ballestas, M. E., Komatsu, T., & Kaye, K. M. (2007). Kaposi's sarcoma
885   herpesvirus C-terminal LANA concentrates at pericentromeric and peri-telomeric regions
886   of a subset of mitotic chromosomes. *Virology, 357*(2), 149-157.
887   https://doi.org/10.1016/j.virol.2006.07.052
888 Khmelinskii, A., & Schiebel, E. (2008). Assembling the spindle midzone in the right place at the
889   right time. *Cell Cycle, 7*(3), 283-286.
890   https://doi.org/10.4161/cc.7.3.5349
891 Krithivas, A., Fujimuro, M., Weidner, M., Young, D. B., & Hayward, S. D. (2002). Protein
892   interactions targeting the latency-associated nuclear antigen of Kaposi's sarcoma-
893   associated herpesvirus to cell chromosomes. *J Virol, 76*(22), 11596-11604.
894   https://dx.doi.org/10.1128/JVI.76.22.11596-11604.2002
895 Kruitwagen, T., Chymkowitch, P., Denoth-Lippuner, A., Enserink, J., & Barral, Y. (2018).
896   Centromeres License the Mitotic Condensation of Yeast Chromosome Arms. *Cell,*
897   *175*(3), 780-795 e715.
898   https://doi.org/10.1016/j.cell.2018.09.012
899 Kueng, S., Oppikofer, M., & Gasser, S. M. (2013). SIR proteins and the assembly of silent
900   chromatin in budding yeast. *Annu Rev Genet, 47*, 275-306.
901   https://doi.org/10.1146/annurev-genet-021313-173730
902 Kupiec, M. (2014). Biology of telomeres: lessons from budding yeast. *FEMS Microbiol Rev,*
903   *38*(2), 144-171.
904   https://doi.org/10.1111/1574-6976.12054
905 Lavoie, B. D., Hogan, E., & Koshland, D. (2004). In vivo requirements for rDNA chromosome
906   condensation reveal two cell-cycle-regulated pathways for mitotic chromosome folding.
907   *Genes Dev, 18*(1), 76-87.
908   https://doi.org/10.1101/gad.1150404
909 Lefrancois, P., Auerbach, R. K., Yellman, C. M., Roeder, G. S., & Snyder, M. (2013).
910   Centromere-like regions in the budding yeast genome. *PLoS Genet, 9*(1), e1003209.
911   https://doi.org/10.1371/journal.pgen.1003209
912 Liu, Y. T., Chang, K. M., Ma, C. H., & Jayaram, M. (2016). Replication-dependent and
913   independent mechanisms for the chromosome-coupled persistence of a selfish genome.
914   *Nucleic Acids Res, 44*(17), 8302-8323.
915   https://doi.org/10.1093/nar/gkw694
916 Liu, Y. T., Ma, C. H., & Jayaram, M. (2013). Co-segregation of yeast plasmid sisters under
917   monopolin-directed mitosis suggests association of plasmid sisters with sister
918   chromatids. *Nucleic Acids Res, 41*(7), 4144-4158.
919   https://doi.org/10.1093/nar/gkt096
920 Liu, Y. T., Sau, S., Ma, C. H., Kachroo, A. H., Rowley, P. A., Chang, K. M., Fan, H. F., &
921   Jayaram, M. (2014). The partitioning and copy number control systems of the selfish
922   yeast plasmid: an optimized molecular design for stable persistence in host cells.
923   *Microbiol Spectr, 2*(5).
924   https://doi.org/10.1128/microbiolspec.PLAS-0003-2013
925 Ma, C.-H., Cui, H., Hajra, S., Rowley, P. A., Fekete, C., Sarkeshik, A., Ghosh, S. K., Yates III, J.
926   R., & Jayaram, M. (2012). Temporal sequence and cell cycle cues in the assembly of
927   host factors at the yeast 2 micron plasmid partitioning locus. *Nucleic Acids Res, 41*(4),
928   2340-2353.
929   http://doi.org/10.1093/nar/gks1338
930 Ma, C.-H., Su, B.-Y., Maciaszek, A., Fan, H.-F., Guga, P., & Jayaram, M. (2019). A Flp-SUMO
931   hybrid recombinase reveals multi-layered copy number control of a selfish DNA element

33

932   through post-translational modification. *PLoS Genet, 15*(6), e1008193.
933   https://doi.org/10.1371/journal.pgen.1008193
934 Ma, C. H., Cui, H., Hajra, S., Rowley, P. A., Fekete, C., Sarkeshik, A., Ghosh, S. K., Yates, J.
935   R., 3rd, & Jayaram, M. (2013). Temporal sequence and cell cycle cues in the assembly
936   of host factors at the yeast 2 micron plasmid partitioning locus. *Nucleic Acids Res, 41*(4),
937   2340-2353.
938   https://doi.org/10.1093/nar/gks1338
939 Machin, F., Quevedo, O., Ramos-Perez, C., & Garcia-Luis, J. (2016). Cdc14 phosphatase:
940   warning, no delay allowed for chromosome segregation! *Curr Genet, 62*(1), 7-13.
941   https://doi.org/10.1007/s00294-015-0502-1
942 Malik, H. S., & Henikoff, S. (2009). Major evolutionary transitions in centromere complexity. *Cell,
943   138*(6), 1067-1082.
944   https://doi.org/10.1016/j.cell.2009.08.036
945 Marston, A. L., Lee, B. H., & Amon, A. (2003). The Cdc14 phosphatase and the FEAR network
946   control meiotic spindle disassembly and chromosome segregation. *Dev Cell, 4*(5), 711-
947   726.
948   https://doi.org/10.1016/S1534-5807(03)00130-8
949 McBride, A. A. (2008). Replication and partitioning of papillomavirus genomes. *Adv Virus Res,
950   72*, 155-205.
951   https://doi.org/10.1016/S0065-3527(08)00404-1
952 Mead, D. J., Gardner, D. C., & Oliver, S. G. (1986). The yeast 2 µ plasmid: strategies for the
953   survival of a selfish DNA. *Mol Gen Genet 205*(3), 417-421.
954   https://doi.org/10.1007/BF00338076
955 Mehta, S., Yang, X. M., Chan, C. S., Dobson, M. J., Jayaram, M., & Velmurugan, S. (2002). The
956   2 micron plasmid purloins the yeast cohesin complex: a mechanism for coupling plasmid
957   partitioning and chromosome segregation? *J Cell Biol, 158*(4), 625-637.
958   https://doi.org/10.1083/jcb.200204136
959 Mehta, S., Yang, X. M., Jayaram, M., & Velmurugan, S. (2005). A novel role for the mitotic
960   spindle during DNA segregation in yeast: promoting 2 microm plasmid-cohesin
961   association. *Mol Cell Biol, 25*(10), 4283-4298.
962   https://doi.org/10.1128/MCB.25.10.4283-4298.2005
963 Michaelis, C., Ciosk, R., & Nasmyth, K. (1997). Cohesins: chromosomal proteins that prevent
964   premature separation of sister chromatids. *Cell, 91*(1), 35-45.
965   https://doi.org/10.1016/s0092-8674(01)80007-6
966 Mittal P., Ghule K., Trakroo D., Prajapati H.K., & Ghosh, S.K. (2020). Meiosis-specific functions
967   of kinesin motors in cohesin removal and maintenance of chromosome integrity in
968   budding yeast. *Mol Cell Biol*; 10.1128/MCB.00386-19.
969   https://doi.org/10.1128/MCB.00386-19
970 Møller, H. D., Parsons, L., Jørgensen, T. S., Botstein, D., & Regenberg, B. (2015).
971   Extrachromosomal circular DNA is common in yeast. *PNAS, 112*(24), E3114-E3122.
972   https://doi.org/10.1073/pnas.1508825112
973 Moquin, S. A., Thomas, S., Whalen, S., Warburton, A., Fernandez, S. G., McBride, A. A.,
974   Pollard, K. S., & Miranda, J. J. L. (2017). The Epstein-Barr virus episome maneuvers
975   between nuclear chromatin compartments during reactivation. *J Virol*.
976   https://doi.org/10.1128/jvi.01413-17
977 Murray, J. A., & Cesareni, G. (1986). Functional analysis of the yeast plasmid partition locus
978   STB. *The EMBO journal, 5*(12), 3391-3399.
979   http://www.ncbi.nlm.nih.gov/pubmed/16453734

980   Murray, J. A., Scarpa, M., Rossi, N., & Cesareni, G. (1987). Antagonistic controls regulate copy
981   number of the yeast 2 mu plasmid. *The EMBO journal, 6*(13), 4205-4212.
982   http://www.ncbi.nlm.nih.gov/pubmed/2832156
983   Mythreye, K., & Bloom, K. S. (2003). Differential kinetochore protein requirements for
984   establishment versus propagation of centromere activity in Saccharomyces cerevisiae. *J
985   Cell Biol, 160*(6), 833-843.
986   https://doi.org/10.1083/jcb.200211116
987   Nanbo, A., Sugden, A., & Sugden, B. (2007). The coupling of synthesis and partitioning of
988   EBV's plasmid replicon is revealed in live cells. *The EMBO journal, 26*(19), 4252-4262.
989   https://doi.org/10.1038/sj.emboj.7601853
990   Ohkuni, K., & Kitagawa, K. (2012). Role of transcription at centromeres in budding yeast.
991   *Transcription, 3*(4), 193-197.
992   https://doi.org/10.4161/trns.20884
993   Oliveira, J. G., Colf, L. A., & McBride, A. A. (2006). Variations in the association of
994   papillomavirus E2 proteins with mitotic chromosomes.*PNAS, 103*(4), 1047-1052.
995   https://doi.org/10.1073/pnas.0507624103
996   Ouspenski, I. I., Cabello, O. A., & Brinkley, B. R. (2000). Chromosome condensation factor
997   Brn1p is required for chromatid separation in mitosis. *Mol Biol Cell, 11*(4), 1305-1313.
998   https://doi.org/10.1091/mbc.11.4.1305
999   Petes, T. D., & Williamson, D. H. (1994). A novel structural form of the 2 micron plasmid of the
1000   yeast Saccharomyces cerevisiae. *Yeast, 10*(10), 1341-1345.
1001   https://doi.org/10.1002/yea.320101011
1002   Poddar, A., Reed, S. C., McPhillips, M. G., Spindler, J. E., & McBride, A. A. (2009). The human
1003   papillomavirus type 8 E2 tethering protein targets the ribosomal DNA loci of host mitotic
1004   chromosomes. *J Virol, 83*(2), 640-650.
1005   https://doi.org/10.1128/jvi.01936-08
1006   Prajapati, H. K., Agarwal, M., Mittal, P., & Ghosh, S. K. (2018). Evidence of Zip1 Promoting
1007   Sister Kinetochore Mono-orientation During Meiosis in Budding Yeast. *G3 (Bethesda,
1008   Md.), 8*(11), 3691-3701.
1009   https://doi.org/10.1534/g3.118.200469
1010   Prajapati, H. K., Rizvi, S. M. A., Rathore, I., & Ghosh, S. K. (2017). Microtubule-associated
1011   proteins, Bik1 and Bim1, are required for faithful partitioning of the endogenous 2 micron
1012   plasmids in budding yeast. *Mol Microbiol, 103*(6), 1046-1064.
1013   https://doi.org/10.1111/mmi.13608
1014   Primig, M., Williams, R. M., Winzeler, E. A., Tevzadze, G. G., Conway, A. R., Hwang, S. Y.,
1015   Davis, R. W., & Esposito, R. E. (2000). The core meiotic transcriptome in budding
1016   yeasts. *Nat Genet, 26*(4), 415-423.
1017   https://doi.org/10.1038/82539
1018   Rabitsch, K. P., Tóth, A., Gálová, M., Schleiffer, A., Schaffner, G., Aigner, E., Rupp, C.,
1019   Penkner, A. M., Moreno-Borchart, A. C., & Primig, M. (2001). A screen for genes
1020   required for meiosis and spore formation based on whole-genome expression. *Curr Biol,
1021   11*(13), 1001-1009.
1022   https://doi.org/10.1016/s0960-9822(01)00274-3
1023   Reid, R. J., Sunjevaric, I., Voth, W. P., Ciccone, S., Du, W., Olsen, A. E., Stillman, D. J., &
1024   Rothstein, R. (2008). Chromosome-scale genetic mapping using a set of 16 conditionally
1025   stable Saccharomyces cerevisiae chromosomes. *Genetics, 180*(4), 1799-1808.
1026   https://dx.doi.org/10.1534/Fgenetics.108.087999
1027   Reynolds, A. E., Murray, A. W., & Szostak, J. W. (1987). Roles of the 2 microns gene products
1028   in stable maintenance of the 2 microns plasmid of Saccharomyces cerevisiae.*Mol Cell

1029   *Biol, 7*(10), 3566-3573.
1030   https://doi.org/10.1128/mcb.7.10.3566
1031 Rizvi, S. M. A., Prajapati, H. K., & Ghosh, S. K. (2018). The 2 micron plasmid: a selfish genetic
1032   element with an optimized survival strategy within Saccharomyces cerevisiae. *Curr*
1033   *Genet, 64*(1), 25-42.
1034   https://doi.org/10.1007/s00294-017-0719-2
1035 Sau, S., Conrad, M. N., Lee, C. Y., Kaback, D. B., Dresser, M. E., & Jayaram, M. (2014). A
1036   selfish DNA element engages a meiosis-specific motor and telomeres for germ-line
1037   propagation. *J Cell Biol, 205*(5), 643-661.
1038   https://doi.org/10.1083/jcb.201312002
1039 Sau, S., Ghosh, S. K., Liu, Y. T., Ma, C. H., & Jayaram, M. (2019). Hitchhiking on
1040   chromosomes: A persistence strategy shared by diverse selfish DNA elements. *Plasmid,*
1041   *102*, 19-28.
1042   https://doi.org/10.1016/j.plasmid.2019.01.004
1043 Sau, S., Liu, Y. T., Ma, C. H., & Jayaram, M. (2015). Stable persistence of the yeast plasmid by
1044   hitchhiking on chromosomes during vegetative and germ-line divisions of host cells. *Mob*
1045   *Genet Elements, 5*(2), 1-8.
1046   https://doi.org/10.1080/2159256x.2015.1031359
1047 Scott-Drew, S., & Murray, J. (1998). Localisation and interaction of the protein components of
1048   the yeast 2 mu circle plasmid partitioning system suggest a mechanism for plasmid
1049   inheritance. *J Cell Sci, 111*(13), 1779-1789.
1050   http://www.ncbi.nlm.nih.gov/pubmed/9625741
1051 Sekhar, V., Reed, S. C., & McBride, A. A. (2010). Interaction of the betapapillomavirus E2
1052   tethering protein with mitotic chromosomes. *J Virol, 84*(1), 543-557.
1053   https://doi.org/10.1128/jvi.01908-09
1054 Sharp, J. A., Krawitz, D. C., Gardner, K. A., Fox, C. A., & Kaufman, P. D. (2003). The budding
1055   yeast silencing protein Sir1 is a functional component of centromeric chromatin. *Genes*
1056   *Dev, 17*(19), 2356-2361.
1057   https://doi.org/10.1101/gad.1131103
1058 Shibata, Y., Kumar, P., Layer, R., Willcox, S., Gagan, J. R., Griffith, J. D., & Dutta, A. (2012).
1059   Extrachromosomal microDNAs and chromosomal microdeletions in normal tissues.
1060   *Science, 336*(6077), 82-86.
1061   https://doi.org/10.1126/science.1213307
1062 Som, T., Armstrong, K. A., Volkert, F. C., & Broach, J. R. (1988). Autoregulation of 2µm circle
1063   gene expression provides a model for maintenance of stable plasmid copy levels. *Cell,*
1064   *52*(1), 27-37.
1065   https://doi.org/10.1016/0092-8674(88)90528-4
1066 Stegmeier, F., & Amon, A. (2004). Closing mitosis: the functions of the Cdc14 phosphatase and
1067   its regulation. *Annu Rev Genet, 38*, 203-232.
1068   https://doi.org/10.1146/annurev.genet.38.072902.093051
1069 Stephens, A. D., Haase, J., Vicci, L., Taylor, R. M., 2nd, & Bloom, K. (2011). Cohesin,
1070   condensin, and the intramolecular centromere loop together generate the mitotic
1071   chromatin spring. *J Cell Biol, 193*(7), 1167-1180.
1072   https://doi.org/10.1083/jcb.201103138
1073 Straight, A. F., Belmont, A. S., Robinett, C. C., & Murray, A. W. (1996). GFP tagging of budding
1074   yeast chromosomes reveals that protein-protein interactions can mediate sister
1075   chromatid cohesion. *Curr Biol, 6*(12), 1599-1608.
1076   https://doi.org/10.1016/S0960-9822(02)70783-5
1077 Sullivan, M., Higuchi, T., Katis, V. L., & Uhlmann, F. (2004). Cdc14 phosphatase induces rDNA
1078   condensation and resolves cohesin-independent cohesion during budding yeast

36

1079   anaphase. *Cell, 117*(4), 471-482.
1080   https://doi.org/10.1016/s0092-8674(04)00415-5
1081 Taddei, A., & Gasser, S. M. (2012). Structure and function in the budding yeast nucleus.
1082   *Genetics, 192*(1), 107-129.
1083   https://doi.org/10.1534/genetics.112.140608
1084 Takeo, S., Lake, C. M., Morais-de-Sá, E., Sunkel, C. E., & Hawley, R. S. (2011). Synaptonemal
1085   complex-dependent centromeric clustering and the initiation of synapsis in Drosophila
1086   oocytes. *Curr Biol, 21*(21), 1845-1851.
1087   https://doi.org/10.1016/j.cub.2011.09.044
1088 Velmurugan, S., Yang, X.-M., Chan, C. S.-M., Dobson, M., & Jayaram, M. (2000). Partitioning of
1089   the 2-μm circle plasmid of Saccharomyces cerevisiae: functional coordination with
1090   chromosome segregation and plasmid-encoded Rep protein distribution. *J Cell Biol,*
1091   *149*(3), 553-566.
1092   https://doi.org/10.1083/jcb.149.3.553
1093 Verzijlbergen, K. F., Nerusheva, O. O., Kelly, D., Kerr, A., Clift, D., de Lima Alves, F.,
1094   Rappsilber, J., & Marston, A. L. (2014). Shugoshin biases chromosomes for biorientation
1095   through condensin recruitment to the pericentromere. *eLife, 3*, e01374.
1096   https://doi.org/10.7554/eLife.01374
1097 Villasante, A., Abad, J. P., & Méndez-Lago, M. (2007). Centromeres were derived from
1098   telomeres during the evolution of the eukaryotic chromosome.*PNAS, 104*(25), 10542-
1099   10547. https://dx.doi.org/10.1073/pnas.0703808104
1100 Volkert, F. C., & Broach, J. R. (1986). Site-specific recombination promotes plasmid
1101   amplification in yeast. *Cell, 46*(4), 541-550.
1102   https://doi.org/10.1016/0092-8674(86)90879-2
1103 Wang, B. D., Eyre, D., Basrai, M., Lichten, M., & Strunnikov, A. (2005). Condensin binding at
1104   distinct and specific chromosomal sites in the Saccharomyces cerevisiae genome. *Mol*
1105   *Cell Biol, 25*(16), 7216-7225.
1106   https://doi.org/10.1128/MCB.25.16.7216-7225.2005
1107 Wong, M. C. V. L., Scott-Drew, S. R. S., Hayes, M. J., Howard, P. J., & Murray, J. A. H. (2002).
1108   RSC2, encoding a component of the RSC nucleosome remodeling complex, is essential
1109   for 2 microm plasmid maintenance in Saccharomyces cerevisiae. *Mol Cell Biol, 22*(12),
1110   4218-4229.
1111   https://doi.org/10.1128/mcb.22.12.4218-4229.2002
1112 Xiong, L., Chen, X. L., Silver, H. R., Ahmed, N. T., & Johnson, E. S. (2009). Deficient SUMO
1113   attachment to Flp recombinase leads to homologous recombination-dependent
1114   hyperamplification of the yeast 2 μm circle plasmid.*Mol Biol Cell, 20*(4), 1241-1251.
1115   https://dx.doi.org/10.1091/mbc.E08-06-0659
1116 Yong-Gonzalez, V., Wang, B.-D., Butylin, P., Ouspenski, I., & Strunnikov, A. (2007). Condensin
1117   function at centromere chromatin facilitates proper kinetochore tension and ensures
1118   correct mitotic segregation of sister chromatids. *Genes to cells : devoted to molecular &*
1119   *cellular mechanisms, 12*(9), 1075-1090.
1120   https://doi.org/10.1111/j.1365-2443.2007.01109.x
1121 Zakian, V. A., Brewer, B. J., & Fangman, W. L. (1979). Replication of each copy of the yeast 2
1122   micron DNA plasmid occurs during the S phase. *Cell, 17*(4), 923-934.
1123   https://doi.org/10.1016/0092-8674(79)90332-5

1124

1125

1126   **Figure Legends-**

1127   **Figure 1. Localization of pSG1-*CEN* plasmid with respect to *CEN V* and *TEL V* during**
1128   **different stages of the cell cycle.**

1129   **A**. The positions of pSG1-*CEN*, along with those of *CEN V* (indicated by arrows) and *TEL V*,
1130   were followed in [Cir$^+$] cells grown in glucose (to keep the *CEN* harbored by the plasmid active).
1131   Representative images from fixed cells are shown in rows at the left, and summarized in the
1132   schematic diagrams at the right. **B**. pSG1 locations proximal to a reference locus (≤ 0.5 μm) or
1133   distal from either of the two reference loci (> 0.5 μm) are shown in the plots. 'N' represents total
1134   number of cells analyzed. Error bars denote the standard deviation of the mean acquired from
1135   three separate experiments. Bar, 5 μm.

1136

1137   **Figure 1 has the following supplement figures:**

1138   **Figure 1- figure supplement 1. The functional states of *CEN* and *STB* in plasmid pSG1**
1139   **under distinct experimental contexts.**

1140   In the pSG1 plasmid, schematically diagrammed at the top, the centromere (*CEN*) is placed
1141   immediately downstream of the *GAL* promoter. The segregation status of the plasmid in a [Cir^0]
1142   or [Cir$^+$] host strain under glucose or galactose as the carbon source is tabulated below. *CEN* is
1143   active in both hosts when the promoter is turned off by glucose repression. It is inactivated by
1144   galactose-induced transcription. The Rep1 and Rep2 proteins provided by the native 2-micron
1145   circle of the [Cir$^+$] strain keep *STB* active, regardless of the carbon source. In the [Cir^0] strain,
1146   lacking Rep1 and Rep2, *STB* is inactive. In the [Cir^0]/galactose context, neither *CEN* nor *STB* is
1147   active. As a result, pSG1 segregates as an *ARS* plasmid. The active and inactive states of *CEN*
1148   or *STB* are indicated by '+' and '-', respectively.

1149

1150   **Figure 1- figure supplement 2. The localization patterns of SPB, *CEN V* and *TEL V* during**
1151   **different stages of the mitotic cell cycle.**

1152   In the experimental strain, SPB was marked with red fluorescence using Spc42 fused to m-
1153   herry. *CEN V* and *TEL V* were tagged by green fluorescence via [TetO]$_n$-[TetR-GFP] interaction.
1154   These two loci were distinguished by their differential brightness ([TetO]$_{224}$ at *CEN* and [TetO]$_{448}$
1155   at *TEL*). **A.** The representative images from fixed cells (left) and their schematic illustrations
1156   (right) denote the positions of the three nuclear landmarks at different stages of the cell cycle.

1157   The arrows and arrowheads point to *CEN V* and *TELV*, respectively. Bar, 5 μm. **B.** The

1158   histograms show distance measurements of *CEN V* and *TEL V* from SPBs that are divided into

1159   two categories (≤ 0.5 μm and > 0.5 μm). 'N' represents total number of cells analyzed. Error

1160   bars denote the standard deviation from the mean values acquired from three independent

1161   experiments.

1162

1163   **Figure 2. Preferred telomere-proximal localization of pSG1-*STB*.**

1164   The localization of pSG1-*STB* ([Cir$^+$]; galactose) with respect to *CEN V* and *TEL V* was scored

1165   in fixed cells at the G1/S (**A**) and metaphase (**C**) stages of the cell cycle. The types of plasmid

1166   localization with respect to reference loci represented by the rows of images at the left are

1167   codified in the corresponding schematic diagrams placed to the right of each row. The

1168   histogram plots in **B** and **D** are based on the data from **A** and **C**, respectively. 'N' represents

1169   total number of cells analyzed. Error bars denote the standard deviation of the mean acquired

1170   from three separate experiments. Bar, 5 μm.

1171   **Figure 2 has the following supplement figures:**

1172

1173   **Figure 2- figure supplement 1. Localization of pSG1-*ARS* in the nuclei of mitotic cells at**

1174   **the G1/S stage.**

1175   **A**. The cell images (left) and the corresponding schematic diagrams (right) represent the three

1176   localization patterns of pSG1-*ARS* assayed in [Cir^0] cells grown in galactose. **B**. The relative

1177   abundance of each pattern is shown in the histogram plot. 'N' represents total number of cells

1178   analyzed. Error bars denote the standard deviation from the mean values acquired from three

1179   independent experiments.

1180

1181   **Figure 2- figure supplement 2. Relative distances of pSG1-*STB* from *CEN V* and *TEL V***

1182   **within the 3D nuclear space.**

1183   **A**. The positioning of the centroids of the fluorescent foci by Z-series sectioning of the nucleus is

1184   schematically shown. Images were captured from the [Cir^0] experimental strain grown in glucose

1185   (pSG1-*CEN*) or galactose (pSG1-*ARS*) or the isogenic [Cir$^+$] strain grown in galactose (pSG1-

1186   *STB*). Image analysis was performed using Imaris 'Slice' tool (see Materials and Methods for

1187   details). **B**-**D**. Plasmid distances from *CEN V* and *TEL V* are shown as dot plots.

1188

1189   **Figure 2- figure supplement 3. Simultaneous localization of pSG1-*STB* with respect to**

1190   ***TEL V* and *TEL VII*.**

1191   The analysis was similar to that described in the legend to Figure 2. The pSG1-*STB* plasmid

1192   ([Cir$^+$]; galactose; [LacO]$_{256}$-[cyan-LacI]) was localized with respect to *TEL V* and *TEL VII* in fixed

1193   G1/S cells. The *TEL V* and *TEL VII* tagged by [TetO]$_n$-[TetR-GFP] were distinguished by the

1194   difference in the brightness of their fluorescence (*TEL V* >> *TEL VII*). 'N' represents total

1195   number of analyzed cells.

1196

1197   **Figure 3. Preferential localization of pSG1-*STB* near telomeres revealed at the anaphase**

1198   **stage of mitosis.**

1199   **A**. The representative images (rows at the left) depict a subset of early anaphase cells ([Cir$^+$];

1200   galactose grown) in which pSG1-*STB* was mapped with respect to well resolved *CEN V*

1201   (indicated by the arrows) and *TEL V*. The pSG1-*STB* positions were classified into three types

1202   as idealized by the schematic diagrams at the right. **B**. The plot shows the relative frequencies

1203   of the three types. 'N' represents total number of cells analyzed. Error bars denote the standard

1204   deviation of the mean acquired from two separate experiments. Bar, 5 μm.

1205

1206   **Figure 4. 2-micron plasmid segregation when Cdc14 inactivation causes missegregation**

1207   **of telomeres or rDNA.**

1208   **A**, **B**. The wild type and *cdc14-3* strains (otherwise isogenic) were arrested in G1 with α-factor at

1209   23°C, and released from arrest at 33°C. Representative images of the four cell types analyzed

1210   are shown in the left panels (pSV5-*STB*, *TELV* in **A**; pSV5-*STB*, rDNA in **B**). The histogram

1211   plots for the quantitative estimates of the cell types are shown at the right. 'N' represents total

1212   number of cells analyzed. Error bars denote the standard deviation of the mean acquired from

1213   three separate experiments. Bar, 5 μm.

1214   **Figure 4 has the following supplement figures:**

1215 **Figure 4- figure supplement 1. *ARS*-plasmid segregation when missegregation of**

1216 **telomeres or rDNA is induced by Cdc14 inactivation.**

1217 **A**, **B**. The experimental protocols were similar to those described under Figure 4, except that

1218 the reporter plasmid employed was pSV6-*ARS*. Plasmid segregation was assayed in

1219 conjunction with that of *TEL V* (**A**) or of rDNA (**B**). The images of cell types (I-IV) and histogram

1220 plots of their quantitative analysis are arranged as in Figure 4. Bar, 5 µm. 'N' represents total

1221 number of cells analyzed. Error bars denote the standard deviation from the mean values

1222 acquired from three independent experiments.

1223

1224 **Figure 4- figure supplement 2. *CEN*-plasmid segregation under Cdc14 inactivation to**

1225 **induce missegregation of telomeres and rDNA**

1226 **A**, **B**. The assays in the wild type and *cdc-14-3* strains (otherwise isogenic) were carried out as

1227 described in the legend for Figure 4 (also Figure 4- figure supplement 1) with pSV7-*CEN* as the

1228 reporter plasmid. Bar, 5 µm. 'N' represents total number of cells analyzed. Error bars denote the

1229 standard deviation from the mean values acquired from three independent experiments.

1230

1231 **Figure 4- figure supplement 3. Segregation of single copy reporter plasmids (pSG1-*STB*,**

1232 **pSG1-*CEN*, and pSG1-*ARS*) with respect to Nop1 under Cdc14 inactivation.**

1233 The partitioning status of the pSG1-reporter plasmid was manipulated as indicated in Figure 1-

1234 figure supplement 1 to obtain pSG1-*STB*, pSG1-*CEN* and pSG1-*ARS*. Segregation assays were

1235 performed at the non-permissive temperature (33°C). Segregation types (I-IV; images at the left)

1236 are quantitated in histogram plots at the right. Bar, 5µm. 'N' represents total number of cells

1237 analyzed. Error bars denote the standard deviation from the mean values acquired from three

1238 independent experiments.

1239 The correlation with Nop1 in segregation is high in the case of pSG1-*STB* (Type 1 + Type IV >>

1240 Type II + Type III), which is not the case for pSG1-*ARS* or pSG1-*CEN*. Equal segregation is

1241 high for pSG1-*CEN* (Type I + Type III >> Type II + Type IV); the opposite is true for pSG1-*ARS*

1242 (Type II + Type IV >> Type I + Type III).

1243

1244 **Figure 5. 2-micron plasmid segregation in cells missegregating either chromosome III or**
1245 **chromosome XII.**

1246 **A.** The experimental strains contained the *GAL1* promoter placed proximal to *CEN III* or *CEN*
1247 *XII* to drive high-level transcription through them under galactose induction. These strains were
1248 engineered to express GFP-LacI and Nop1-RFP for fluorescence tagging pSV5-*STB* and
1249 chromosome XII, respectively. Plasmid and chromosome segregations were assayed in
1250 anaphase cells under uninduced (glucose; *CEN III* and *CEN XII* active) or induced (galactose;
1251 *CEN III or CEN XII* inactive) conditions. The four segregation patterns analyzed (Types I-IV) are
1252 illustrated by representative cell images. **B, C.** The cell fractions showing Type I-IV segregation
1253 are plotted for *CEN III* inactivation (B) and *CEN XII* inactivation (C). 'N' represents total number
1254 of cells analyzed. Error bars denote the standard deviation of the mean acquired from three
1255 separate experiments. Bar, 5 μm.

1256

1257 **Figure 6. Missegregation of *STB*- and *CEN*-plasmids is increased in a condensin-**
1258 **defective strain relative to *ARS*-plasmids.**
1259 **A.** Plasmid loss rates were estimated after 6-7 generations of non-selective growth at 36°C in
1260 the wild type and 4-5 generations in *brn1-60* strains (Materials and Methods). **B.** The
1261 segregation patterns of the fluorescence-tagged reporter plasmids were scored in the same
1262 strains as in (A). 'N' represents total number of colonies counted in (A) and cells analyzed in (B)
1263 . Error bars denote the standard deviation from the mean values acquired from three
1264 independent experiments. p-values were calculated using *t*-test after comparing the values from
1265 WT and *brn1-60.* Bar, 5 μm.

1266

1267 **Figure 7. Brn1 associates with *STB* with the assistance of Rep proteins.**
1268 **A, B.** ChIP analyses were performed using the indicated wild type and mutant strains (Cir[+] or
1269 Cir[0]). Brn1-6HA was immunoprecipitated using an antibody to the HA-tag. The ΔCT values
1270 between an experimental sample and the input DNA were derived from qPCR data after
1271 correcting for primer efficiency/amplification factor (Verzijlbergen et al., 2014). ChIP efficiency
1272 was quantitated as the fraction of the input DNA that was immunoprecipitated [ε^(-ΔCT)], where
1273 ε is the amplification factor). The *TUB2* locus was used as a negative control (no Brn1 binding).
1274 Error bars denote the standard deviation from the mean values acquired from three independent

1275   experiments with minimum two technical replicates for each sample. p-values were calculated

1276   using *t*-test after comparing the values from WT and *cdc14-3*.

1277

1278   **Figure 7 has the following supplement figures:**

1279   **Figure 7- figure supplement 1. In a monohybrid assay, Brn1 interacts with the *STB* locus.**

1280   The reporter construct for the monohybrid, schematically illustrated at the top, includes the *STB*

1281   locus as an artificial UAS (Upstream activating sequence) of the *HIS3* gene expressed from its

1282   native promoter. A test protein was expressed as a fusion to the *GAL4* activation domain under

1283   the control of the constitutive *ADH* promoter from a 2-micron derived plasmid vector (carrying

1284   the *LEU2* marker). The left and right columns show growth on plates lacking leucine and

1285   histidine in the absence and presence of 40 mM 3-AT (3-amino 1,2,4-triazole). The assays were

1286   performed in isogenic strains containing the 2-micron plasmid ([Cir$^+$]) (**A**) or lacking it ([Cir^0] (**B**).

1287   The latter strain lacks Rep1 and Rep2 expressed from the endogenous plasmid. Rep1, which is

1288   known to interact with *STB* (Sengupta et al., 2001) served as a positive control. The negative

1289   control is labeled 'VA', for vector alone.

1290

1291   **Figure 7- figure supplement 2. Brn1 interacts with Rep1 and Rep2 in dihybrid assays**

1292   **performed in a [Cir$^+$] strain.**

1293   The dihybrid system based on the *LEU2* reporter (Finely and Brent, 1997) is schematically

1294   diagrammed at the top. The 'bait' and 'prey' proteins were expressed as hybrid proteins fused to

1295   the LexA repressor and B42 activation domain, respectively. These *CEN*-based expression

1296   vectors were designed for inducible expression from the *GAL* promoter, and harbored *HIS3* (VB;

1297   bait expression vector) or *TRP1* (VA; prey expression vector) as selectable markers. For a given

1298   protein pair, the protein to the left of the plus sign was the bait; the one to the right was the

1299   potential prey. The Rep1 (bait)-Rep2 (prey) combination served as the positive control.

1300

A.

| pSG1:CFP | CEN V - TEL V:GFP | pSG1 CEN V-TEL V | Spc42 - mcherry | Merged |

G1/S Phase

Metaphase

Anaphase

B.

N= 80

% Cells

TEL V (≤ 0.5 μm)   CEN V (≤ 0.5 μm)   > 0.5 μm

● SPB ● CEN V ○ TEL V ● pSG1-CEN
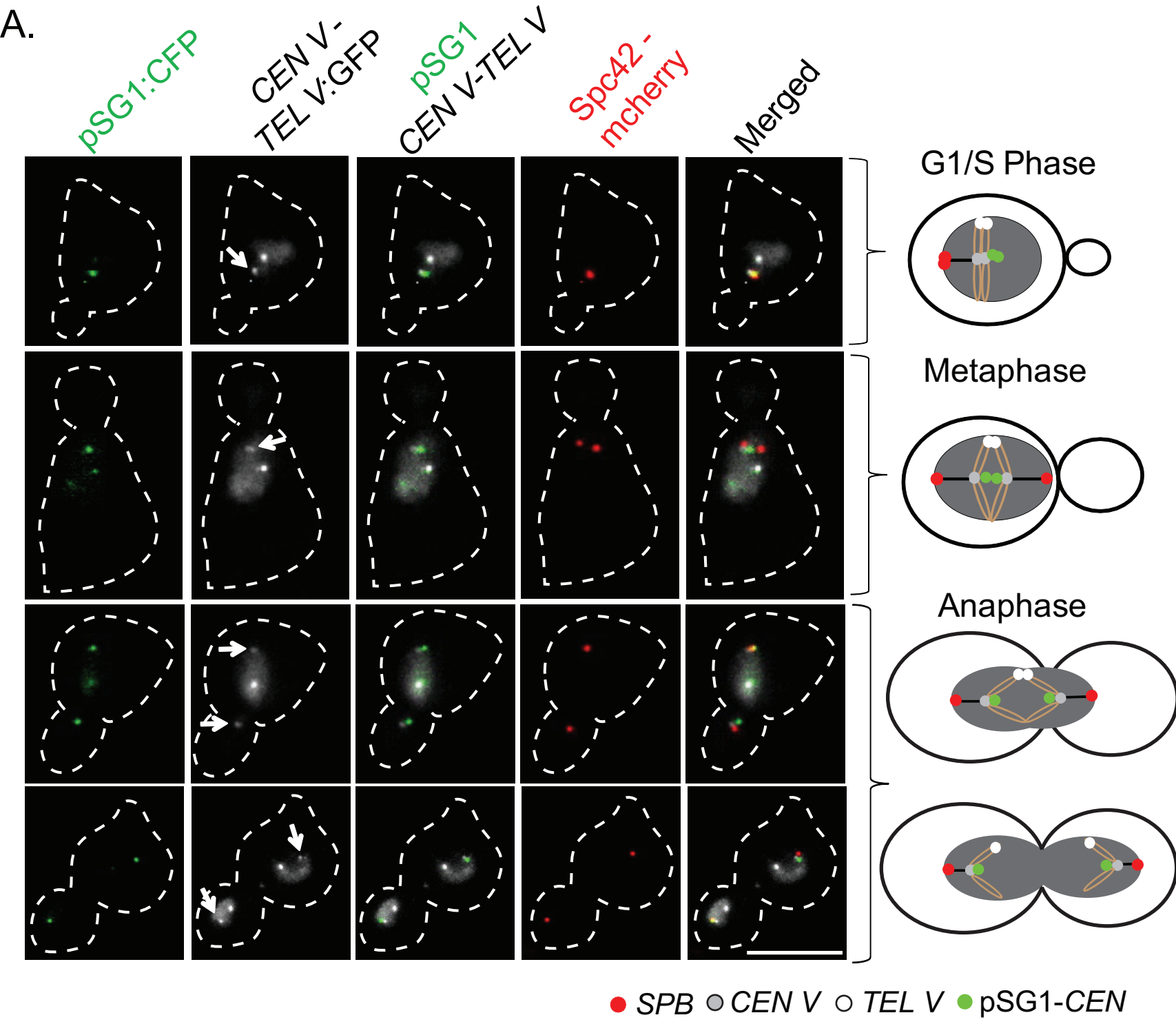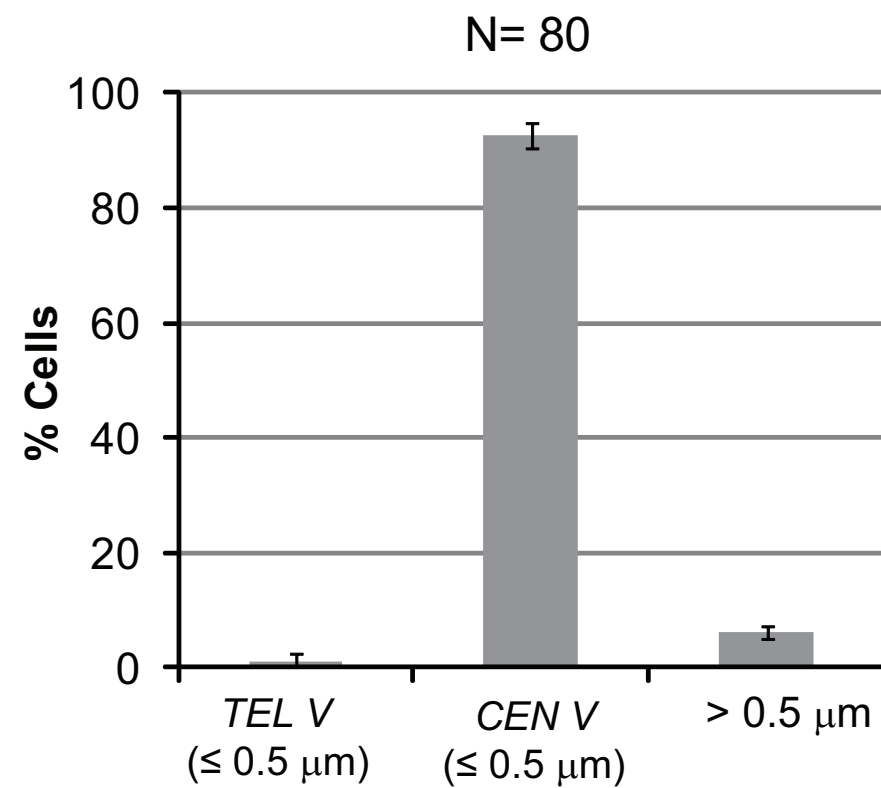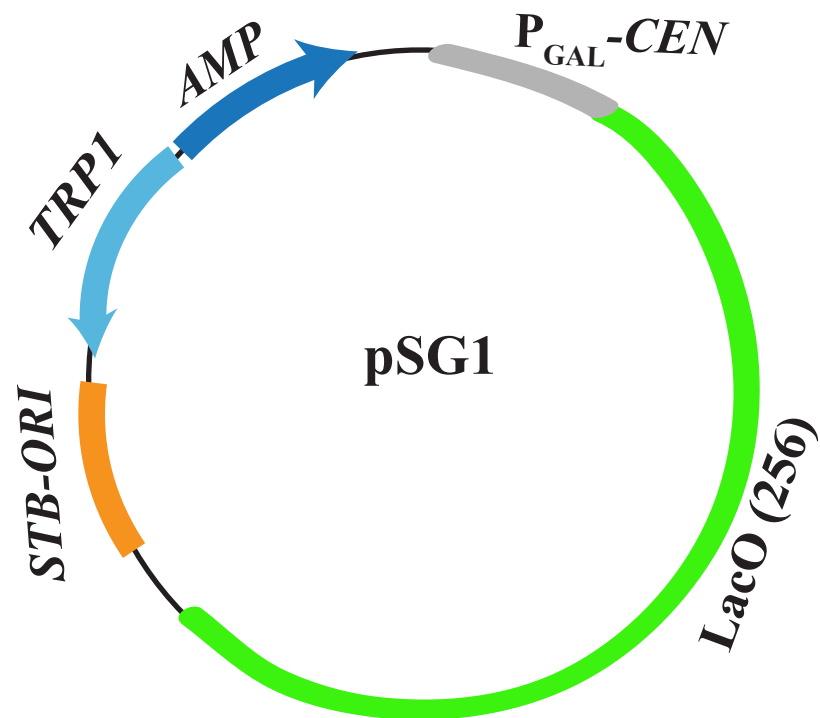
Carbon Source	[Cir^0]		[Cir$^+$]	
	CEN	*STB*	*CEN*	*STB*
Glucose	+	-	+	+
Galactose	-	-	-	+

A.

Spc42_mcherry | CEN V-TEL V:GFP | Merged

G1 Phase

S Phase

Metaphase

Anaphase

● SPB ◉ CEN V ○ TEL V

B.

N= 90

■ ≤ 0.5 µm   ■ > 0.5 µm

% Cells
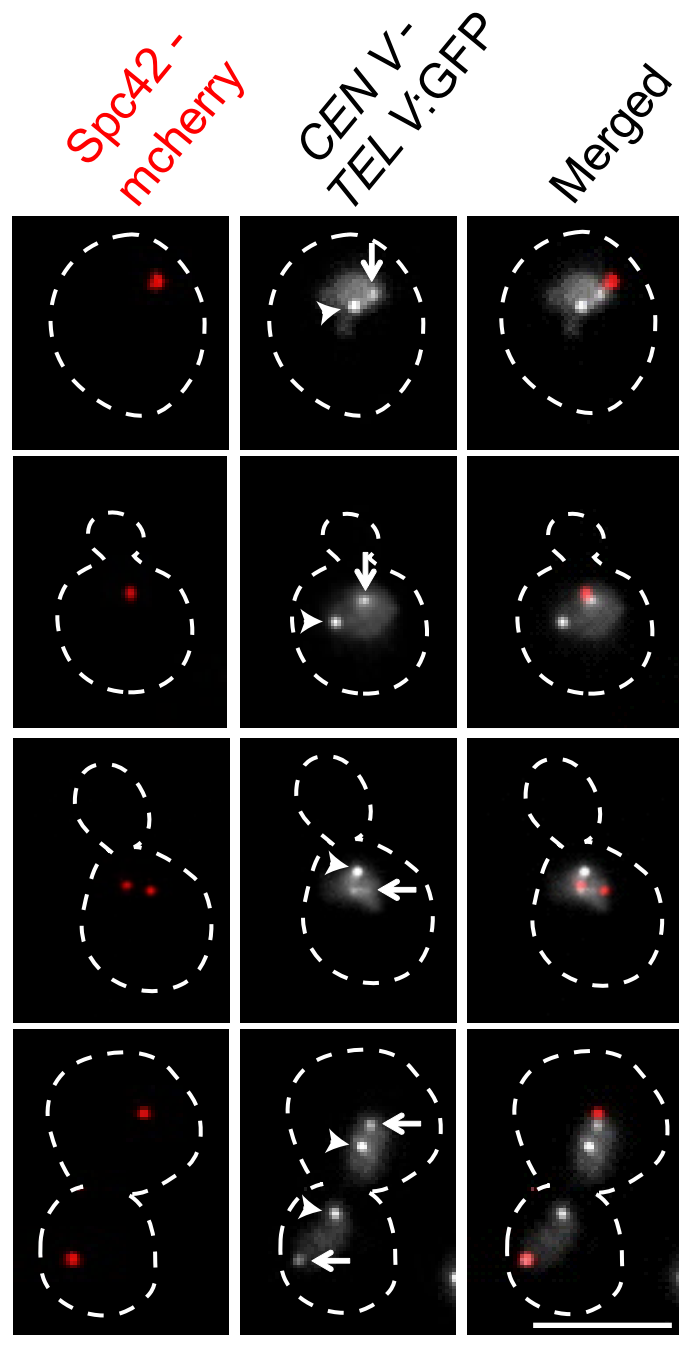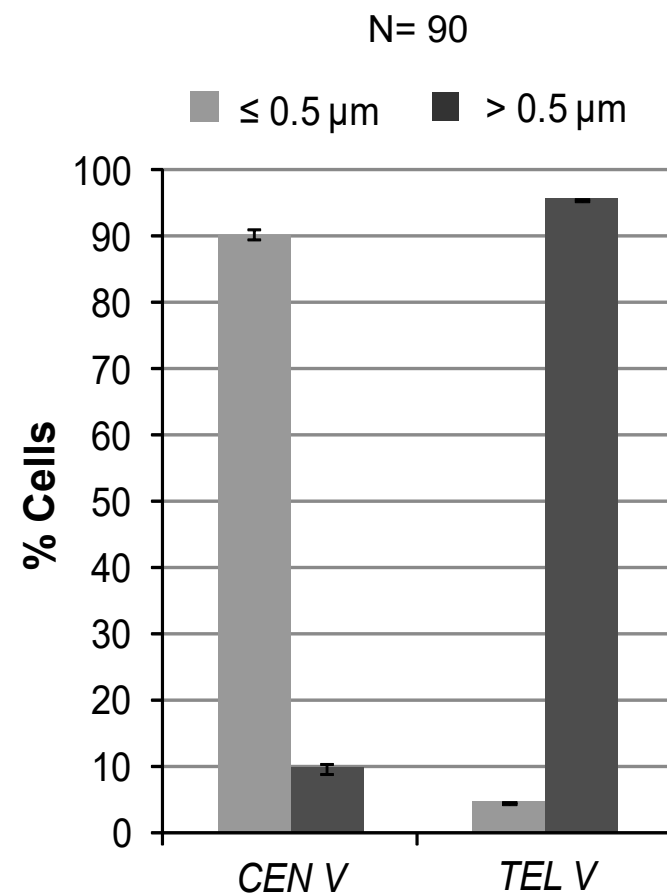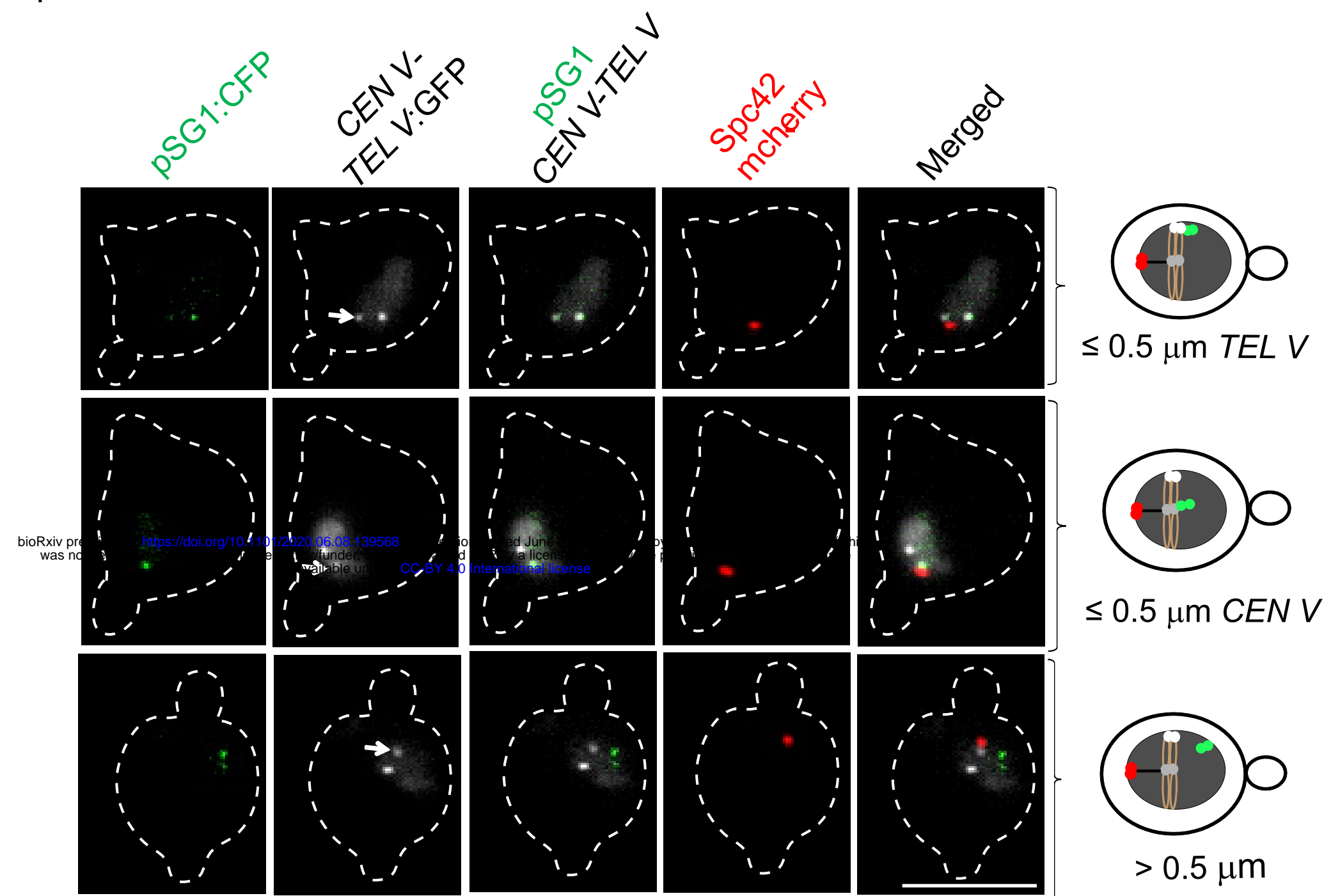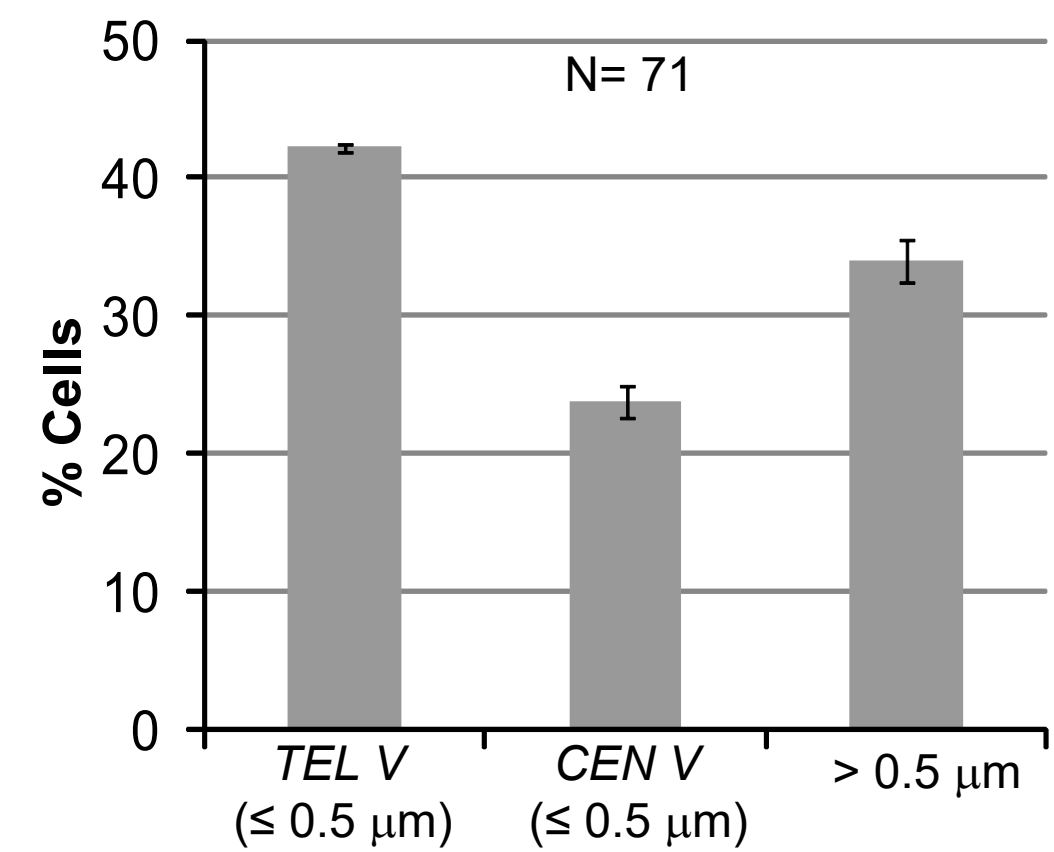
A. pSG1-*STB* / G1-S

C. pSG1-*STB* / metaphase

B.

D.

● *SPB*   ● *CEN V*   ○ *TEL V*   ● pSG1-*STB*
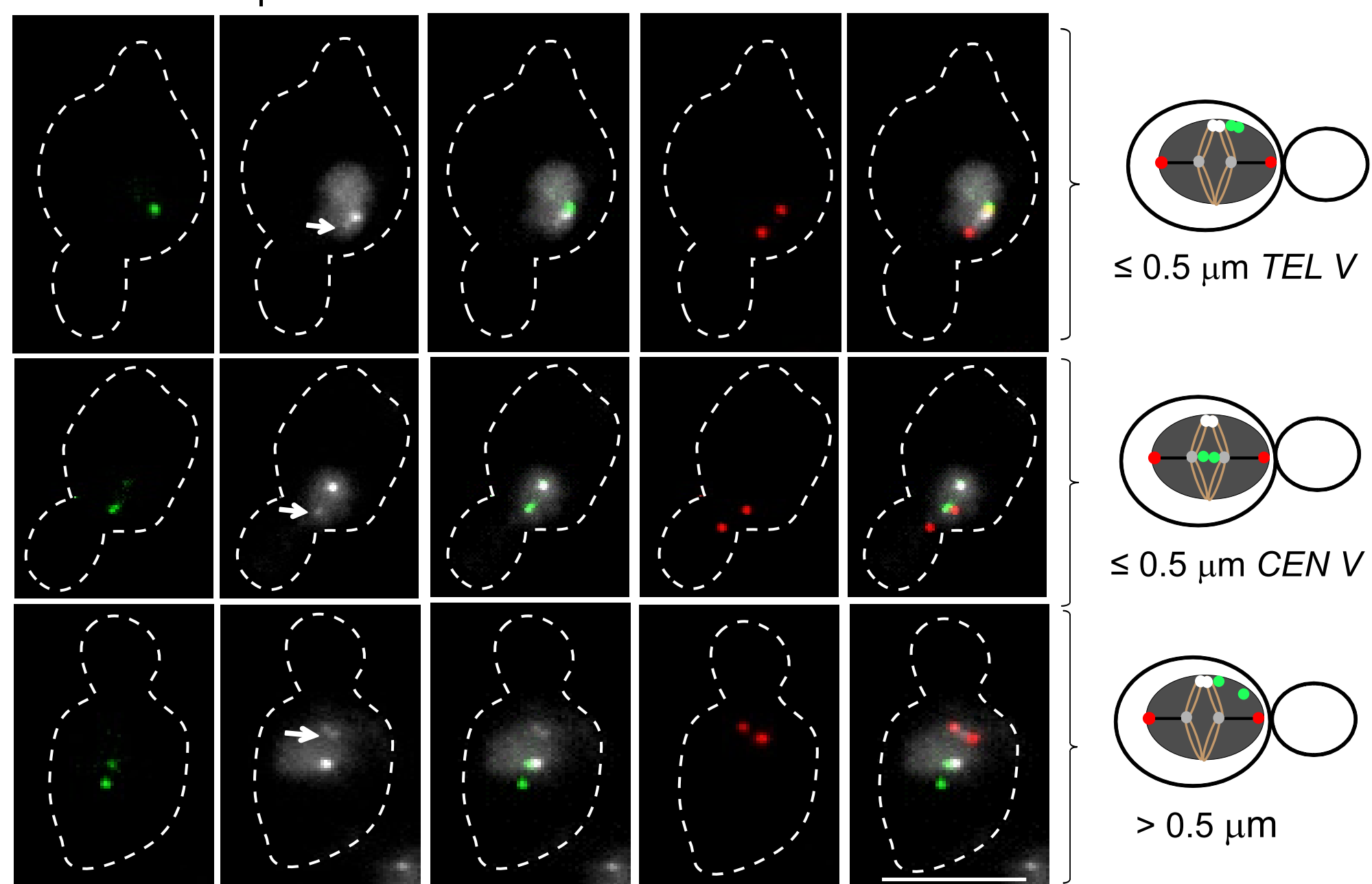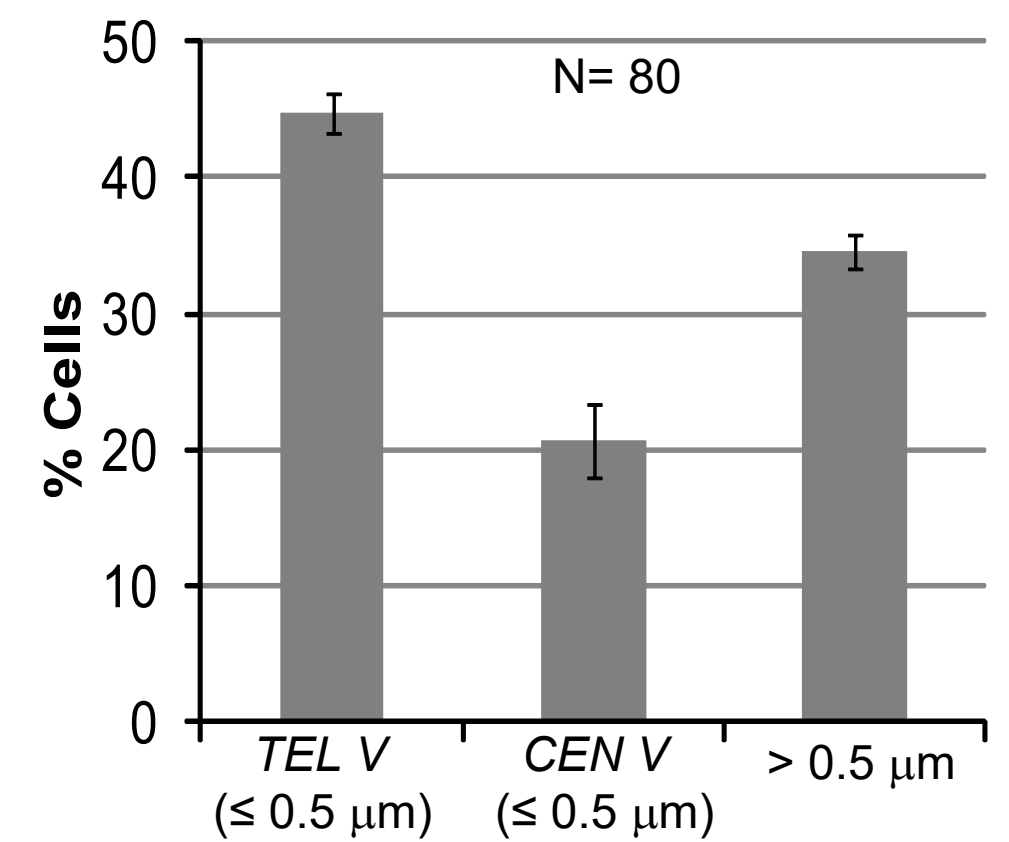
A. Localization of pSG1-*ARS* plasmid during G1/S

pSG1:CFP | *CEN V-TEL V:GFP* | *pSG1 CEN V-TEL V* | *Spc42-mcherry* | Merged

≤ 0.5 μm *TEL V*

≤ 0.5 μm *CEN V*

> 0.5 μm

B.

N= 68

% Cells

TEL V (≤ 0.5 μm)   *CEN V* (≤ 0.5 μm)   > 0.5 μm
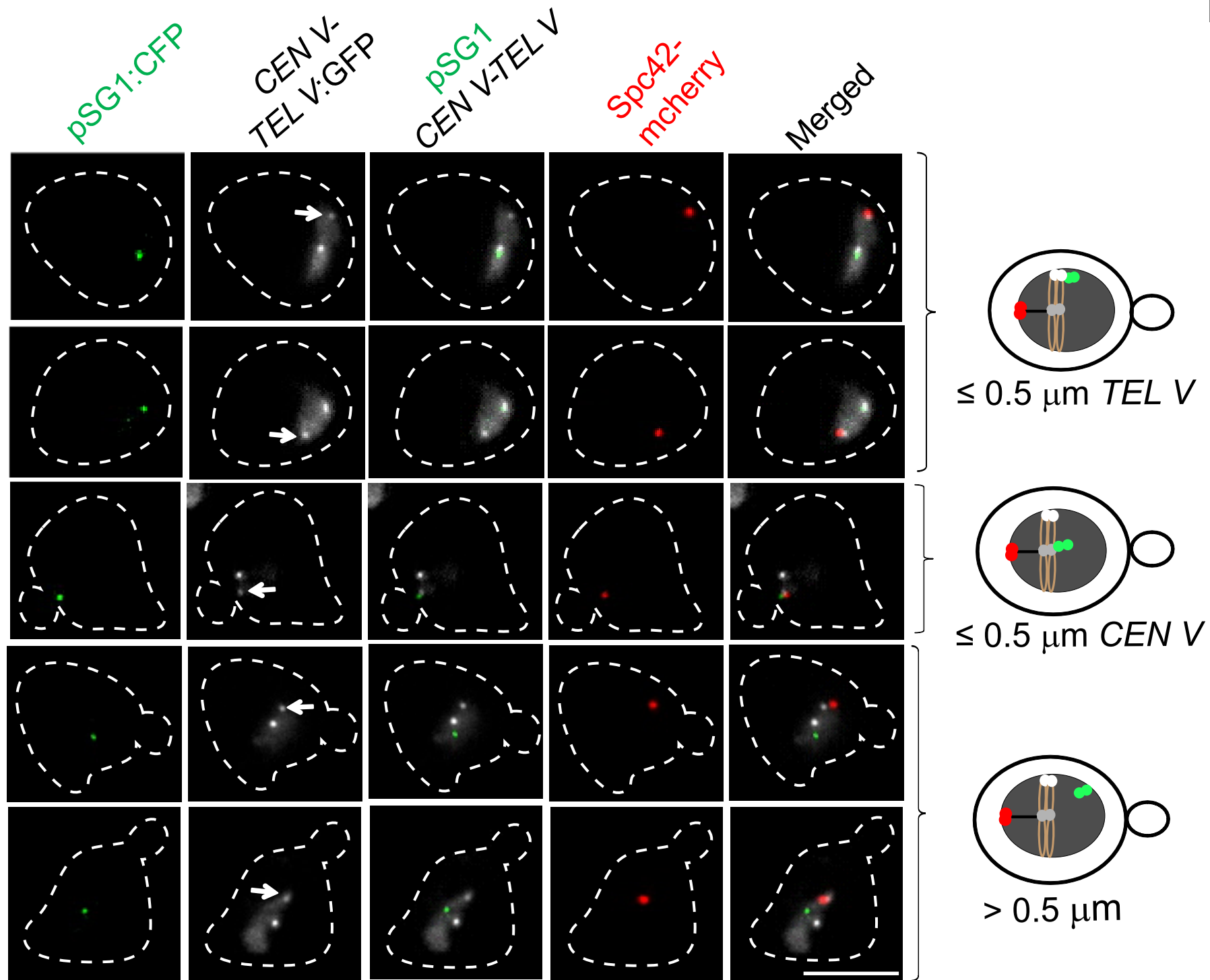
● *SPB* ◉ *CEN V* ○ *TEL V* ● pSG1-*ARS*
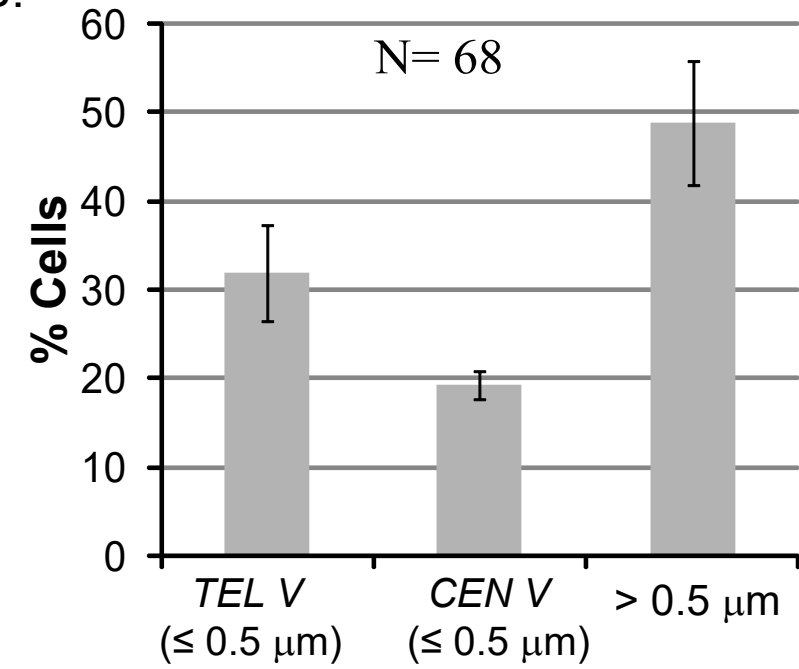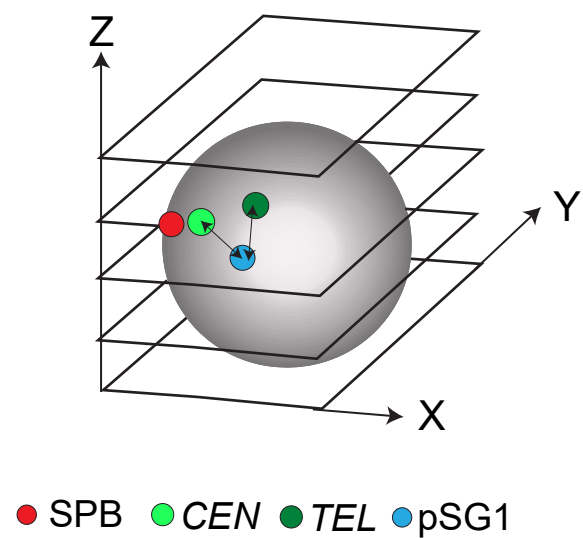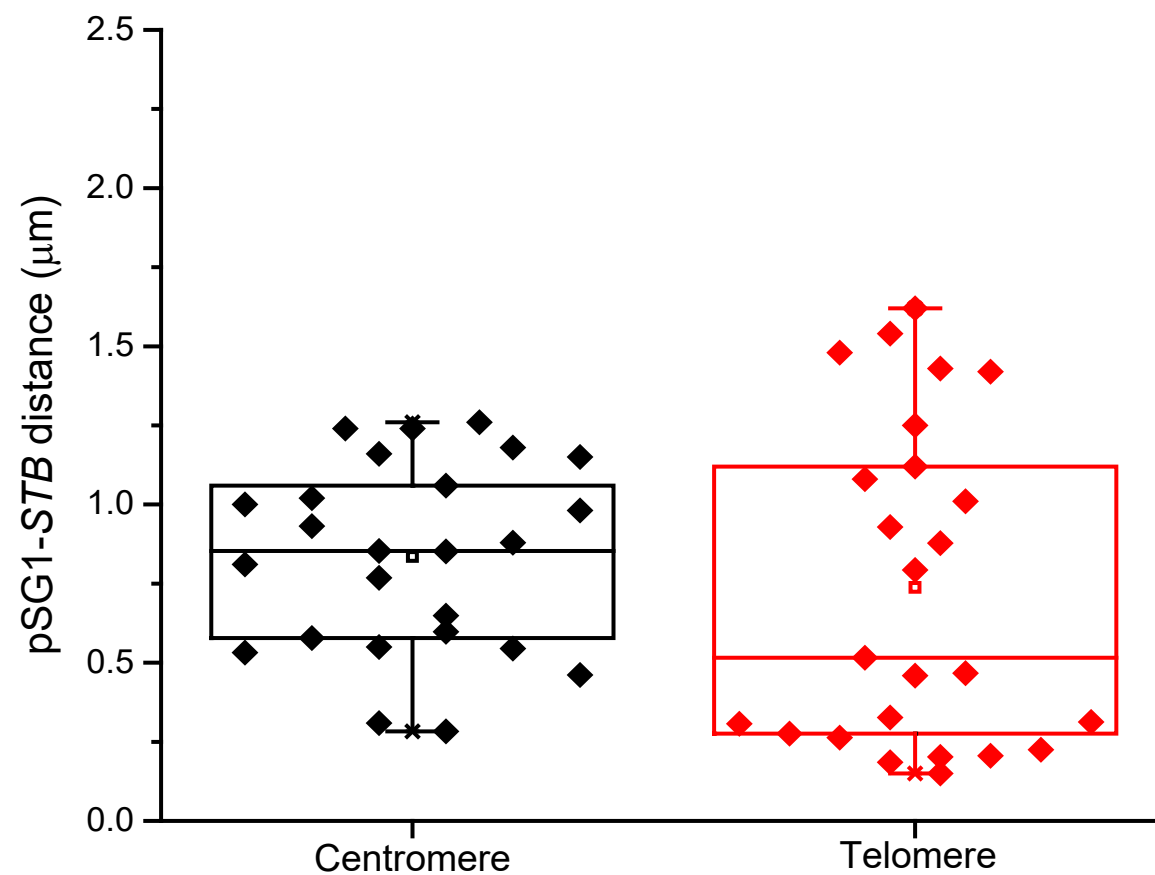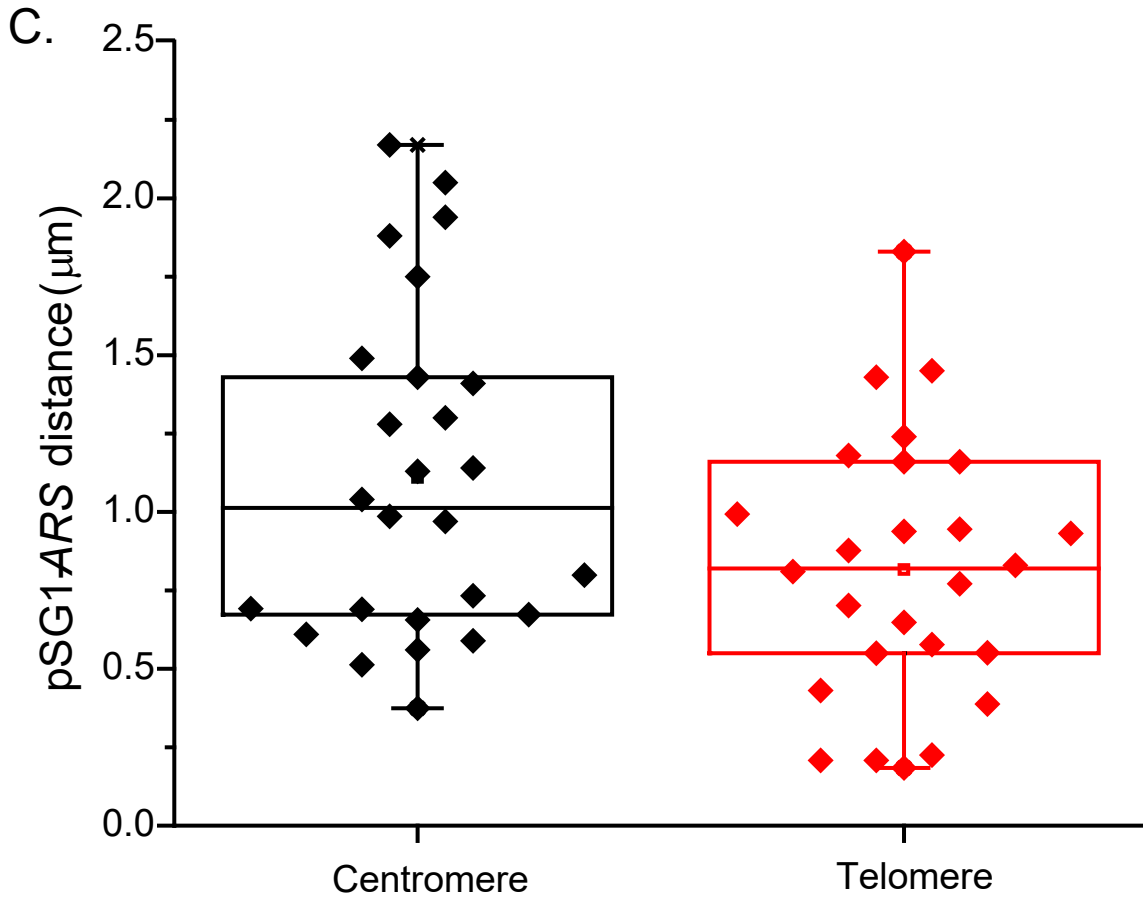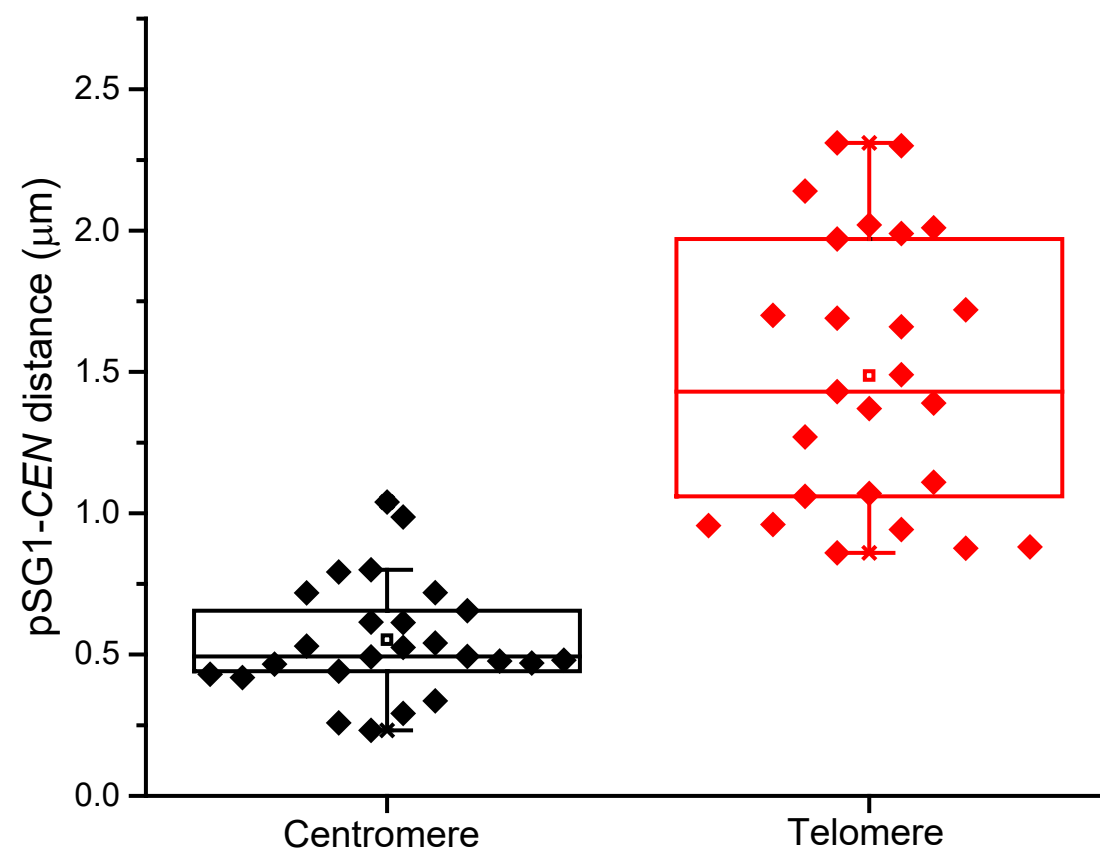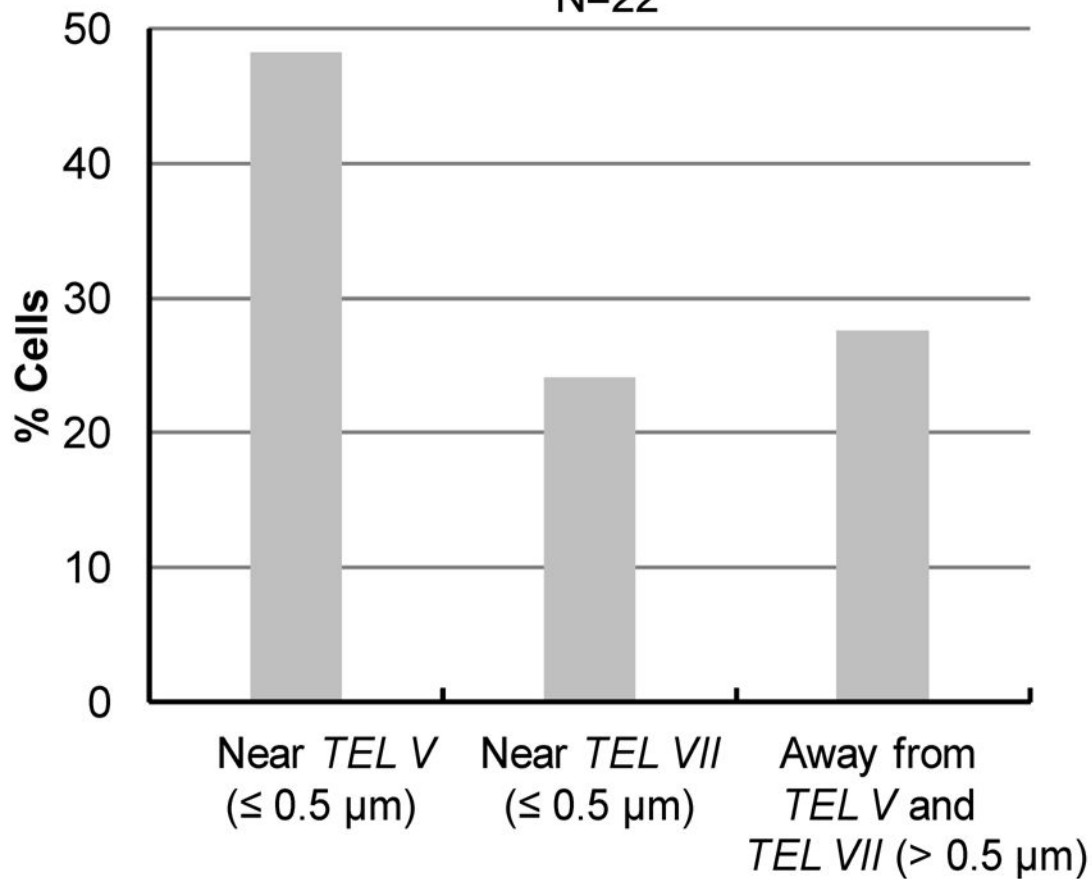
A. pSG1-*STB* /anaphase

B.
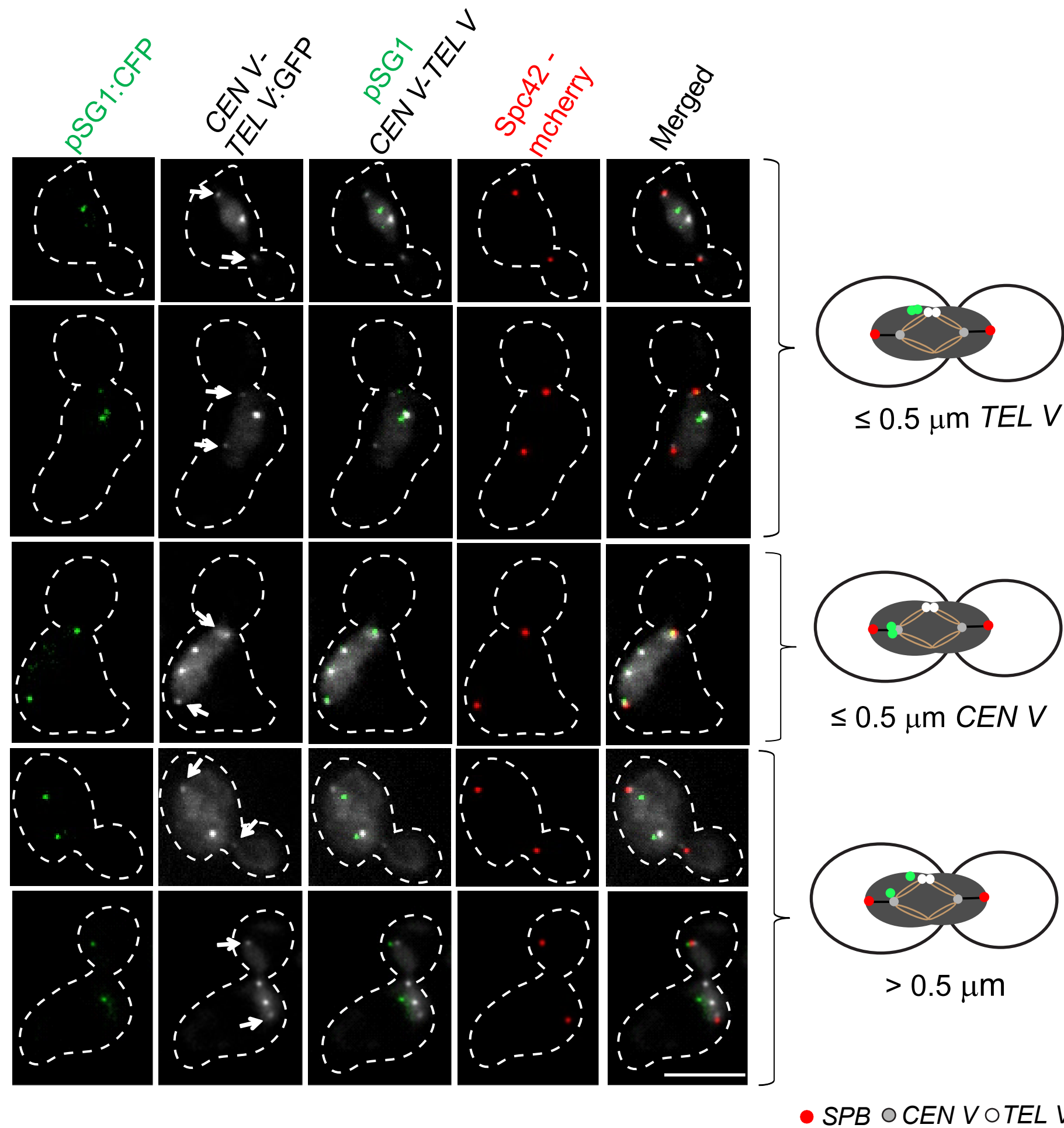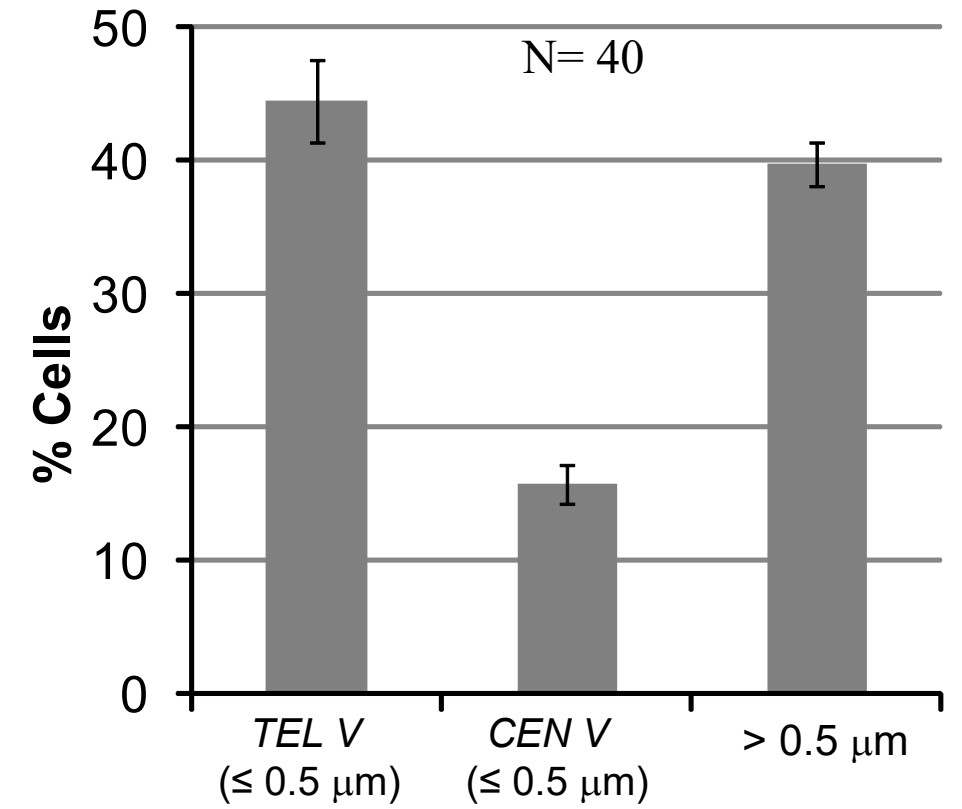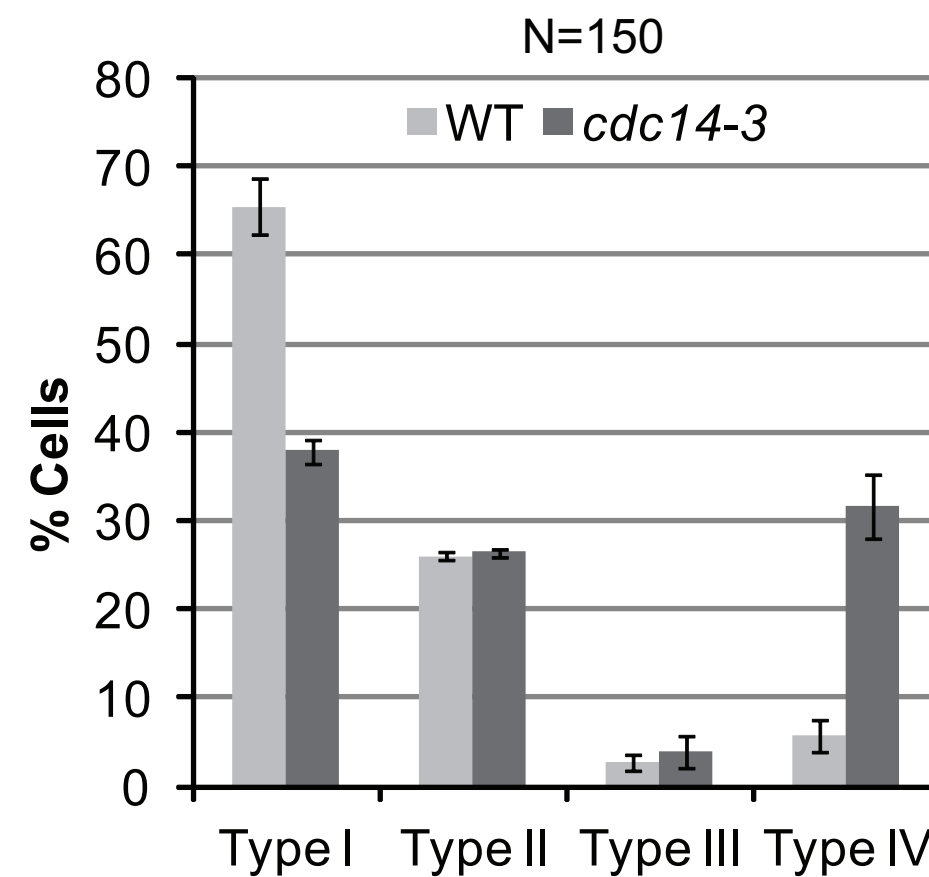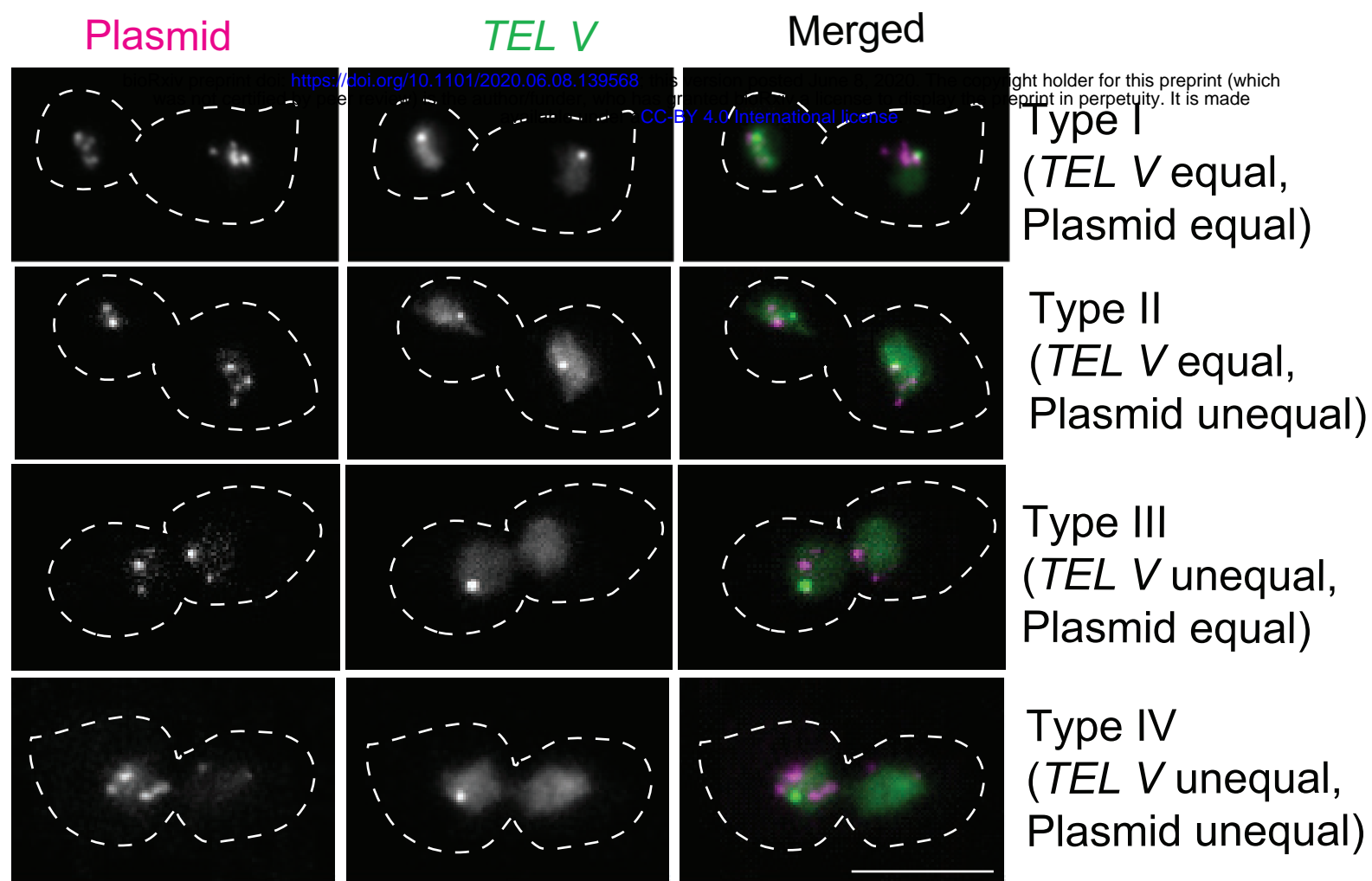
● *SPB* ◯ *CEN V* ○ *TEL V* ● pSG1-*STB*
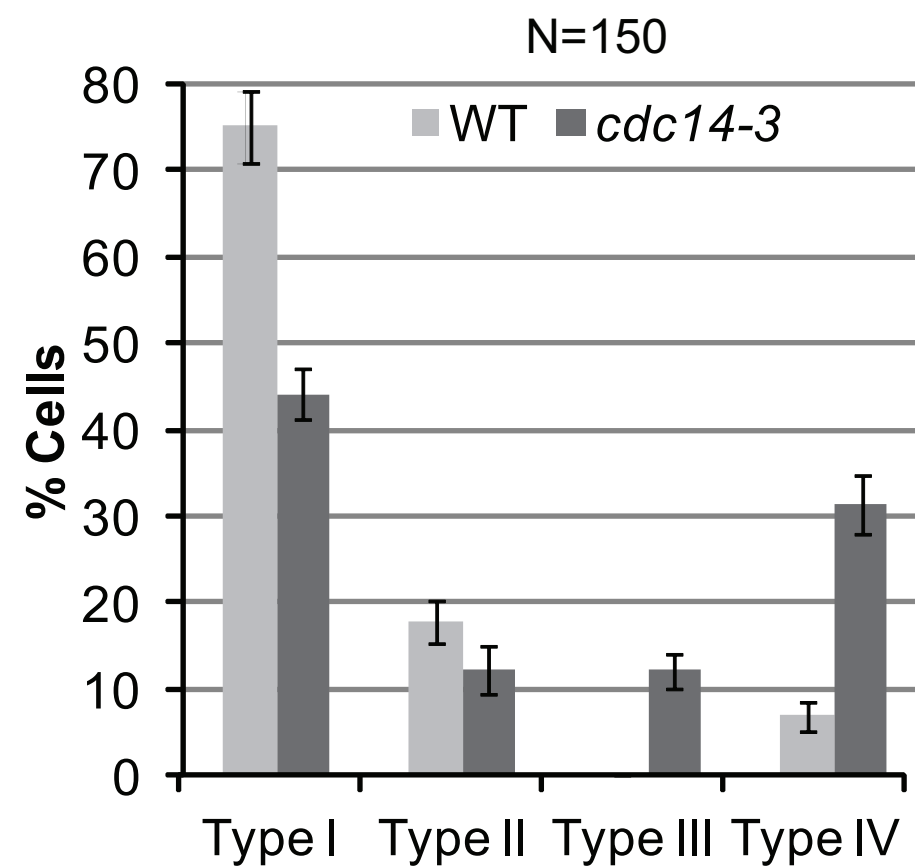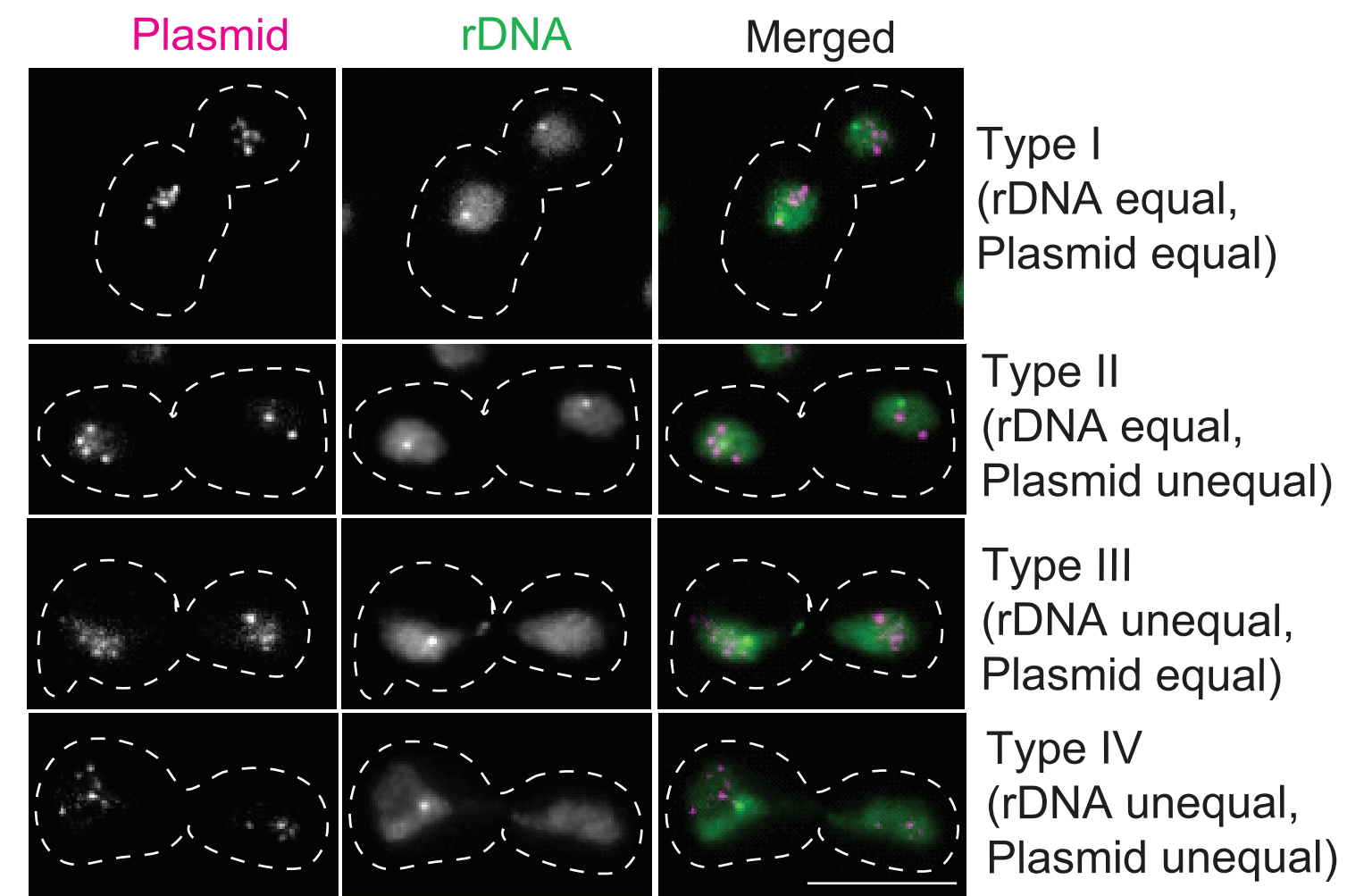
A.
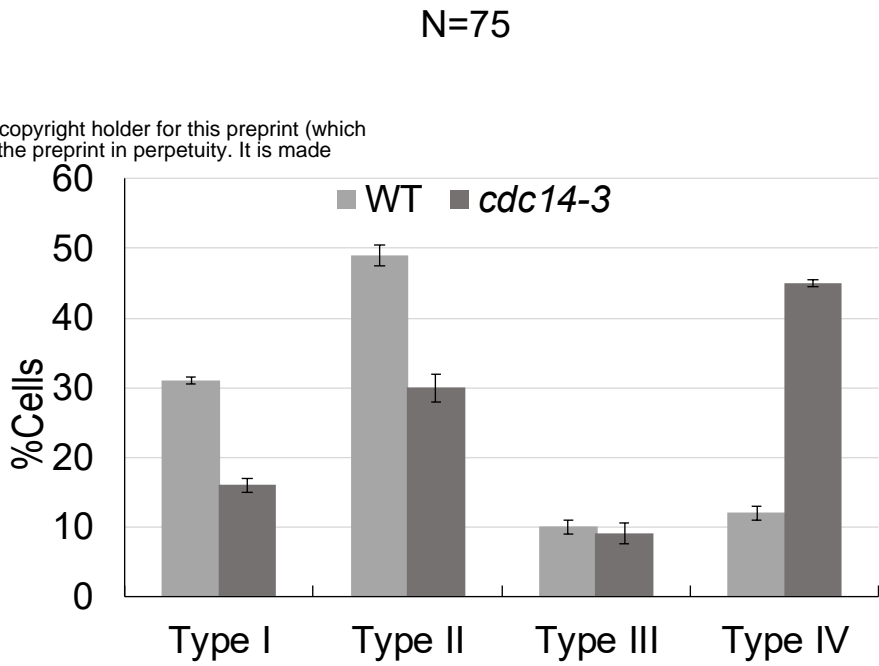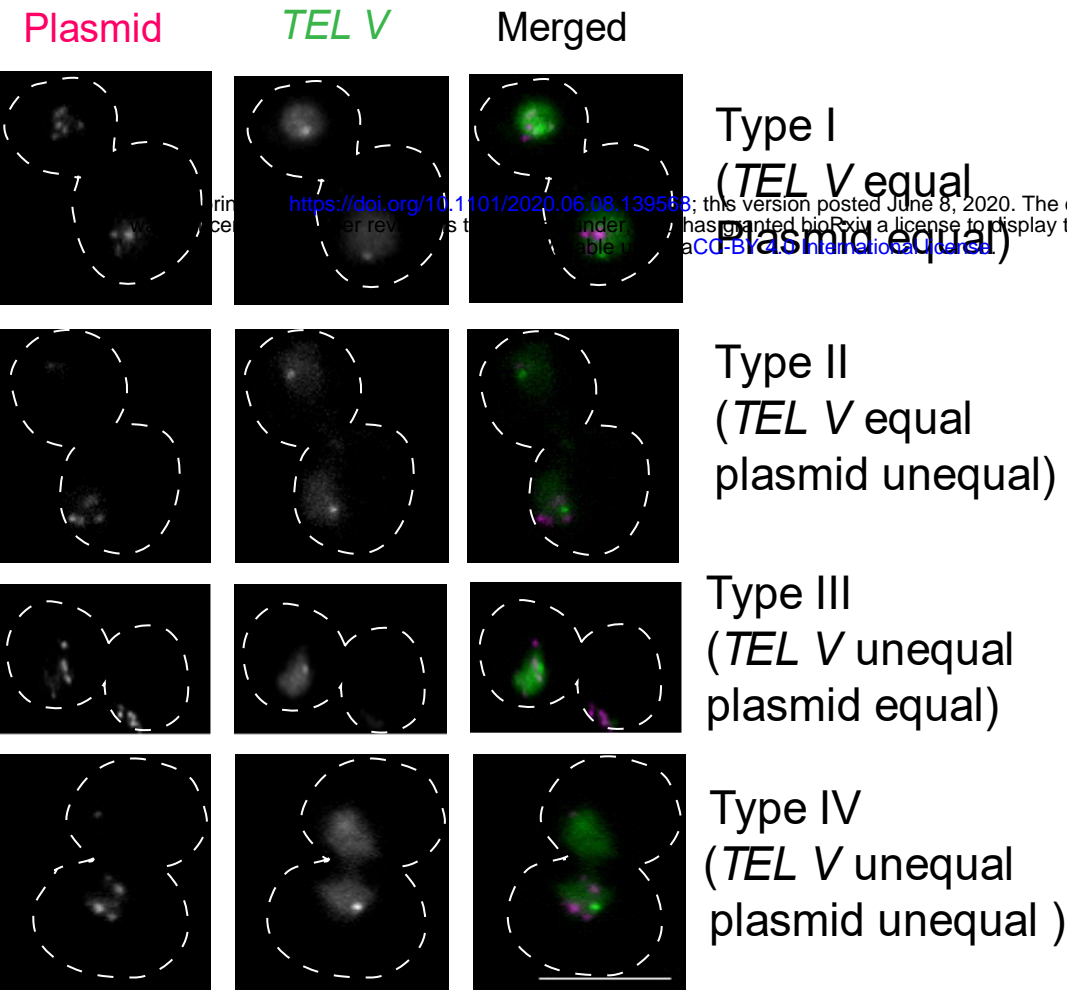
B.
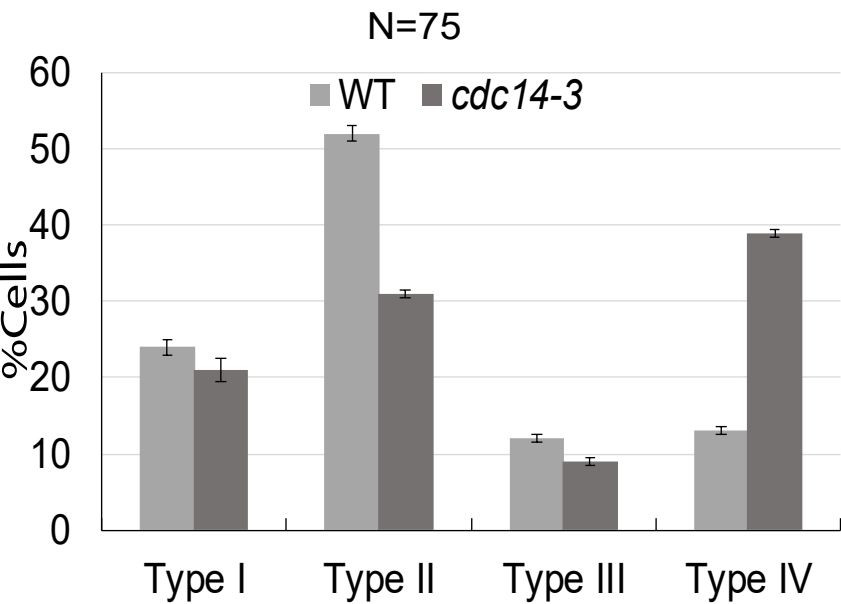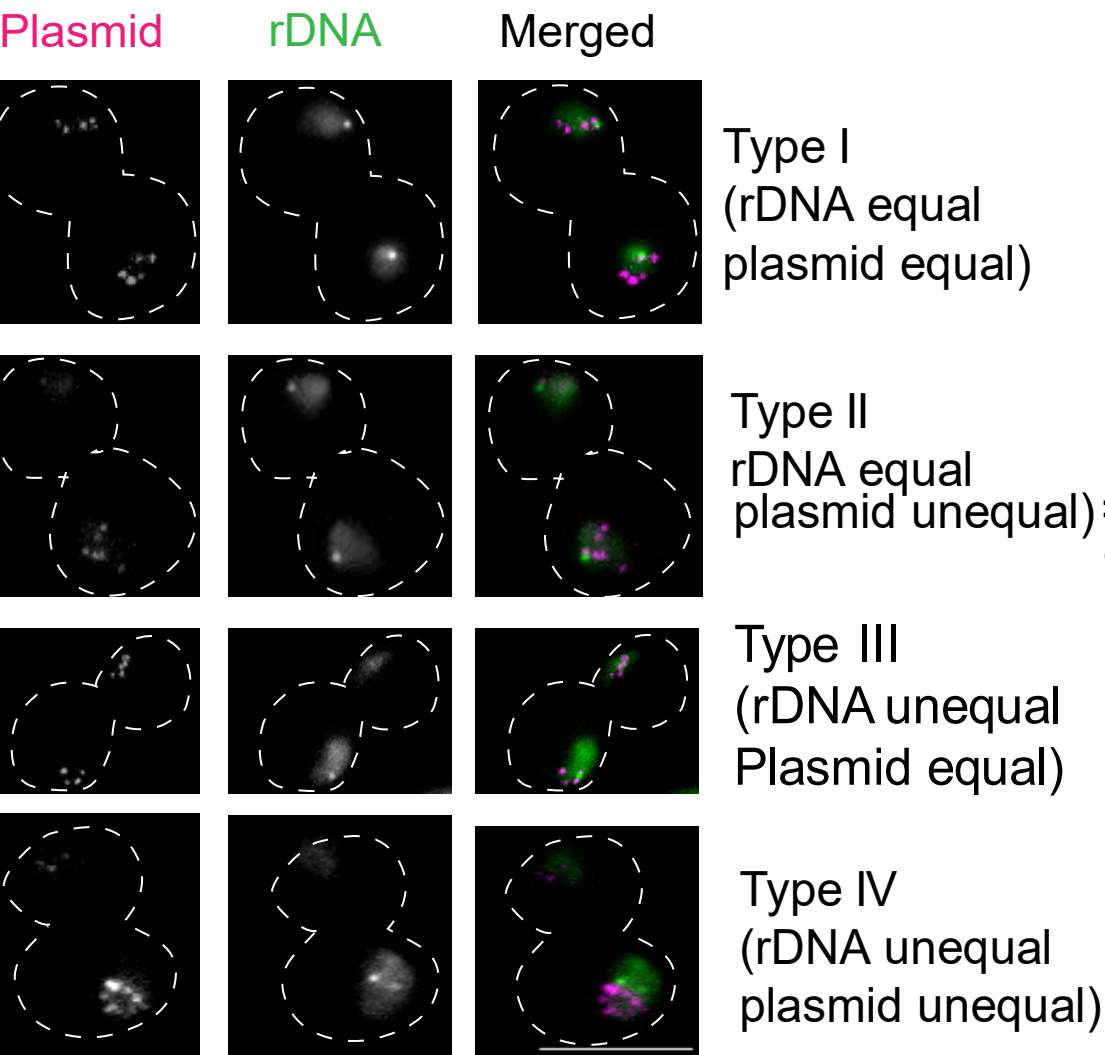
A

| Plasmid | *TEL V* | Merged |
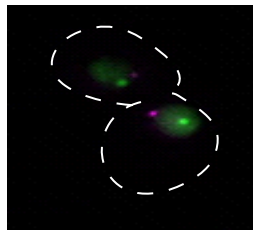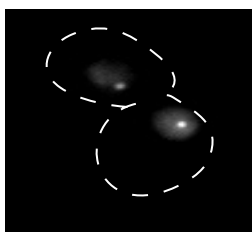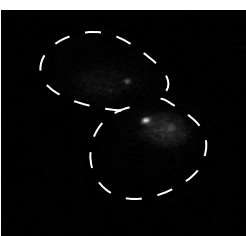
Type I
(*TEL V* equal

plasmid equal)
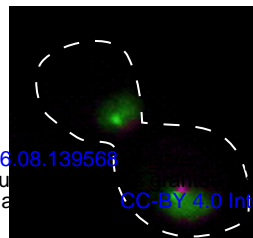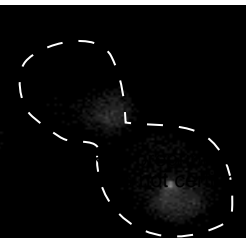
Type II
(*TEL V* equal
plasmid unequal)
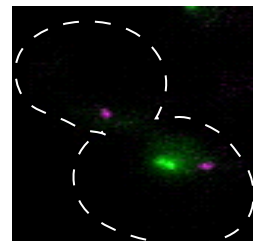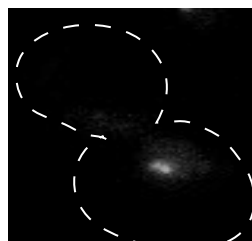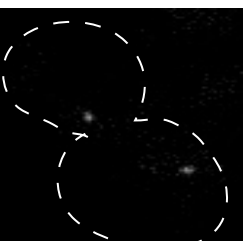
Type III
(*TEL V* unequal
plasmid equal)
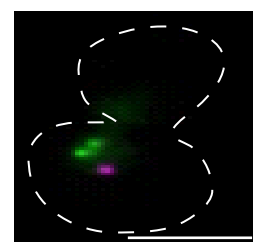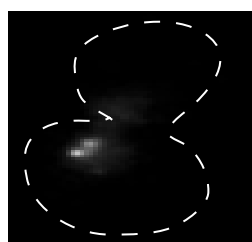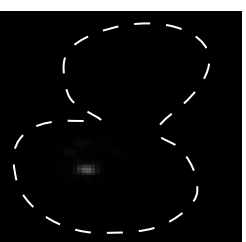
Type IV
(*TEL V* unequal
plasmid unequal)

N=75
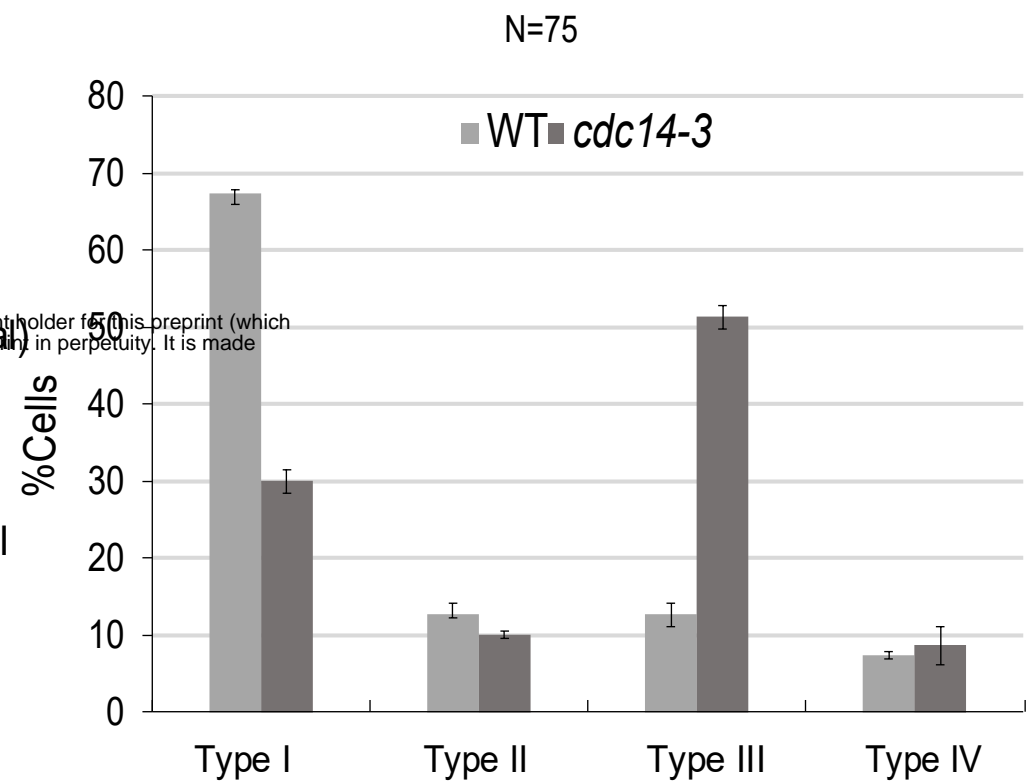
B.

| Plasmid | rDNA | Merged |
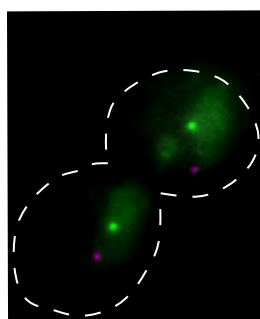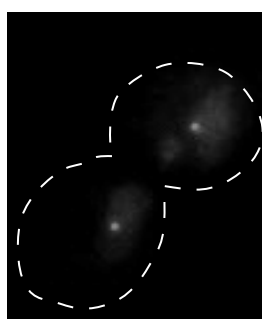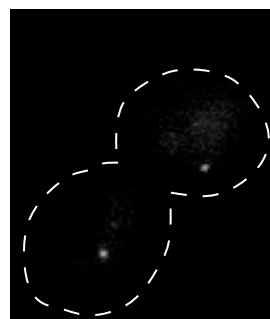
Type I
(rDNA equal
plasmid equal)
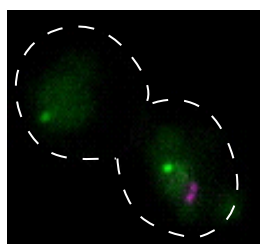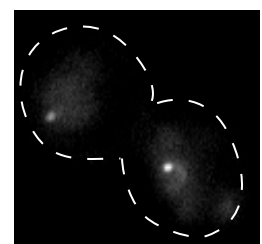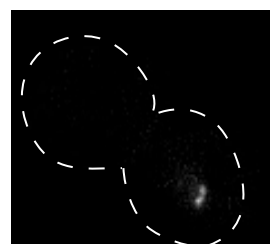
Type II
rDNA equal
plasmid unequal)
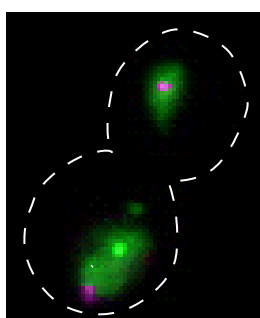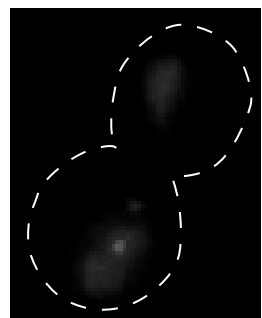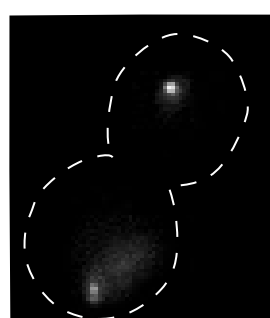
Type III
(rDNA unequal
Plasmid equal)
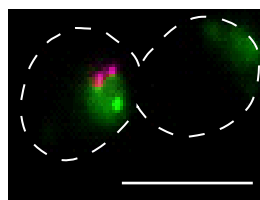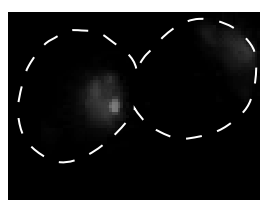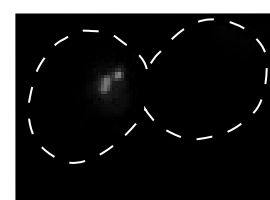
Type IV
(rDNA unequal
plasmid unequal)
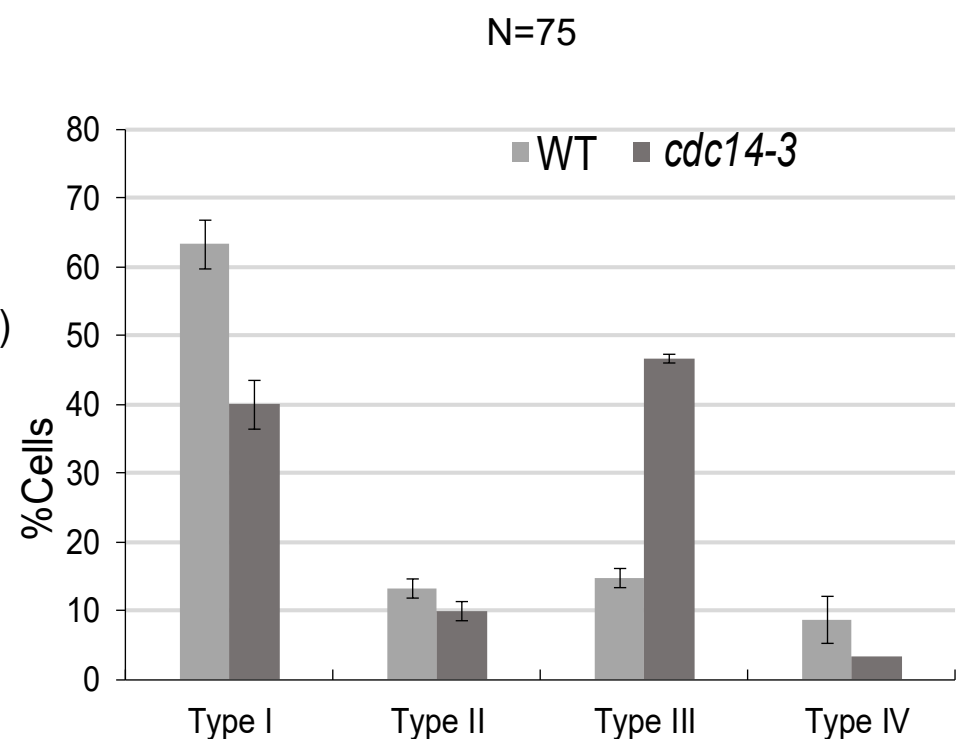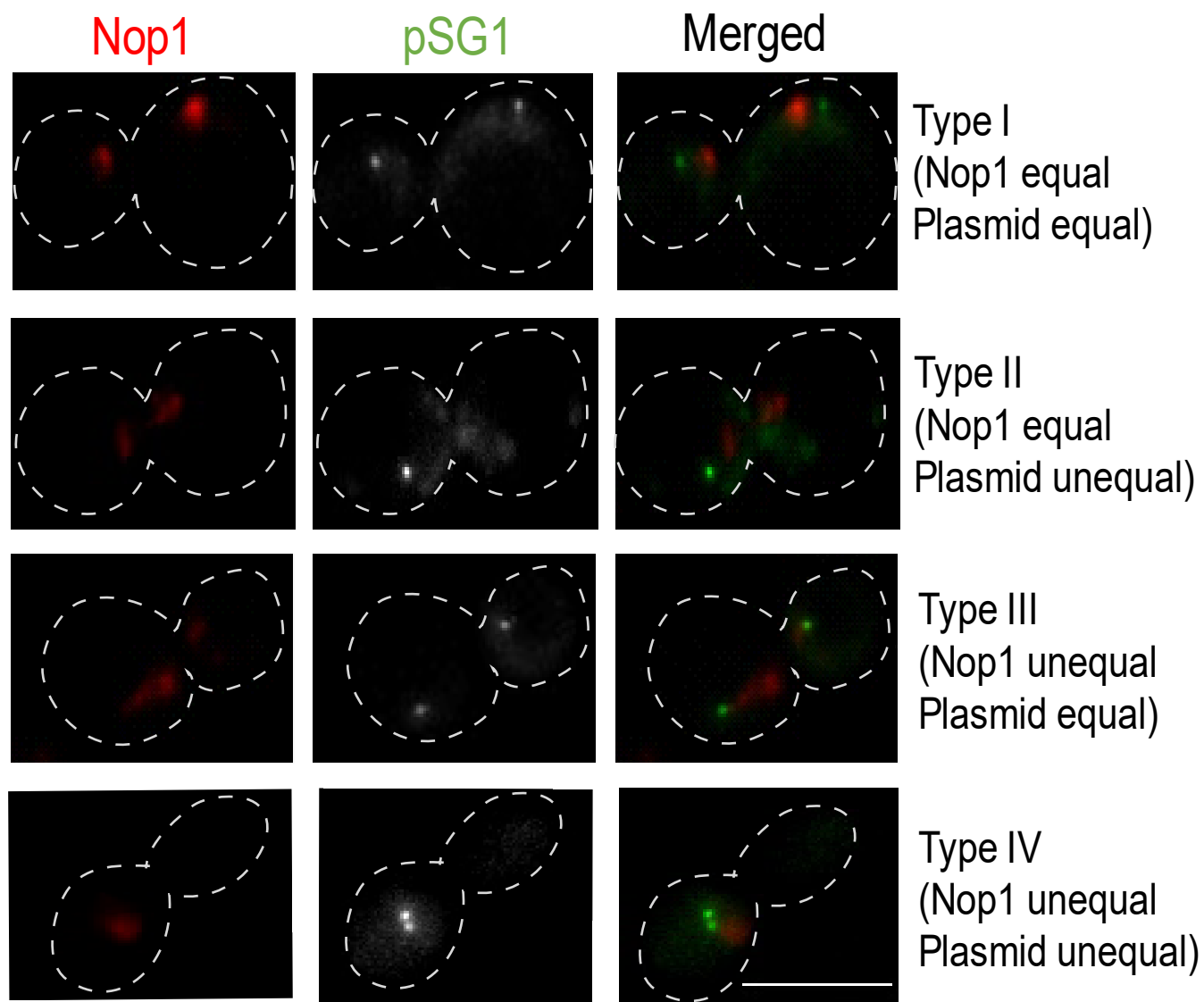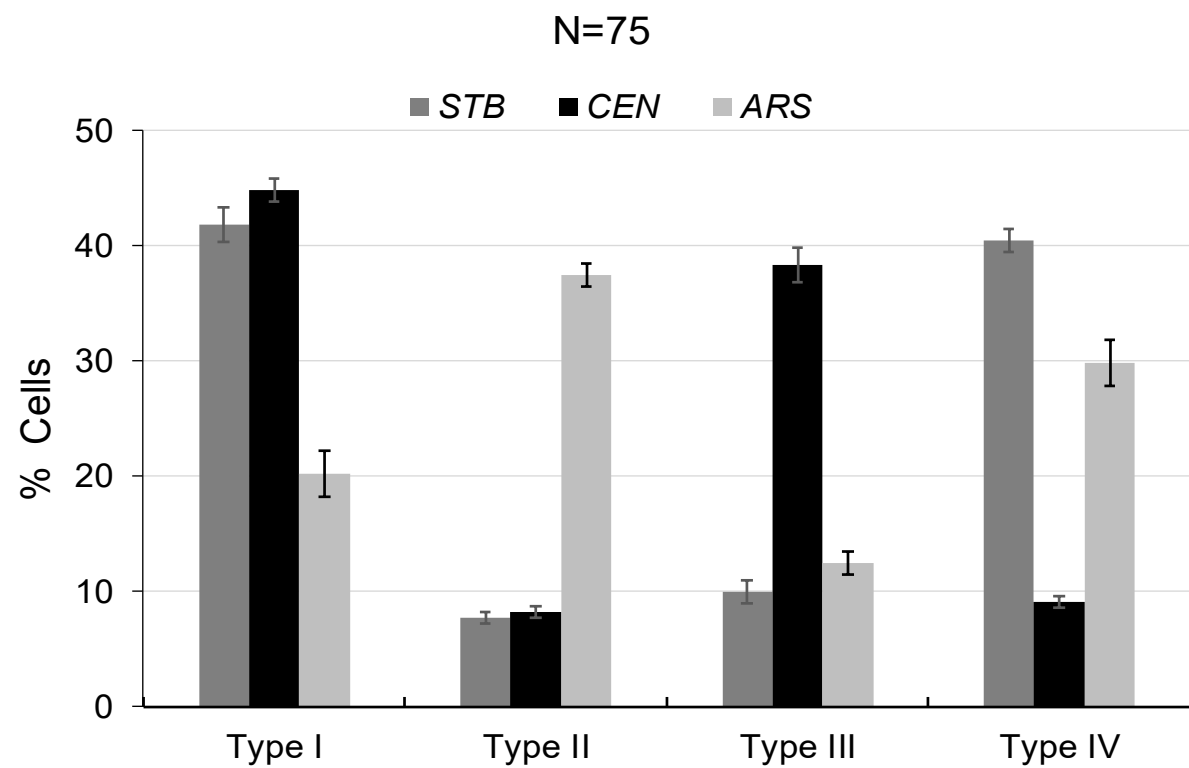
N=75

A.

B.

A.

Nop1	pSG1	Merged	
			Type I (Nop1 equal Plasmid equal)
			Type II (Nop1 equal Plasmid unequal)
			Type III (Nop1 unequal Plasmid equal)
			Type IV (Nop1 unequal Plasmid unequal)

B.

N=75

A.

Nop1 Plasmid DAPI Merged

Type I
(Nop1 equal,
Plasmid equal)

Type II
(Nop1 equal,
Plasmid unequal)

Type III
(Nop1 unequal,
Plasmid equal)

Type IV
(Nop1 unequal,
Plasmid unequal)

B.

N=150

P_{GAL1}-CEN III

% Cells

Glu
Gal

Type I   Type II   Type III   Type IV

C.

N=150

P_{GAL1}-CEN XII

% Cells

Glu
Gal

Type I   Type II   Type III   Type IV
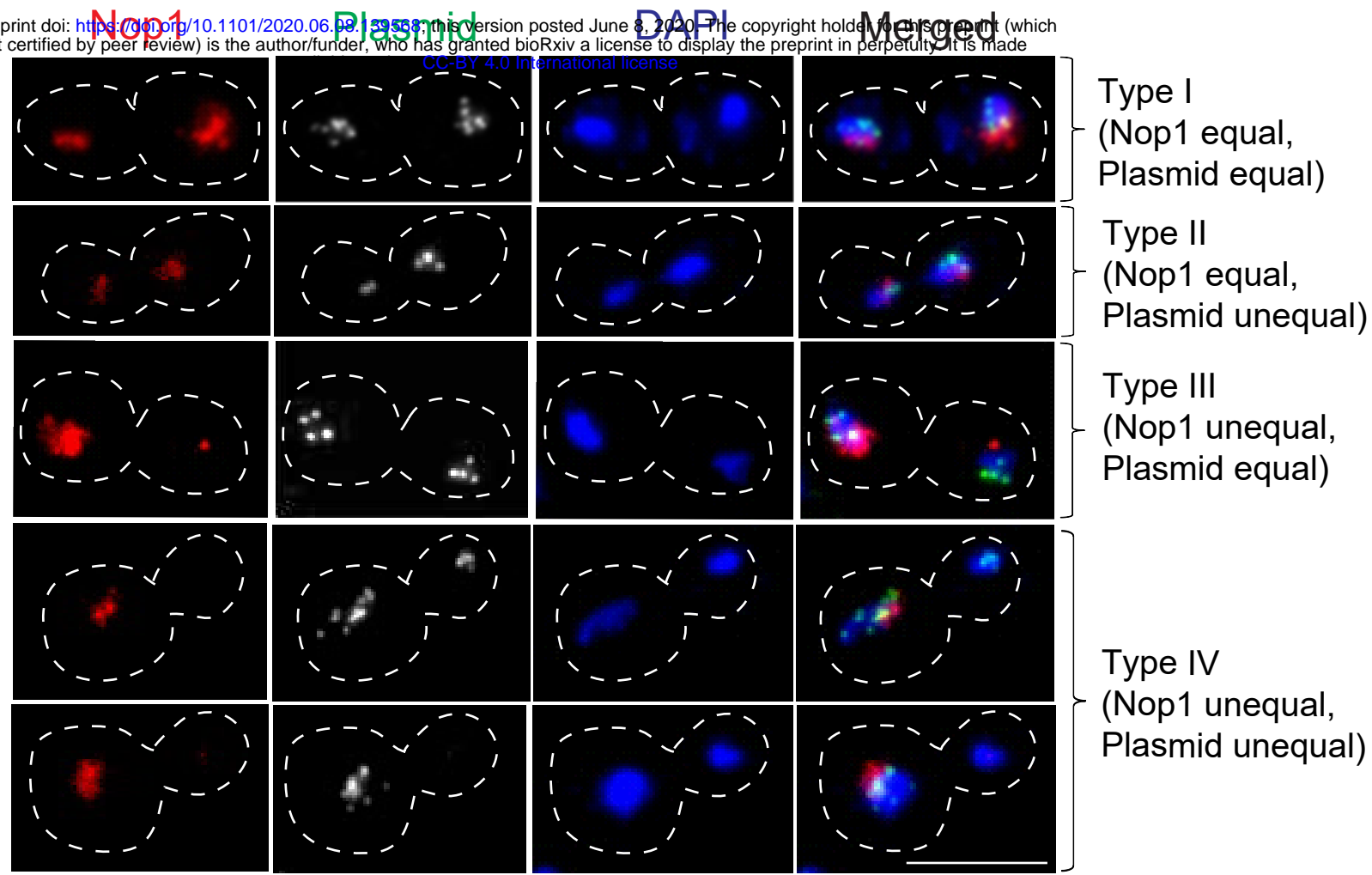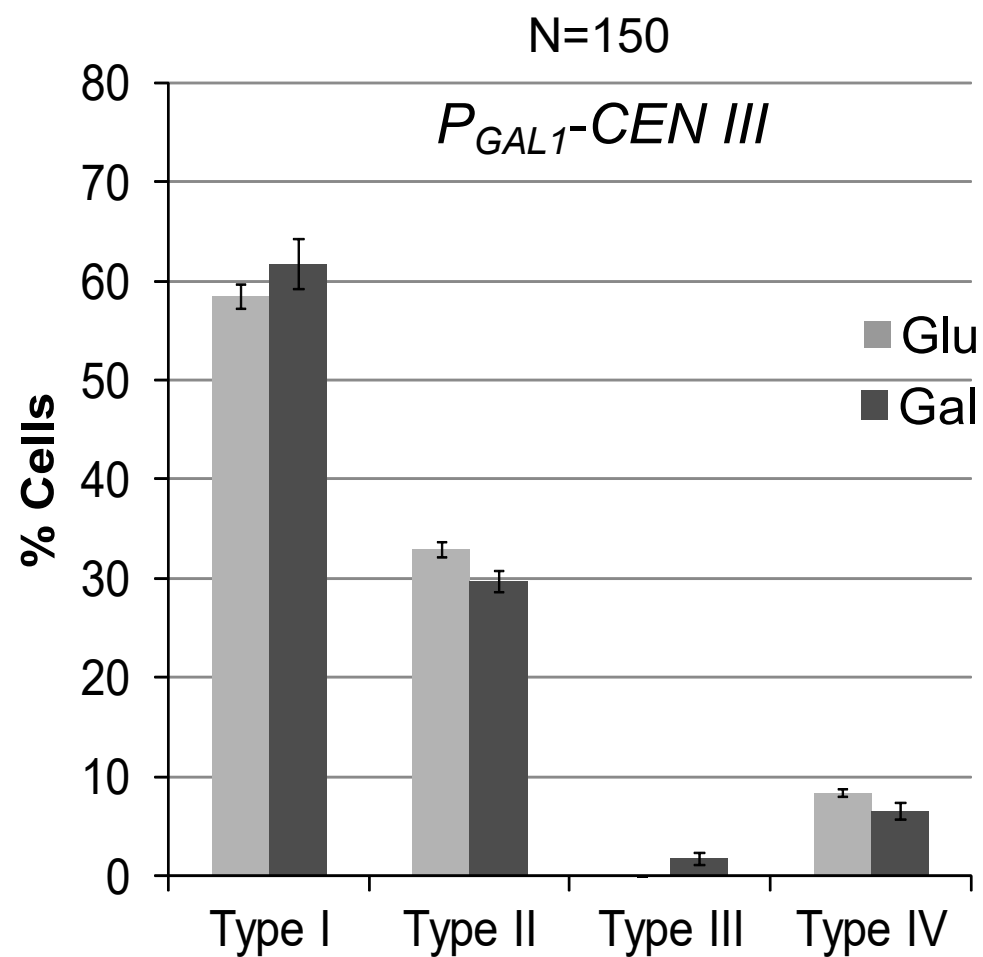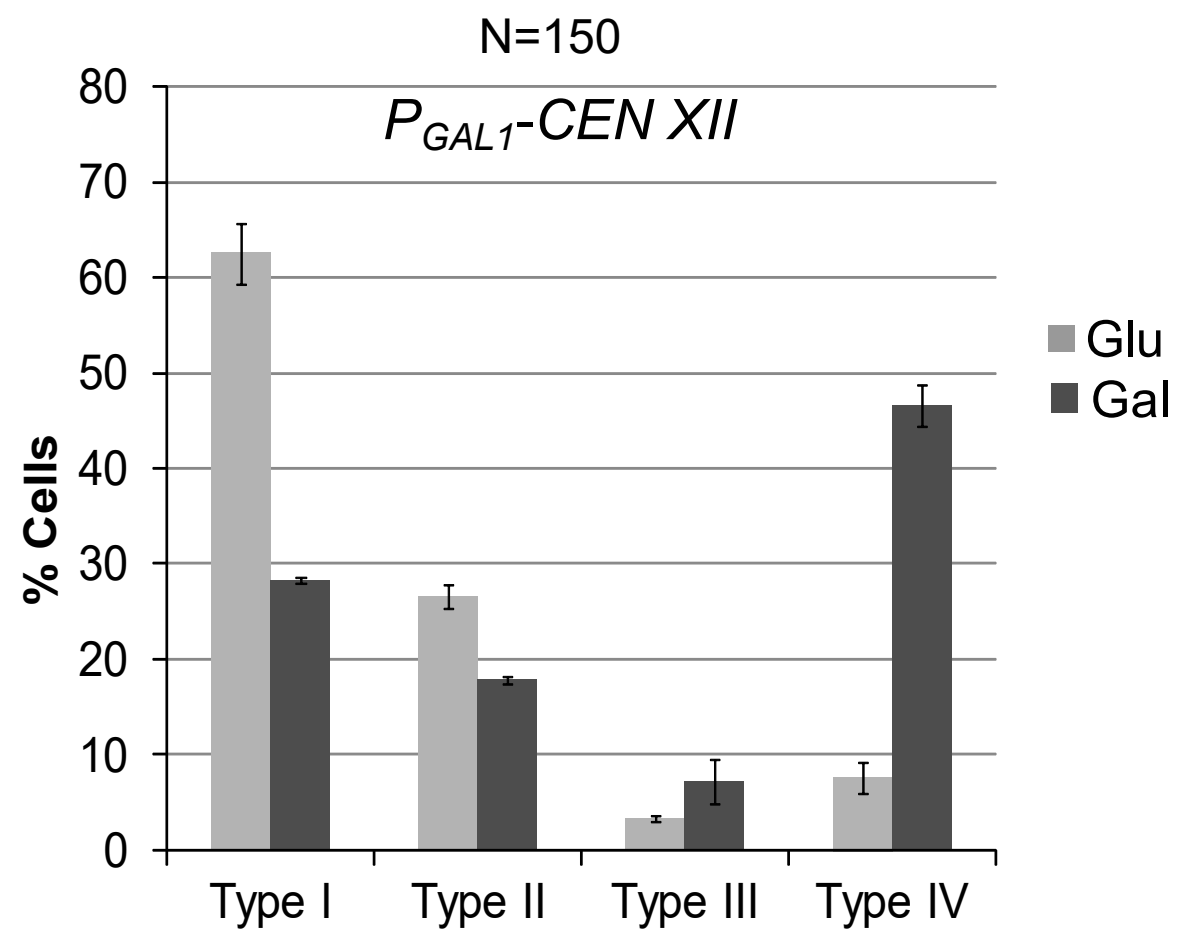
A.
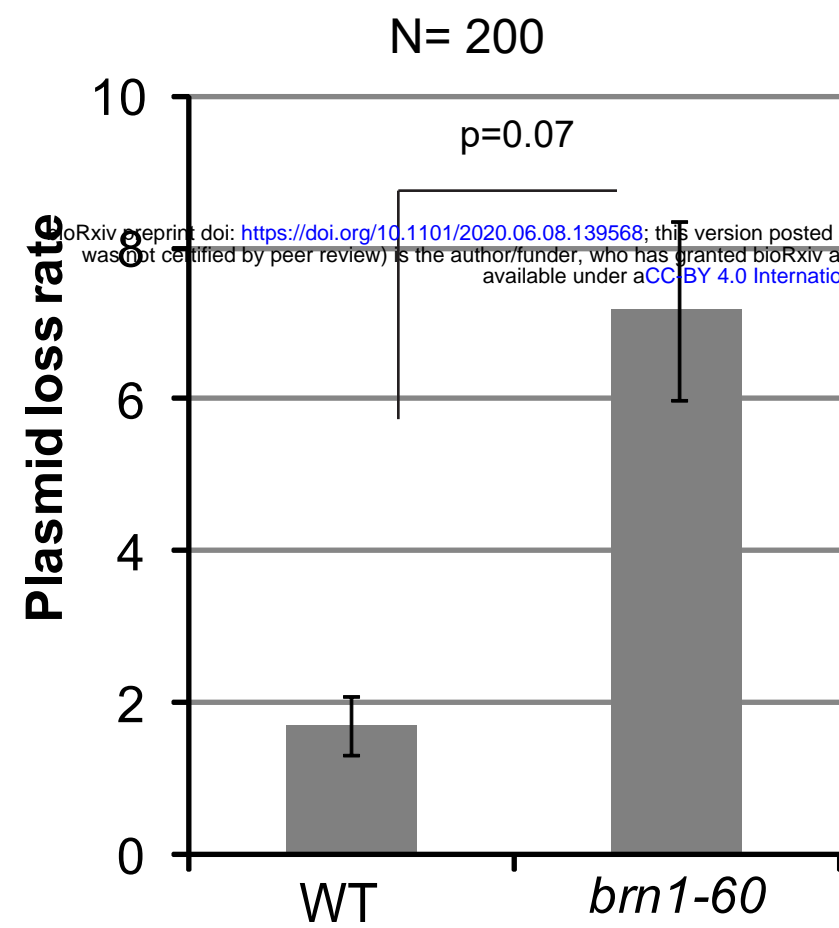
STB plasmid
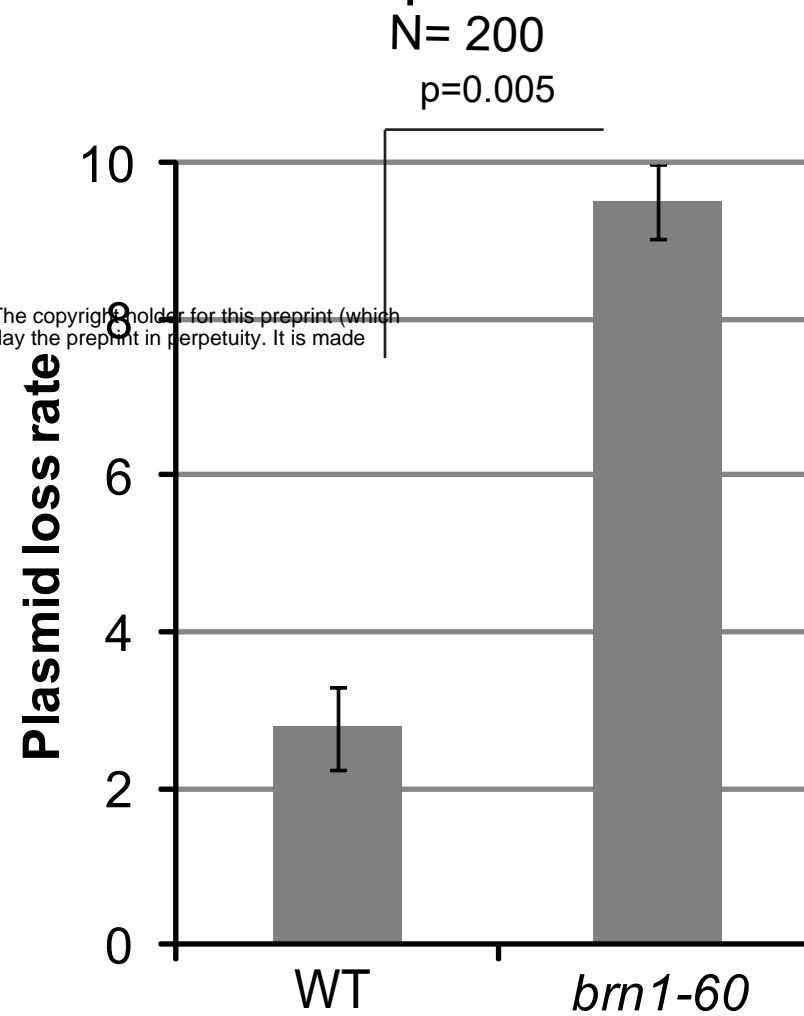
CEN plasmid

ARS plasmid

B.

STB plasmid

CEN plasmid

ARS plasmid

A.

BRN1-6HA/ [Cir⁺]   BRN1-6HA/cdc14-3 [Cir⁺]

Ab ⟶ Brn1-6HA

	WCE	+ Ab	-Ab	WCE	+Ab	- Ab
STB						
CEN3						
TUB2						

□ WT   ■ cdc14-3

ChIP efficiency (Fraction of input)

p=0.020

p = 0.039

TUB2   STB   CEN3

B.

BRN1-6HA/[Cir⁰]   BRN1-6HA/cdc14-3 [Cir⁰]

Ab ⟶ Brn1-6HA

	WCE	+Ab	- Ab	WCE	+Ab	-Ab
STB						
CEN3						
TUB2						

□ WT   ■ cdc14-3

ChIP efficiency (Fraction of input)

p=0.030

TUB2   STB   CEN3

A.

B.

Glucose

Galactose

Bait
LexA/BD
LexA-binding sites
LEU2

B42/AD
Prey
Bait
LexA/BD
LexA-binding sites
LEU2

-His -Trp Glu

-His -Leu -Trp Glu

-His -Leu -Trp Gal

VB + Brn1

Brn1 + VA

Rep1 + Rep2

Rep1 + Brn1

Rep2 + Brn1

Brn1 + Rep1

Brn1 + Rep2